Doctoral theses at NTNU, 2022:311

Inger Berge Hagen

Topics on Marine Collision Avoidance

Doctoral thesis

NTNU
Norwegian University of Science and Technology
Thesis for the Degree of
Philosophiae Doctor
Faculty of Information Technology and Electrical Engineering
Department of Engineering Cybernetics

NTNU
Norwegian University of
Science and Technology

Inger Berge Hagen

Topics on Marine Collision Avoidance

Thesis for the Degree of Philosophiae Doctor

Trondheim, November 2022

Norwegian University of Science and Technology
Faculty of Information Technology and Electrical Engineering
Department of Engineering Cybernetics

NTNU
Norwegian University of
Science and Technology

NTNU
Norwegian University of Science and Technology

Thesis for the Degree of Philosophiae Doctor

Faculty of Information Technology and Electrical Engineering
Department of Engineering Cybernetics

ISBN 978-82-326-6737-6 (printed ver.)
ISBN 978-82-326-5298-3 (electronic ver.)
ISSN 1503-8181 (printed ver.)
ISSN 2703-8084 (online ver.)

Doctoral theses at NTNU, 2022:311

Printed by NTNU Grafisk senter

Summary

The increasing number of both industrial and academic initiatives towards maritime autonomy is a clear indication that this is an active and rapidly expanding field. This thesis presents developments contributing to the future realization of autonomous surface vehicles (ASVs), and is divided into three parts according to the topics treated. The first part is dedicated to the tracking of kayaks in urban environments, while the second and third part concerns the development and evaluation of collision avoidance algorithms. The red line that connects these topics is found in the thesis' main objective, namely to contribute to the ability of ASVs to safely navigate waters shared with vessels under conventional human control.

Part one of the thesis applies this objective to the field of target tracking . The result is a method for extended object tracking (EOT) that employs measurements from a light detection and ranging (lidar) sensor to track the movements of a kayak. Kayaks are small, narrow vessels and kayaking is often practiced on urban waterways as a means of exercise or decompression. The choice of target model was brought on by the fact that easy access to existing infrastructure in metropolitan areas has framed these as one of the prime locations for the early deployment of autonomous vessels. Such applications has triggered the need for research on novel tracking methods capable of handling the distinct environments and vessel types of such locations, to which this work contributes.

While the first part of the thesis focuses on the ASV's ability to sense and interpret its surroundings, the second and third part are dedicated to assuring that it reacts to this information in an appropriate manner. This includes the development of a collision avoidance algorithm designed to produce behaviors that adhere to the International Regulations for Preventing Collisions at Sea (COLREGs). Achieving this is crucial for ASVs ability to interact safely with vessels operated by humans and thus an important step towards future deployment. The presented method is also easily integrated into existing guidance and control systems currently in use on marine vessels, which allowed for the execution of the on-water experiments presented in this part.

Also presented is a method for evaluating the behavior produced by collision avoidance algorithms. This contribution can be seen as a tool in the process of refining existing algorithms, capable of identifying problematic behaviors from simulated trajectories without the need for manual inspection. It can also be viewed in the context of system verification for ASVs, where such methods will be an important element.

The work on evaluation is complemented by a study into the collision avoidance

behaviors displayed by conventional maritime vessels in normal operation. This was motivated by the need for more well defined criteria for COLREGs compliant behavior, both with respect to the evaluation process, but also for the collision avoidance algorithms themselves. The term *COLREGs compliant* is commonly used to describe algorithms that comply with the qualitative behaviors prescribed in Rules 13-17, sometimes also including parts of Rule 8. However, many of the rules allude to the use of human judgment, for instance when stating that vessels should pass each other at a safe distance, or that maneuvers should be readily apparent to the other vessel. The inclusion of such considerations in collision avoidance algorithms require a formal definition in terms of parameters and numerical values, along with their dependence on situation specific factors and parameters. While this requirement could not be fully met, the study does give useful insights into what factors may influence vessel behavior along with a presentation of the statistics obtained.

In addition to the chapters on the topics mentioned above, this thesis includes an introductory chapter aimed at giving a deeper understanding of the motivation behind the presented work, along with some relevant background and context regarding the contributions. The concluding chapter is dedicated to summarize the achieved outcomes and outlines possible directions for future exploration.

Preface

This thesis was submitted as a partial fulfillment of the requirements for the degree of Philosophiae Doctor (PhD) at the Department of Engineering Cybernetics (ITK) at the Norwegian University of Science and Technology (NTNU). The work was carried out under the supervision of Associate Professor Edmund Førland Brekke with Professor Tor Arne Johansen as my co-supervisor. The work has been funded primarily by the project "Autonomous All-Electric Passenger Ferries for Urban Water Transport (Autoferry)" through the NTNU Digital Transformation initiative, and by Kongsberg Maritime as part of the University Technology Center (UTC) for research on Ship Performance and Cyber-Physical Systems at NTNU and Sintef Ocean. The research was also supported by the Research Council of Norway (NFR) through the Center of Excellence on Autonomous Marine Operations and Systems (NTNU AMOS), grant number 223254.

From the start of my PhD I have been a part of the Autoferry project, lead by Associate Professor Morten Breivik. Through this project and also through my affiliation with AMOS, I have had the opportunity to meet people from both the industry and the academic world who has helped widen my perspective on the field of marine autonomy. My work on collision avoidance also brought me into the UTC project which has provided me with new insights on the topic and given me the opportunity to co-supervise three master students.

My own journey into marine autonomy also started with my master's thesis [30], where I implemented a basic version of an model predictive control (MPC)-based collision avoidance algorithm [49]. This implementation included all the cost-function elements from the original paper, except a grounding cost, and performed well in very carefully designed simulation scenarios. This implementation was used as a foundation for the work presented in Chapter 3. However, several additions and changes were necessary before the implementation could be considered for on-water experiments. The most significant being the addition of way-point handling and guidance prediction in the model used for simulating the own ship's alternative trajectories. This greatly improved the implementations' prediction accuracy and contributed to its robustness, which is evident from the results, both those presented in this thesis but also from later sea-trials [55].

Acknowledgments

I first of all would like to thank my main supervisor Edmund, for giving me the opportunity of doing this PhD. You have been a great support, and I truly appreciate

the engagement you have shown towards my work and the interesting discussions this has lead to. I would also like to thank Tor Arne who has been my co-supervisor, but also supervised the work on my master's thesis which got me started with marine autonomy in the first place. You have heard this before, but your response-time and to the point answers to any email is amazing. I am also grateful for the valuable input and feedback provided by Morten Skogvold and Sverre Rye Torben from Kongsberg Maritime, through their involvement in the UTC project. The last couple of years I have also had the pleasure of co-supervising three master students; Olav, Karen and Martin. Working with you was a joy, and I appreciate how your many questions really made me think and rethink everything.

Throughout the work on my PhD I have also been lucky to have the support of good colleagues, many of which I now consider friends. The star of the show is without doubt my former office mate Gunhild. From discussions on lambda-calculus to emotional support. Through all the ups and downs of a PhD, you have been there and I truly value your friendship.

Other honorable mentions goes to Glenn and Håkon, you really made the second floor the place to be. From kindhearted pranks to sledding in the park during lunch, you have brought so much fun to my time at ITK. Thank you.

A special thanks also goes to all my colleagues who has joined in on our Thursday activities; bouldering, the amazing skiing/taco-buffet combo, go-carting, swimming lessons and so much more. This has been a highlight in my week and I have thoroughly enjoyed spending time with you. The guys at the office down at Nyhavna also deserves big thanks, not the least for making working in an open office space a very tolerable experience.

I would also like to thank Giorgio, who I first met as the co-supervisor of my master's thesis. I have greatly appreciated your willingness to share your knowledge and understanding of marine collision avoidance though numerous discussions. And maybe even more, your constant good mood and sense of humor.

Finally, to my family, thank you for the unconditional love and support you have always shown me. My mum, who wants the world for me, and exchanges phone calls with texts to not bother me while I'm writing my thesis. My dad, who once worried that I would never get around to university education, but supported my choices none the less. (You can relax now, I'm educated.) And to Emilien, you have been there for me through the work on my master's thesis and now also for my PhD. I don't know what to say but thank you.

Contents

Acronyms

AIS automatic identification system.
ANEES averaged normalized estimation error squared.
ARPA automatic radar plotting aid.
ASV autonomous surface vehicle.

COG course over ground.
COLAV collision avoidance.
COLREGs International Regulations for Preventing Collisions at Sea.
CPA closest point of approach.
CV constant velocity.

DBSCAN density-based spatial clustering of applications with noise.
DCPA distance to CPA.
DOF degrees of freedom.

ECDIS Electronic Chart Display and Information System.
EKF extended Kalman filter.
EMSA European Maritime Safety Agency.
ENC electronic navigational charts.
EOT extended object tracking.

FOV field of view.

GP Gaussian process.
GPDA generalized probabilistic data association.

IMO International Maritime Organization.

lidar light detection and ranging.
LOS line-of-sight.

MASS maritime autonomous surface ships.

MMSI Maritime Mobile Service Identity.
MOO multi-objective optimization.
MSS minimum sample set.

NAC Norwegian Coastal Administration.
NED North-East-Down.
NM nautical mile.

OOW officers on watch.

PDAF probabilistic data association filter.

RANSAC random sample consensus.
RMSE root mean square error.

SBMPC scenario-based model predictive control.
SOG speed over ground.
SOLAS International Convention for the Safety of Life at Sea.
STL signal temporal logic.

TCPA time to closest point of approach.

UTC coordinated universal time.

VHF very high frequency.

Chapter 1

Introduction

This chapter presents the motivation behind the topics covered in this thesis along with relevant background material. It concludes with an outline of the remaining chapters, including an overview of the topic and main contribution of each.

1.1 Motivation

Automation has long been employed as a means to reduce the extent of time and effort required to complete every-day tasks. Just think of how the washing machine revolutionized the labor intensive and time-consuming process of doing laundry [76]. In other settings, automation is a method for cost reduction and increased production quality and outcome consistency, as with robots operating in industrial production lines. In surveillance and monitoring operations, reducing the cost and effort needed to complete a task can also make it possible to expand both the area and time frame of the operation. For instance, the use of drones to monitor the condition of power lines speeds up the inspection process, especially in areas that are hard to access, thereby permitting more frequent checkups and more efficient maintenance. This is also an example of a task where automation can reduce human exposure to dangerous environments, an advantage made even more clear by the use of underwater robots operating at depths posing serious risks to human divers. Automation has clearly had a big influence on the every-day life of human beings and as the number and extent of the tasks being automated keeps increasing we are moving towards a world where machines can operate autonomously, possibly contributing to further improvements to human safety and well-being.

While the two terms *automation* and *autonomy* may appear similar, the difference between them is vast. While automation applies to the automatic execution of specific pre-defined tasks with an equally well-defined expected outcome, autonomy implies the capability of acting independently in an uncertain environment, making judgments in a manner mimicking that of humans. The distinction between the two has been exemplified by the automotive industry through the development of so-called self-driving cars. The drivers of modern cars are aided by a multitude of advanced driver-assistance system (ADAS) features such as adaptive cruise control, active lane centering and automatic distance control. Despite the appar-

a Washing machine handling the labor intensive task of cleaning fabrics. Source: Adapted from [80].

b Surveillance drone monitoring power-lines. Source: Adapted from [80].

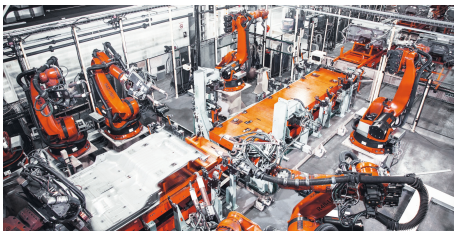

c Industrial robots handling spot welding. Courtesy of KUKA Group.

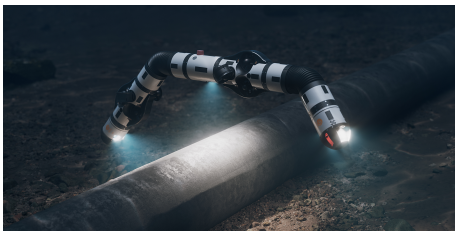

d Underwater inspection and intervention robot performing dual side pipe inspection. Courtesy of Eelume.

Figure 1.1: Examples of automated tasks that either reduce the human work load or exposure to danger, increases output consistency or reduces costs.

ent capabilities of these systems, the driver is still required to remain engaged and ready to take control of the vehicle at any time. According to the levels of driving automation, as defined in SAE J3016 [44], this equates Level 2 which is classified as an assisted mode. Level 3 is the lowest level that can be classified as an autonomous mode, such vehicles are capable of operating autonomously under limited conditions, allowing the driver to take their attention off the road. However, if the conditions are no longer met, the vehicle will alert the driver, who must be ready and able to take over the task of driving. While not yet widely available, vehicles equipped with Level 3 features are slowly making their way into the market. In March 2021, Honda released a limited number of the Legend Hybrid EX equipped with a level 3 traffic jam pilot ADAS (TJPA) for leasing sales in Japan [39]. Later the same year Mercedes-Benz secured international approval for their DRIVE PILOT system which is available for order as an optional extra for selected models from May 2022 [63].

The transportation sector's interest in automation and autonomy is also present within the maritime domain, made apparent by a myriad of projects and initiatives from the industry, academics and authorities. One industry-driven project that stands out is the construction of the *Yara Birkeland*, a cooperation between the fertilizer manufacturer Yara and the technology company Kongsberg. The vessel, which was put into commercial operation in the spring of 2022, will go through a gradual transition towards full autonomy over a two-year period and is predicted to become the world's first fully autonomous, zero-emission container ship [100].

Another example, which involves both industry and academic partners, is the centre for research-based innovation (SFI) SFI AutoShip at NTNU, Trondheim, officially started in 2020. The project concerns several topics related to autonomous transportation operations at sea and its focus points include the development of enabling technologies, new business models and concepts along with a focus on risk monitoring and the legal aspects ships without a captain [79]. Regulatory initiatives aimed to facilitate the transition into autonomy are also taking place. In June 2021, the International Maritime Organization (IMO), a United Nations (UN) specialized agency and the standard-setting authority for safety, security and environmental performance for international shipping, completed a regulatory scoping exercise assessing how maritime autonomous surface ships (MASS) could be regulated [46]. Also at national level the interest is apparent; In 2016, an agreement between the Norwegian Maritime Authority and Norwegian Coastal Administration opened up the Trondheim fjord to become the world's first test area for autonomous ships[81] facilitating both research and development. Similar areas has since been established at other locations in Norway and abroad [47].

The potential advantages giving rise to the interest are many, some examples are the increase of operational safety, improved working conditions, reductions in fuel consumption and increased cargo capacity [75]. While many of the envisioned benefits can be achieved through controlling vessels remotely from dedicated shore control centers (SCCs), it can be argued that the vessels must be capable of a certain level of autonomy, as a fall-back in case of communication failures. A higher level of autonomy will also decrease the need for external intervention and allow for more efficient manning of such centers. The appropriate level of autonomy may also depend on the type of vessel along with the area and type of operation [48]. Combining different levels of autonomy and remote control has the potential to open up for new concepts and solutions within the maritime transportation sector meaning that, also in the future, vessels running autonomously must be capable of operating in waters shared with vessels under human control.

A central aspect with regards to the deployment of autonomous surface vehicles (ASVs) is their behavior in encounters with other vessels. For conventional vessels, such behavior is governed by rules set out by the International Regulations for Preventing Collisions at Sea (COLREGs) [42]. While a regulatory framework is yet to be developed for ASVs, common sense would suggest that they should operate according to similar rules. This is also supported by the IMO's scoping exercise on MASS [61] which recommends that future regulations for autonomous ships should align closely with the COLREGs. Robust, COLREGs compliant collision avoidance is therefore a key technology in the development of ASVs.

As the enabling technologies mature, the issue of how to verify the performance of such systems has become more pertinent. Due to the high complexity of such systems, simulation-based verification has been suggested as a viable approach. This will, among other things, require methods for automatic evaluation of the collision avoidance behavior displayed by the autonomous vessels. It also calls for a more precise definition of the COLREGs, which in many instances refer to the use of human judgment, in order to properly define the evaluation criteria.

However, the outcome of all collision avoidance methods rely on receiving accurate updates about the ASV's surroundings. This information is provided by the

situational awareness module, where data recorded by multiple sensors are combined and interpreted into a consistent world view. Information related to dynamic obstacles, usually other vessels, is provided by the tracking system. A good tracking system is therefore essential for predictable collision avoidance behavior.

1.2 Background

This section presents background information related to the topics treated in this thesis and established the context in which the presented work was accomplished.

1.2.1 Tracking

Lookouts still play an important part in navigation, continuously monitoring the sea for objects that may be an obstacle to navigation or may cause harm to the ship. They are however aided in their task by aids for detection and tracking, this goes back as far as 1935 and the introduction of the first practical radar system. First used to detect incoming aircrafts, it played a crucial role during the battle of Great Britain during the second world war. The invention was soon introduced to commercial vessels and today radar is a requirement from the IMO.

Another aid to tracking is the automatic identification system (AIS) system. The system allows vessels equipped with transceivers to transmit information related their own state and voyage and receive the same information from other vessels. While originally vessel-based, the network has since been extended to include terrestrial-based AIS (T-AIS) and satellite-based AIS (S-AIS) making the system truly global. AIS is a requirement for International Convention for the Safety of Life at Sea (SOLAS) vessels. Information from radar and AIS can be visualized through an Electronic Chart Display and Information System (ECDIS), a tool approved by IMO as an alternative to paper nautical charts, which integrates and displays the sensor information into electronic navigational charts (ENCs) along with the own ship's information.

While the above mentioned aids significantly facilitates navigation in congested waters they do have their limitations. The minimum range of marine radars is primarily determined by the pulse length of the transmitted signals, but can also be extended due to electronic considerations. Sea returns may also clutter the received signals both within and beyond the minimum range. When in the proximity of land or large targets side-lobe echos may also prevent the detection of close targets, small targets that are also close may also escape the lower edge of the vertical beam.

Detection through AIS is limited to vessels equipped with an AIS transceiver. While this is mandatory equipment for SOLAS vessels and many smaller vessels also carry simpler and cheaper transceivers (AIS class B), it can not be the relied upon as the sole method for obstacle detection and tracking. Employing other exteroceptive sensors that can detect other vessels, and provide information regarding measures such as position, course, speed and size, without inter-vessel communication is therefore essential for reliable tracking. This is especially true when operating in areas constricted by land and at locations where smaller vessels are likely to be encountered.

A very likely first use-case for autonomous vessels, which will face both these challenges, is that of the urban ferry. Urban areas often have the infrastructure necessary to enable proper monitoring and possible remote control of such vessels which alleviates many of the problems related to communication and safety that autonomous vessels would face on long-distance voyages. The traffic in such areas is however often made up of smaller vessels making it necessary to employ sensors and tracking methods capable of dealing with vessels such as kayaks that are both highly maneuverable and lies low in the water.

Operating in such limited spaces also increases the importance of precise knowledge about the extent of encountered vessel. This encourages the use of tracking methods that explicitly includes estimates of the target's size, known as extended object tracking (EOT) methods [26]. For such estimates to be accurate, EOT methods should be combined with high-resolution sensors, such as the light detection and ranging (lidar) [77, 78].

1.2.2 Marine Collision Avoidance

Obstacle avoidance is an essential feature of any vehicle intended for autonomous operation, so also at sea. The importance of solving this problem has led to the conception of numerous methods applying different approaches to this challenge [91]. These methods can generally be divided into two categories. *Global*, also known as *deliberate*, algorithms provides a plan for the vessel's long-term movements, generally employing prior information regarding static obstacles such as land. *Local*, or *reactive* algorithms on the other hand, deal with obstacles not known in advance, including dynamic obstacles such as other vessels. Reactive methods are characterized by the limited amount of information employed in their decision making process. This gives them the advantage of being computationally cheap but also limits their motion planning capabilities which can cause sub-optimal behavior in complex situations.

In order to fully exploit available prior information and also be capable of handling unexpected obstacles, the two approaches can be combined. This was for instance done in [94], where the deliberate A* algorithm is used for long-term path planning while discrepancies between the prior information and the experienced environment are handled by the reactive dynamic window (DW) algorithm. However, this does not remedy the lack of short-term planning, which is also an issue with respect to the monitoring of such vessels. The lack of information regarding future movements makes it hard to make informed decisions with respect to the necessity of a remote operator intervening in the situation.

The concept of a plan is an important advantage of model predictive control (MPC) based methods, which provides a prediction of the vessel's movements for a pre-defined time-horizon. Its formulation also admit balanced prioritization of multiple objectives of different importance, such as avoiding collision, abiding the COLREGs and staying on the planned path [15].

Computational power is often a restricting factor when it comes to the use of MPC based methods, especially when it comes to smaller ASVs. As the power of computers increases and their size decreases this has become less of an issue. However, the risk is still there that an optimal solution can not be found within the

time limits posed by the real-time system. As proposed in [49] this can be solved by reducing the algorithm's search space to a limited number of possible control behaviors.

1.2.3 Evaluation of Collision Avoidance Behaviors

The steady advances towards marine autonomy, both in terms of enabling technologies but also regarding the regulatory frameworks, emphasizes the need for formal verification methods for such systems. The high complexity level that characterizes ASVs makes simulation-based testing an appealing solution when combined with a formalized framework ensuring sufficient test-coverage and the provision of confidence levels denoting the results' reliability [89].

A simulation-based approach will also require automatic evaluation of the COLREGs compliance levels of the method being tested, based on the simulated trajectories. So far, most attempts at automatic evaluation has been limited [72, 89]. The exception is the set of metrics developed by Woerner [96] which was primarily used for real-time evaluation of vessel behavior, but also forms a suitable basis for the development of simulation-based evaluation platforms.

However, evaluation results will depend heavily on the parameter values chosen to define COLREGs compliant behavior, which, due to the intentional vagueness of the rules, are not self-evident. While sanctioned qualitative behaviors are clearly defined, e.g., for head on situations, both vessels must make a starboard turn, quantitative properties are left to the judgment of the navigator, e.g. the action must be *made in ample time*, c.f. Rule 8 (a). This implies that no single value will be appropriate for all encounters and multiple factors must be taken into consideration when deciding on the timing of the maneuver.

One possible approach to identify influencing factors and parameterizing COLREGs compliant behaviors is through the study of how the rules are currently being practiced at sea. This has been done with respect to the concept of ship domain, i.e. an area around the own ship that navigators prefer to keep empty, based on data gathered by radar [21, 23]. The ship domain's size and shape can be seen as a representation of how navigators' perception of *safe distance*, c.f. Rule 8 (d) varies according to an obstacle's position relative to the own ship. The introduction of AIS which provides more detailed information about the vessels and their movements has since allowed for the inclusion of additional factors in the study of ship domain properties.

1.3 Research Objectives

Conventional marine tracking systems often combine the use of radar with clustering methods, in order to create a point measurement to use in the estimation of an obstacle's state [95]. Due to the radar's long minimum range and the loss of information related to the target's size, such systems are not suitable for environments where close encounters with small vessels are likely to occur. As mentioned in the previous section, urban ferries are a likely early application for ASVs, and as waterways in metropolitan areas are often narrow and trafficked by vessels of

all sizes, this will necessitate the employment of methods and sensors capable of handling these challenges. One example of a high-resolution sensor that can handle close encounters is the lidar. The use of lidar in combination with an EOT method, which retains information regarding the extent of the object being tracked, therefore seems like a suitable approach for urban ferries. The combination has been tested for boats, using an elliptical target model [77, 78], but whether the use of simpler models is more suitable for very narrow vessels, such as kayaks, is still to be explored.

The restricted maneuvering space available to vessels traveling the rivers and channels that usually make up the waterways in urban areas pose an additional constraint on collision avoidance behavior. Furthermore, the traffic is also often governed by local rules which may require site specific adaptations. It therefore seems expedient to work towards the development of a flexible, COLREGs compliant collision avoidance algorithm for open water encounters, that can easily be modified to include a different rule set or additional restrictions. While several popular collision avoidance algorithms have been adapted to also include COLREGs considerations [4, 57, 94], many does not incorporate vessel dynamics and are limited in their ability to include further considerations. Such limitations are not an issue with MPC-based approaches [15, 49], where both vessel models and additional considerations can easily be included. And while the computational costs and the occurrence of local minima, often associated with MPC methods, is a deterrent with respect to implementation within real-time systems, these problems can be mitigated through optimization over a finite set [49]. Such an approach therefore pose a promising avenue for further research and may help to extend the somewhat limited results from filed tests of collision avoidance algorithms [91].

A natural follow-up to a collision avoidance algorithm claiming COLREGs compliance is a method for evaluating to what degree this claim is met. Such a method will also be an important element in future simulation-based verification platforms for ASVs [89, 90]. The research on methods for evaluation of COLREGs compliance has been limited, but a notable contribution is the set of metrics developed by Woerner [96]. The metrics attempt to quantify the safety and COLREGs performance of vessels and have since their introduction also been employed in the context of simulation-based testing [69, 82]. However, many details surrounding the values of weights and tuning parameters, and also the methods employed to identify and measure maneuvers remain unspecified.

While the weights in this case determine the influence of each metric on the total score, the tuning is used to define the desired behavior. The issue in this originates from the COLREGs' reliance on the human use of judgment, a problem that has been remarked upon by many [69, 82, 90]. While several studies have investigated the rules' concept of *safe distance* by means of radar or AIS data recording vessel behavior [23, 29, 73], information regarding other behavioral traits is still lacking.

The research questions outlined in the previous paragraphs has lead to the consideration of the following tasks in this thesis.

- Develop a method for EOT tailored to the tracking of kayaks in close encounters. The method should be designed to employ measurements obtained by a lidar sensor, and should be tested on real lidar data.

- Develop an MPC based collision avoidance algorithm capable of producing COLREGs compliant behavior. The method should be designed to be suitable for implementation within existing guidance and control architectures on marine vessels.
- Develop an algorithm that can provide unbiased evaluation of the degree of COLREGs compliance in a vessel's behavior in encounters with other vessels. The evaluation should be made based on trajectory data originating from either simulations or on-water encounters.
- Analyze data regarding the collision avoidance behaviors of human controlled vessels from historical AIS data, and study the quantitative properties of vessel behavior in encounters where the qualitative behaviors align with the COLREGs. Efforts should also be made to identify any factors that may influence the decisions made.

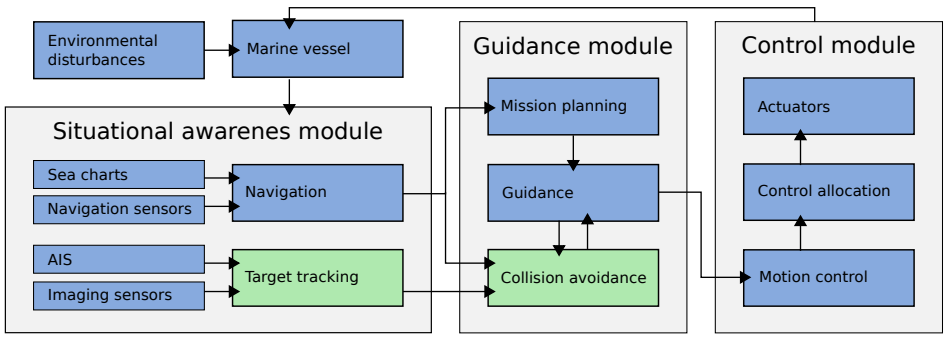

a Control architecture and information flow of an ASV.

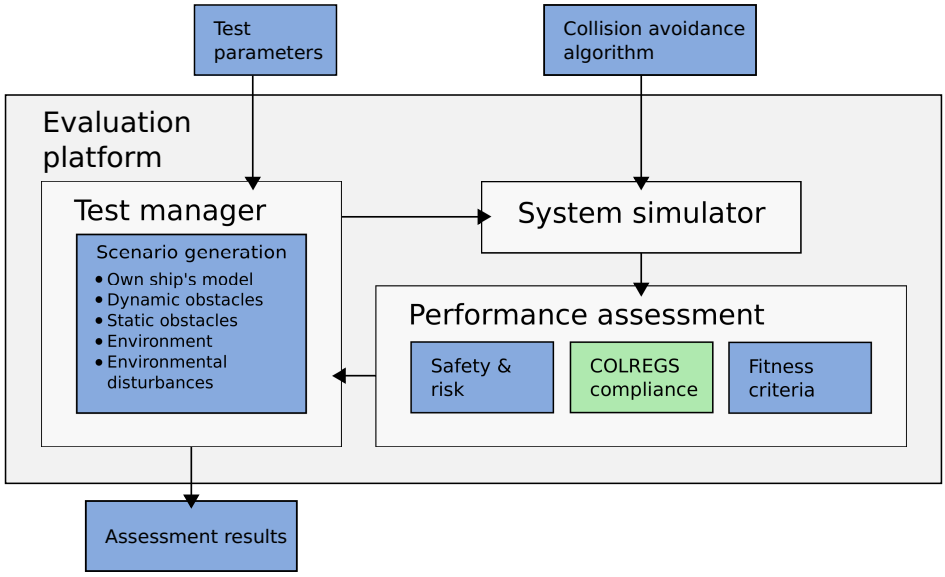

b The proposed architecture of a verification framework for collision avoidance algorithms.

Figure 1.2: Overview of systems forming the context of the topics treated in this thesis. Modules directly related to the presented work are marked in green.

1.4 Contribution and Outline

The main segment of this thesis contains six chapters, excluding this introduction and a concluding chapter, and is divided into three parts, each of which treats a topic essential to the future deployment of ASVs, see Figure 1.2. This section outlines the topic and contribution of each of these chapters.

Part I: Tracking

Chapter 2: Tracking in Urban Waters

Publications:

[31] Inger Berge Hagen and Edmund Brekke. Kayak tracking using a direct lidar model. In *Global Oceans 2020: Singapore–US Gulf Coast*, pages 1–7. IEEE, 2020.

Topic: This chapter proposes a direct approach for EOT using lidar measurements. The method does not use any clustering operations, but processes individual laser beams directly in an extended Kalman filter (EKF), and resolves data association by means of techniques reminiscent of the probabilistic data association filter (PDAF). The method is particularly tailored to tracking of kayaks, and parameterizes the shape of the kayak as a stick whose length is part of the state vector. The proposed method is evaluated through a simulation study and tested on real lidar data.

Contribution: The contribution of this chapter is a tracking method using lidar measurements and is suitable for tracking small vessels, specifically kayaks, in close encounters. This includes a method for direct association between lidar measurements and the kayak, inspired by PDAF techniques. Also presented is a method for hypothesis generation employing the random sample consensus (RANSAC) method.

Part II: Collision Avoidance

Chapter 3: Scenario-based Model Predictive Control in Marine Collision Avoidance

Publications:

[32] Inger Berge Hagen, D. Kwame Minde Kufoalor, Edmund Førland Brekke, and Tor Arne Johansen. MPC-based Collision Avoidance Strategy for Existing Marine Vessel Guidance Systems. In *IEEE International Conference on Robotics and Automation*, Brisbane, QLD, 2018.

Topic: This chapter presents a viable approach for incorporating collision avoidance strategies into existing guidance and control systems on marine vessels. The proposed method facilitates the use of scenario-based MPC for collision avoidance

on marine vessels and does not rely on an accurate model of the guidance system to achieve vessel behaviors that are compliant with the COLREGs. Rather, it depends on transitional costs in the MPC objective for collision avoidance maneuvers that are being executed by the marine vessel. Hence, it is straightforward to implement the MPC collision avoidance on different vessels without specific knowledge of the vessel's guidance strategy. Moreover, it offers the possibility to switch between different (possibly application specific) guidance strategies on the same vessel while running the same MPC collision avoidance algorithm. The method was tested in full scale experiments that show the viability of the method in different collision avoidance scenarios. The same implementation has since been tested in sea-trials facing more complex multi-vessel scenarios[55].

Contribution: The contribution of this chapter is a collision avoidance algorithm compatible with implementation within existing guidance and control architectures. Experiments show that the algorithm produces COLREGs compliant behavior in the main COLREGs scenarios and is also capable of aborting a maneuver if necessary due to drastic changes in the situation.

Chapter 4: Extending the SBMPC with Additional Decision Steps

Publications:

[34] Inger Berge Hagen, D. Kwame Minde Kufoalor, Edmund Førland Brekke, and Tor Arne Johansen. Scenario-based model predictive control with several steps for colregs compliant ship collision avoidance. In *14th IFAC Conference on Control Applications in Marine Systems, Robotics and Vehicles (CAMS)*, 2022. in press.

Topic: The question investigated in this chapter is whether additional decision steps in the scenario-based model predictive control (SBMPC) method, presented in the previous chapter, have the potential to improve vessel behavior. The original method functions by predicting alternative paths resulting from a finite number of alternative control behaviors, then selecting which behavior to apply by use of a cost function and was originally formulated to allow switching between several behaviors on the prediction horizon. However, the implementation presented in Chapter 3 is limited to a single control step at the start of the prediction horizon. To compare the single-step and multi-step SBMPC, a simulation study was performed, where different configurations for the number, positioning and possible control actions were tested. In the course of the simulation study it became clear that identifying situations producing a significant difference between the two methods was difficult to identify and the multi-step SBMPC led to only minor improvements in very few scenarios. Nevertheless, multi-step decisions can be visualized to give better situational awareness, and also have additional benefits with other trajectory parameterizations and less uncertain predictions of other ship trajectories.

Contribution: The main contribution of this chapter with respect to improvements in the method is the identification of a return point on the predicted trajectory where modifications to the control behaviors set by the guidance module are no longer necessary. The addition of this unspecified decision point does not affect the vessel's behavior in two-vessel encounters, but provides a more accurate prediction of the vessel's future movements. If used in real-time visualizations this will significantly improve the observers' understanding of the situation.

While the configurations of decision points, alternative control behaviors and scenarios tested only showed minor improvements to the vessel's behavior, the results illustrate the robustness of the original implantation.

Part III: Evaluation

Chapter 5: Evaluation of Safety and COLREGs Compliance in Collision Avoidance Situations

Publications:

[36] Inger Berge Hagen, Olav Vassbotn, Morten Skogvold, Tor Arne Johansen, and Edmund Førland Brekke. Safety and COLREGS Evaluation for Marine Collision Avoidance Algorithms. *Ocean Engineering*, 2022. unpublished/under revision.

Topic: This chapter presents a comprehensive method for automatic evaluation of collision avoidance maneuvers in terms of safety and COLREGs compliance. A large part of the chapter is dedicated to the presentation of the score and penalty functions used in the evaluation process, including their mathematical expressions and function plots. Also included is an explanation of the technique used for classifying encounters according to the COLREGs rules applicable to each vessel and the method used to detect maneuvers in the trajectory data. The chapter concludes with a presentation of the evaluation scores of seven vessels based on trajectories from both simulated and real-life collision avoidance situations, along with the tuning parameters used for each scenario. The results demonstrate the method' ability to correctly determine the situation type and identify and penalize undesired behaviors.

Contribution: The contribution of this chapter is a method for evaluating the COLREGs compliance and safety of vessel behavior in collision avoidance encounters, based on records of the vessels' trajectories. Also presented is the technique used for maneuver detection, along with the mathematical expressions for the score and penalty functions employed in the evaluation process. The tuning values used in the examples are also available.

Chapter 6: Grounding Hazard Considerations in Collision Avoidance Evaluation

Publications:

[35] Inger Berge Hagen, Martin Navarsete Murvold, Tor Arne Johansen, and Edmund Førland Brekke. Grounding Hazard Considerations in Evaluation of COLREGS Collision Avoidance Algorithms. *IEEE Transactions on Intelligent Transportation Systems*, 2022. unpublished/under revision.

Topic: The method presented in the previous chapter focused on the evaluation of vessel behavior in open water encounters. This chapter extends the domain of this method to also cover coastal waters where the vessel's movements may be restricted by land or shallows. Grounding hazards may impair give-way vessels' ability to make maneuvers sufficiently large to meet the COLREGs requirement of being readily apparent to other vessels. They may also force stand-on vessels to take action despite their obligation to not change their course or speed.

The extensions proposed in this chapter test whether the behavior invoking selected penalties may be caused by grounding hazards. If this is the case, a compensation is calculated based on the severeness of the restrictions formed by the hazard. The effect of these compensations is displayed through the comparison of evaluation results with and without the inclusion of grounding considerations. The results show that grounding hazards preventing COLREGs compliant behavior does lead to compensation being given, also that the size of the compensation corresponds to the restrictiveness of the danger.

Contribution: The contribution of this chapter includes two methods capable of detecting grounding hazards preventing vessels to act in accordance with the COLREGs. Separate methods were developed for vessels with stand-on and give-way responsibilities, and will in both cases lead to compensations proportional to the restrictiveness of the hazards. Also included is a method checking the entire trajectory of the vessel being evaluated for intersections with land or shallows.

Chapter 7: Identifying Parameters for Collision Avoidance Behaviors

Publications:

[33] Inger Berge Hagen, Karen Solem Knutsen, Tor Arne Johansen, and Edmund Førland Brekke. Identification of COLREGS Parameters from Historical AIS-data. *Journal of Navigation*, 2022. unpublished/under revision.

Topic: Reliable anti-collision control algorithms conforming with the rules regulating traffic at sea, the COLREGs, is essential for the deployment of autonomous vessels in waters shared with other ships. The development of such methods is an active field of research, however, little attention has been given to the references to good seamanship in the rules and how these are interpreted by experienced

mariners. This paper presents a method for exploiting historical AIS data in order to obtain parameters indicating the prevalent practices at sea in encounters with high collision risk. The method has been tested on data gathered in areas off the Norwegian coast over several years. Statistics on relevant parameters from the resulting data set and the relation between them is presented. The results indicate that the strongest influence on vessel behavior is the type of situation and the amount of land and grounding hazards in the vessel's proximity.

Contribution: The contribution of this chapter includes an approach to identify collision avoidance encounters within historical AIS data. The method allows for the selection of encounters where the vessels' qualitative behavior adheres to the COLREGs and the extraction of properties characterizing the situation and the behavior of the involved vessels. The results presented in this chapter reveal some of the factors that influence vessel behavior in collision avoidance situations. They also indicate appropriate ranges for parameters used to define COLREGs compliant behavior within the context of both collision avoidance algorithms and verification.

Part I

Tracking

Chapter 2

Tracking in Urban Waters

This chapter is based on :

[31] Inger Berge Hagen and Edmund Brekke. Kayak tracking using a direct lidar model. In *Global Oceans 2020: Singapore–US Gulf Coast*, pages 1–7. IEEE, 2020.

2.1 Introduction

ASVs have been getting increased attention within the maritime industry as they are potentially cost-saving and remove the need for placing human operators in hazardous environments and situations. However, the automation of surface vessels does come with its own set of challenges. On the one side there are technical challenges such as the demand for increased reliability and robustness of the vessel and its systems. Stable communication links are also a necessity, both for monitoring purposes and the possibility of remote control in case of emergencies. Additionally, these systems require access to qualified personnel, capable of running and maintaining them. Other challenges are more directly related to the automation of the vessel itself, notably developing methods for collision avoidance and situational awareness.

To focus on the more automation related challenges it is desirable to concentrate on vessels traveling relatively short distances in coastal or urban waters where issues associated with communication and monitoring are greatly reduced and, if necessary, remote operation is an option. Urban ferries are therefore a natural choice as an experimental platform as they both follow a predefined itinerary within a restricted area and are generally close to existing infrastructures.

The challenges pertaining to autonomy will however not decrease. One example is the great variety in vessel types that may be encountered in such areas, anything from large barges to narrow and low-lying kayaks should be expected. Any ASV that operate in areas close to the shore should therefore have the ability to detect and track kayaks. The operating space can also be very restricted, e.g. a city canal. This combined with an often high traffic density will leave little space for evasive maneuvers and safety margins. Having accurate knowledge of both the position and extent of surrounding vessels is therefore crucial to safe operations.

It is also imperative that any collision avoidance maneuvers are made in a predictable and safe manner. It follows that information pertaining to the speed and heading of other vessels, along with corresponding uncertainty measures, is necessary for the planning of collision free trajectories that uphold acceptable safety margins.

The information needed by the tracking system is obtained via sensors, the most common in use for marine applications being the marine radar. In conventional tracking systems it is assumed that a target generates at most one measurement per scan. In cases where multiple returns are received, clustering techniques are used to join measurements that are likely to originate from the same target. Relevant information about target extent can thus be lost.

To retain information about target extent a high-resolution sensor, yielding multiple measurements per target, can be combined with an EOT [26] approach where the extent of a target is included in its estimated state vector. The lidar sensor is an example of such a high-resolution sensor which in combination with different EOT approaches has been employed for the tracking of cars [25], pedestrians [27, 28] and boats [77, 78].

The ellipse is a common model for marine vessels and is used in both [78] and [77]. The former [78] presents the generalized probabilistic data association (GPDA) filter which combines a random matrix approach with probabilistic data association. In the latter [77], the random matrix approach was replaced with the contour tracking from [24] and the two methods were compared, both in simulations and on real lidar data. In both cases contour tracking outperformed the random matrix approach, motivating further research into more direct methods where the inherent structure of the measurements is exploited.

While an elliptic approximation is suitable for many marine vessels, the highly structured lidar measurements will for the particular case of a kayak target, produce returns along a very narrow shape, see Figure 2.1. It then becomes questionable whether one can estimate the parameters (short and long axes) of a full ellipse, and a simpler stick model with only the long axis retained is a viable alternative. This simple stick approximation also maintains the inherent structure in the lidar measurements.

We have investigated the feasibility of tracking a kayak by means of lidar, and we present a singe-target EOT method tailored to the stick approximation. The data association is based on principles and assumptions similar to the ones underlying the PDAF [2]. A key challenge in EOT is to sample an appropriately diverse set of data association hypotheses. We explore sampling techniques based on RANSAC, a brief description of which can be found in [6]. RANSAC was also the basis for the tracking methods presented in [93] and [67].

2.2 Problem formulation

Our aim being to demonstrate the feasibility of using a direct measurement model, the problem has been limited to tracking a target located within the range of a stationary lidar sensor and issues such as target birth and death has been left for later work.

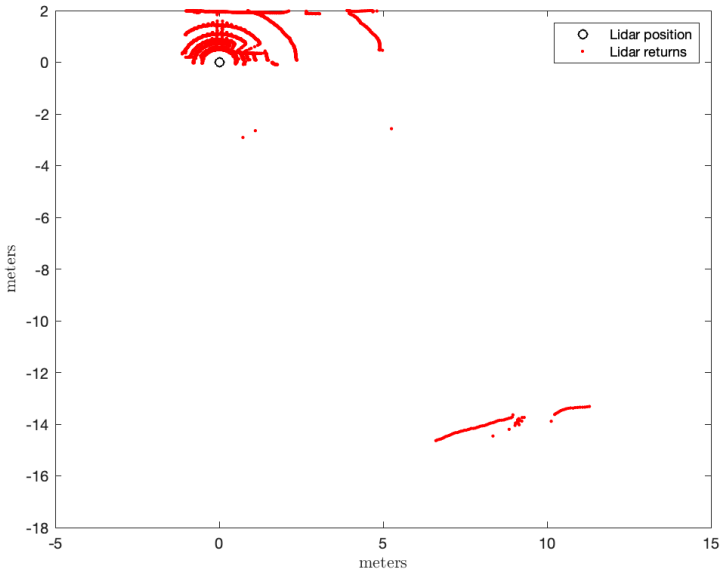

Figure 2.1: Measurements from a Velodyne VLP16 lidar, see specifications in Table 2.3, showing a kayak projected on to a plane. The returns from the kayak forms the line in the bottom right corner.

2.2.1 State model

The state vector at time step k is denoted by $\boldsymbol{x}_k = [x_k, y_k, u_k, v_k, \phi_k, l_k]$, where (x_k, y_k) signifies the position of the target's centroid in Cartesian coordinates, (u_k, v_k) the velocities, ϕ_k the heading and l_k the length of the target. The dynamic evolution of the target state is modeled by a linear Gaussian model

$$\boldsymbol{x}_k = \boldsymbol{F}\boldsymbol{x}_{k-1} + \boldsymbol{q}_k, \quad p(\boldsymbol{q}_k) = \mathcal{N}(\boldsymbol{q}_k; \boldsymbol{0}, \boldsymbol{Q}), \tag{2.1}$$

where the matrices are given by the discrete-time constant velocity model

$$\boldsymbol{F} = \begin{bmatrix} \boldsymbol{I}_2 & \boldsymbol{A} \\ \boldsymbol{0}_4 & \boldsymbol{I}_4 \end{bmatrix}, \quad \boldsymbol{A} = \begin{bmatrix} T_s \boldsymbol{I}_2 & \boldsymbol{0}_2 \end{bmatrix}, \tag{2.2}$$

$$\boldsymbol{Q} = \begin{bmatrix} \boldsymbol{B} \otimes \boldsymbol{I}_2 & \boldsymbol{0} \\ \boldsymbol{0} & \boldsymbol{C} \end{bmatrix}, \ \boldsymbol{B} = \sigma_p^2 \begin{bmatrix} \frac{T_s^3}{3} & \frac{T_s^2}{2} \\ \frac{T_s^2}{2} & T_s \end{bmatrix}, \ \boldsymbol{C} = \begin{bmatrix} \sigma_a^2 T_s & 0 \\ 0 & \sigma_l^2 \end{bmatrix}, \tag{2.3}$$

where $\boldsymbol{I}_n$ is the $n \times n$ identity matrix and $\boldsymbol{0}_m$ is a $m \times m$ zero matrix. The sample time is denoted T_s and the noise covariance for the acceleration and length is given by σ_a^2 and σ_l respectively.

2.2.2 Measurement model

Lidar sensors calculate distances by emitting laser light and measuring the reflected light. The 3D position of a return relative to the sensor is thus given by the mea-

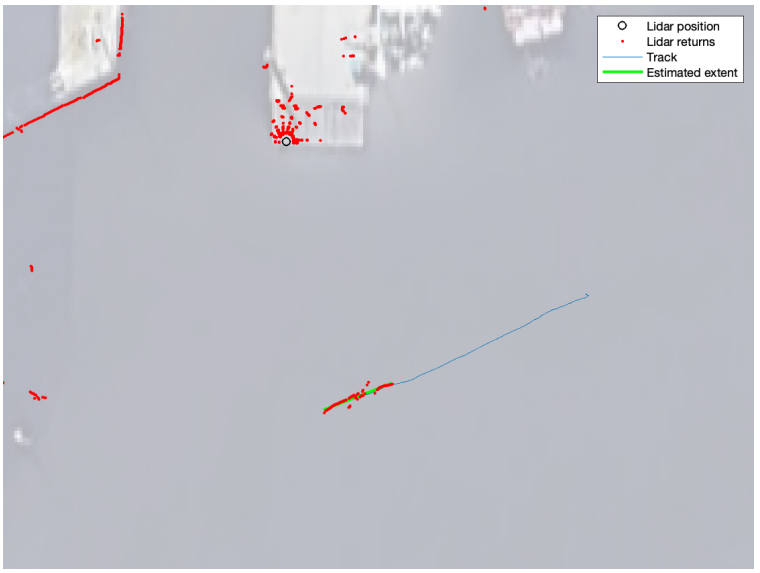

Figure 2.2: Lidar data with track on kayak and its estimated extent. The data were collected with the Velodyne VLP16 lidar, with specifications as in Table 2.3.

sured distance along with the horizontal and vertical angle of the laser beam which together form a measurement, denoted $\boldsymbol{z} = [r\ \theta]^\intercal$. In the following sections it is assumed that the sensor is a side-looking 2D lidar emitting laser beams at fixed angular intervals.

The radial component r_k^j for a measurement will be within the interval $[0, R_{max}]$, where R_{max} is the maximum range of the sensor. The angular component is given by the angle of the beam that contains the detection. The set of candidate measurements for target association is selected by forming an elliptical validation gate around the predicted target extent. The area and orientation of the gate is decided by mapping the unit circle onto an ellipse by the transformation matrix:

$$\boldsymbol{T} = \boldsymbol{S}\boldsymbol{R}^\intercal + \sqrt{\boldsymbol{L}}\boldsymbol{V}^\intercal, \tag{2.4}$$

where the first term accounts for the predicted extent $\bar{l}_k$ and heading $\bar{\phi}_k$. It consist of the rotation matrix $\boldsymbol{R}$ and the scaling matrix $\boldsymbol{S}$.

$$\boldsymbol{R} = \begin{bmatrix} \cos\bar{\phi}_k & -\sin\bar{\phi}_k \\ \sin\bar{\phi}_k & \cos\bar{\phi}_k \end{bmatrix} \quad \boldsymbol{S} = \begin{bmatrix} \bar{l}_k & 0 \\ 0 & 1 \end{bmatrix}, \tag{2.5}$$

The second term is the contribution from the covariance of the position, where $\boldsymbol{V}$ is a matrix whose columns are the eigenvectors of $\boldsymbol{Q}_{1:2,1:2}$ and $\boldsymbol{L}$ is the diagonal matrix whose non-zero elements are the corresponding eigenvalues. As measurements can only appear on the beams the volume of the validation region V_k is equal to the length of the beams within this region.

The list of target generated measurements falling within the gate is denoted $Z_{T,k} = \{\boldsymbol{z}_k^j\}_{j=1}^{\nu_k}$, the list of clutter measurements $Z_{C,k} = \{\boldsymbol{z}_k^j\}_{j=1}^{\mu_k}$, ν_k and μ_k

denote the number of measurements. The list

$$Z_k = \{\boldsymbol{z}_k^j\}_{j=1}^{m_k}, \quad m_k = \mu_k + \nu_k \tag{2.6}$$

contains all validated measurements collected at time step k. Sensor properties assure that Z_k is ordered according to the angular component of the measurements so that $\theta_k^j < \theta_k^{j+1}$.

The measurement likelihood for the list of measurements can then be expressed as:

$$p(Z_k|\boldsymbol{x}_k) = \prod_{\boldsymbol{z}_k^j \in Z_{C,k}} p^c(\boldsymbol{z}_k^j) \prod_{\boldsymbol{z}_k^j \in Z_{T,k}} p^d(\boldsymbol{z}_k^j|\boldsymbol{x}_k). \tag{2.7}$$

Each factor in the above expression can be seen as a mixture:

$$p^c(\boldsymbol{z}_k^j) = P_{FA} p^{c1}(\boldsymbol{z}_k^j) + (1 - P_{FA}) p^{c0}(\boldsymbol{z}_k^j) \tag{2.8a}$$

$$p^d(\boldsymbol{z}_j^j) = P_D p^{d1}(\boldsymbol{z}_k^j) + (1 - P_D) p^{d0}(\boldsymbol{z}_k^j)., \tag{2.8b}$$

where P_{FA} denotes the probability of false alarms and P_D the number of detections. The first term in Equation 2.8a denotes the clutter distribution, the first term in 2.8b the measurement likelihood for a single measurement. It should be noted that while the expressions in Equation 2.8 can be seen as a virtual model, they do however give a mathematical correct representation.

2.2.3 Hypothesis Generation

When a list of measurements Z_k is received, a random sample consensus (RANSAC) method is employed to generate n_k linear models, fitted to the measurements. The method works by drawing a minimum sample set (MSS) from the measurements, then fitting a linear model to the MSS. The compatibility of the remaining measurements with the model is tested by calculating the euclidean distance to the line and measurements within a certain distance are added to the hypothesis. This process is repeated for a fixed number of iterations N. The resulting hypotheses are ranked using a scoring function and those with scores below a chosen threshold is rejected such that $n_k \leq N$ hypotheses are retained, each separating the measurements into two sets

$$\begin{aligned} \mathcal{D}_k^i &= \{\boldsymbol{z} \in Z_k; \boldsymbol{z} \text{ is an inlier of model } i\} \\ \mathcal{C}_k^i &= \{\boldsymbol{z} \in Z_k; \boldsymbol{z} \notin \mathcal{D}_k^i\}, \end{aligned} \tag{2.9}$$

where the measurements contained in $\mathcal{D}^i$ are considered target originated (inliers), and those in $\mathcal{C}^i$ are considered clutter (outliers).

The hypothesis should also include misdetections, to achieve this we define the set $\mathcal{G}_k$ as a set containing one measurement for each beam that falls within the gate at time k. For beams that does not contain a real measurement, the radial component is set to the hyper maximal range, denoted R_{hm} as to not confuse them with any real measurements. This allows the introduction of the following sets:

$$\begin{aligned} \mathcal{T}_k^i &= \{\boldsymbol{z} : \boldsymbol{z} \in \mathcal{G}_k \wedge min_\theta(\mathcal{D}^i) \leq \theta \leq max_\theta(\mathcal{D}^i)\} \\ \mathcal{M}_k^i &= \mathcal{T}_k^i \setminus \mathcal{D} \end{aligned} \tag{2.10}$$

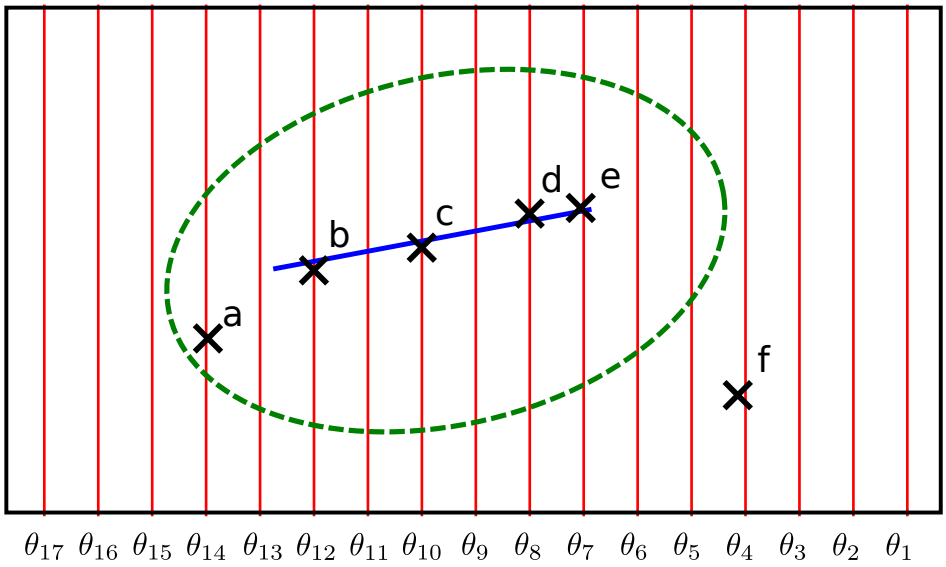

Figure 2.3: Sets generated under the hypothesis that measurements b, c, d and e are target originated, gate marked with (- -). Inliers $\mathcal{D} = \{\boldsymbol{z}_b, \boldsymbol{z}_c, \boldsymbol{z}_d, \boldsymbol{z}_e\}$, outliers $\mathcal{C} = \{\boldsymbol{z}_a\}$, measurements from all gated beams $\mathcal{G} = \{\boldsymbol{z}_{\theta_j}\}_{j=5}^{14}$ where $\boldsymbol{z}_{\theta_j} = [R_{hm}\ \theta_j]^\intercal$, target intersecting beam measurements $\mathcal{T} = \{\boldsymbol{z}_{\theta_j}\}_{j=57}^{12}$ and misdetections $\mathcal{M} = \{\boldsymbol{z}_{\theta_9}\ \boldsymbol{z}_{\theta_{11}}\}$.

where $\mathcal{T}_k^i$ is the set of beams that intersect with the target and $\mathcal{M}_k^i$ is the set of beams with misdetections[1].

Together, the sets $\mathcal{D}^i, \mathcal{C}^i$ and $\mathcal{M}^i$ form an association hypothesis $a_k^i = \{\mathcal{D}^i, \mathcal{C}^i, \mathcal{M}^i\}$. The set of all association hypotheses generated at time k is $\mathcal{A}_k = \{a_k^i\}_{i=1}^{n_k}$. An illustration showing these sets for a given hypothesis can be found in Figure 2.3.

2.2.4 Hypotheses dependent innovations

A key difference between standard single-tracking and EOT is that in the context of EOT the innovation, i.e. the difference between prediction and measurements, must be calculated for multiple measurements per target. In general there will be a difference between the set of beams touched by the predicted kayak and the beams touched by the real kayak. To deal with this discrepancy within the EKF/PDAF framework the concept of virtual measurements is introduced. This approach is explained in the following paragraphs, and illustrated by an example in Figure 2.4.

Prediction

Given a predicted target state $\bar{\boldsymbol{x}}_k$, intersection points between the lidar beams and predicted target extent is calculated. Each point is then converted into polar

[1]The set $\mathcal{T}_k^i$ can be extended to form additional hypotheses assuming misdetections at the target's endpoints.

coordinates according to the following nonlinear equation

$$\begin{aligned} \boldsymbol{z} &= [r\ \theta]^\intercal \\ &= \left[\sqrt{x^2+y^2}\ \ \operatorname{atan2}(y,x)\right]^\intercal . \end{aligned} \tag{2.11}$$

This yields a list of predicted measurements $\bar{Z}'_k$ where each element is on the form described in Equation 2.11. A visualized example is shown in Figure 2.4a.

Endpoint Angle Calculation

The definition of the association hypotheses, Section 2.2.3 can be utilized to approximate the extent of the target. For a given association hypothesis a^i_k, a rough estimate of the endpoints is half-way between a beam covered by the target and a beam not covered by the target. The lower and upper angles of the hypothesized target extent are denoted $\hat{\theta}^l_k$ and $\hat{\theta}^u_k$ respectively. For the predicted extent, the endpoint angles $\bar{\theta}^l_k$ and $\bar{\theta}^u_k$ are calculated from the state vector. All angles are illustrated in Figure 2.4b.

Extension

To compare predictions and actual measurements that lie on the same beam, the length parameter l_k of the predicted state $\bar{\boldsymbol{x}}_k$ is extended to cover beams that have target originated measurements, shown in Figure 2.4c.

Removal

The final step is to remove any predictions that do not align with real measurements. The list of predictions $\bar{Z}'_k$ and the set target originated measurements $\mathcal{D}^i_k$ are now of equal size, as shown in Figure 2.4c.

Restructuring

The angular components of the remaining measurements are deterministically given and can therefore be removed. To amend for the information loss in the extension and removal step, the endpoint angles are then included. This restructuring is performed on both $\bar{Z}'_k$ and $\mathcal{D}^i_k$ resulting in two virtual measurement lists $\bar{Z}^i_k$ (predictions) and $\hat{Z}^i_k$ (target measurement). Both lists are on the form $Z = [\boldsymbol{r}^\intercal,\ \theta^l,\ \theta^u]^\intercal$, where $\boldsymbol{r}$ is a column vector containing the radial component of the remaining measurements.

The above previously described steps are performed in the nonlinear measurement function

$$\bar{Z}^i_k = \boldsymbol{h}_i(\bar{\boldsymbol{x}}_k). \tag{2.12}$$

The Jacobian of the hypothesis conditioned measurement function is found by finite difference, linearizing around the predicted state vector $\bar{\boldsymbol{x}}_k$ and hypothesized target measurements $\hat{Z}^{i\prime}_k$.

$$\boldsymbol{H}^i_k = \frac{\mathrm{d}\boldsymbol{h}}{\mathrm{d}\boldsymbol{x}}\Big|_{\bar{\boldsymbol{x}}_k, \hat{Z}^{i\prime}_k} \tag{2.13}$$

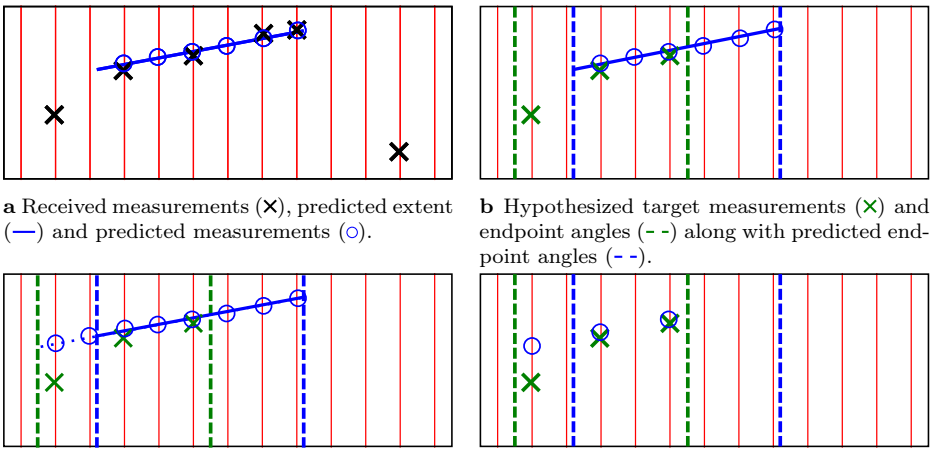

a Received measurements (×), predicted extent (—) and predicted measurements (○).

b Hypothesized target measurements (×) and endpoint angles (- -) along with predicted endpoint angles (- -).

c Extending the predicted target extent (⋯) resulting in two additional measurement predictions.

d Removal of predictions that does not align with the current hypothesis.

Figure 2.4: Illustration of predicted measurements as a function of the predicted state and a given association event.

The covariance for each of the radial measurements is σ_r^2, these are collected in the vector $\boldsymbol{\sigma}_r$. The distributions of the two endpoint angles are approximated by Gaussians giving the covariance matrix $\boldsymbol{R}_k^i$.

$$\boldsymbol{A} = \text{diag}(\boldsymbol{\sigma}_r) \quad \boldsymbol{B} = \begin{bmatrix} \frac{\sigma_\theta^2}{12} & 0 \\ 0 & \frac{\sigma_\theta^2}{12} \end{bmatrix} \quad \boldsymbol{R}_k^i = \begin{bmatrix} \boldsymbol{A} & \boldsymbol{0} \\ \boldsymbol{0} & \boldsymbol{B} \end{bmatrix} \tag{2.14}$$

2.3 Tracking approach

According to the total probability theorem the posterior density of the target can be written as

$$p_k(\boldsymbol{x}_k) = \sum_{\mathcal{A}_k} p(\boldsymbol{x}_k | a_k^i, Z_{1:k}) \mathrm{P}(a_k^i | Z_{1:k}) \tag{2.15}$$

where $Z_{1:k} = \{Z_l\}_{l=1}^k$ is the cumulative set of measurements at time step k.

2.3.1 State and Covariance Update

The event-conditional densities are given by

$$\begin{aligned} p(\boldsymbol{x}_k | a_k^i, Z_{1:k}) &\propto p(Z_k | \boldsymbol{x}_k, a_k^i) p(\boldsymbol{x}_k | Z_{1:k-1}) \\ &= \prod_{\boldsymbol{z}_k^j \in \mathcal{C}^i} p^c(\boldsymbol{z}_k^j) \prod_{\boldsymbol{z}_k^j \in \mathcal{D}^i} p(\boldsymbol{z}_k^j | \boldsymbol{x}_k)\ p(\boldsymbol{x}_k | Z_{1:k-1}) \\ &= \frac{1}{V_k^{\phi_k^i}} \mathcal{N}(\hat{Z}_k^i; \boldsymbol{h}_i(\bar{\boldsymbol{x}}_k), \boldsymbol{R}_k^i) \mathcal{N}(\boldsymbol{x}_k; \bar{\boldsymbol{x}}_k, \bar{\boldsymbol{P}}_k) \\ &\propto \mathcal{N}(\boldsymbol{x}_k; \hat{\boldsymbol{x}}_k^i, \hat{\boldsymbol{P}}_k^i) \end{aligned} \tag{2.16}$$

where V_k is the total beam length within the gate. This results in the following expressions for the filter:

$$\begin{aligned} \boldsymbol{S}_k^i &= \boldsymbol{H}_k^i \bar{\boldsymbol{P}}_k \boldsymbol{H}_k^{i\intercal} + \boldsymbol{R}_k^i & \boldsymbol{W}_k^i &= \bar{\boldsymbol{P}}_k \boldsymbol{H}_k^{i\intercal} \boldsymbol{S}_k^{i\,-1} \\ \boldsymbol{\nu}_k^i &= \hat{\boldsymbol{Z}}_k^i - \boldsymbol{h}_i(\bar{\boldsymbol{x}}_k) & \hat{\boldsymbol{x}}_k^i &= \bar{\boldsymbol{x}}_k + \boldsymbol{W}_k^i \boldsymbol{\nu}_k^i \\ \hat{\boldsymbol{P}}_k^i &= (\boldsymbol{H}_k^{i\intercal} \boldsymbol{R}_k^{i\,-1} \boldsymbol{H}_k^i + \bar{\boldsymbol{P}}_k^{-1})^{-1} \end{aligned}$$

The covariance of the updated state is

$$\hat{\boldsymbol{P}}_k = \boldsymbol{P}_k^c + \tilde{\boldsymbol{P}}_k \tag{2.17}$$

where the spread of innovation term is given by

$$\begin{aligned} \tilde{\boldsymbol{P}}_k = \sum_{i=1}^{n_k} \beta_k^i \left[\bar{\boldsymbol{x}}_k + \boldsymbol{K}_k^i \boldsymbol{\nu}_k^i\right] \left[\bar{\boldsymbol{x}} + \boldsymbol{\nu}_k^i \boldsymbol{K}_k^i\right]^\intercal \\ - \left[\bar{\boldsymbol{x}}_k + \boldsymbol{K}_k^i \boldsymbol{\nu}_k^i\right] \left[\bar{\boldsymbol{x}} + \boldsymbol{\nu}_k^i \boldsymbol{K}_k^i\right]^\intercal \end{aligned} \tag{2.18}$$

where $\beta_k^i \triangleq \mathrm{P}\{a_k^i\}$. The covariance of the state updated with the correct measurement is

$$\boldsymbol{P}_k^c = \sum_{i=1}^{n_k} \beta_k^i (\boldsymbol{H}_k^{i\intercal} \boldsymbol{R}_k^{i\,-1} \boldsymbol{H}_k^i + \bar{\boldsymbol{P}}_k^{-1})^{-1}. \tag{2.19}$$

The Equations (2.19) and (2.18) are derived in a similar manner to the expressions used in the PDAF [2], but without a zero hypothesis.

2.3.2 Association Probabilities

The measurement likelihood for a given hypothesis is given by

$$p(Z_k|\boldsymbol{x}_k) = \prod_{\boldsymbol{z}_k^j \in \mathcal{N}_k^i} p^c(\boldsymbol{z}_k^j) \prod_{\boldsymbol{z}_k^j \in \mathcal{T}^i} p^d(\boldsymbol{z}_k^j|\boldsymbol{x}_k), \tag{2.20}$$

where $\mathcal{N}_k^i = \mathcal{G}_k \setminus \mathcal{T}_k^i$, i.e. measurements that fall within the gate, but are not associated with the target under the i^{th} hypothesis. As described in Section 2.2.2, each factor in the above expression can be seen as a mixture:

$$p^c(\boldsymbol{z}_k^j) = P_{FA} p^{c1}(\boldsymbol{z}_k^j) + (1 - P_{FA}) p^{c0}(\boldsymbol{z}_k^j) \tag{2.8a}$$

$$p^d(\boldsymbol{z}_j^j) = P_D p^{d1}(\boldsymbol{z}_k^j) + (1 - P_D) p^{d0}(\boldsymbol{z}_k^j). \tag{2.8b}$$

The first term in each of the expressions in Equation 2.8 denotes the clutter distribution and measurement likelihood respectively. The last term in each of the equations represent the likelihood of a missed clutter measurement and a missed detection respectively and can be defined as

$$p^{c0}(\boldsymbol{z}_k^j) \triangleq \delta(r_k^j - R_{hm}) \tag{2.22a}$$

$$p^{d0}(\boldsymbol{z}_k^j) \triangleq \delta(r_k^j - R_{hm}), \tag{2.22b}$$

where $\delta(\cdot)$ is the Dirac delta function and r_k^j is the radial component of measurement $\boldsymbol{z}_k^j$. This definition allows for these terms to be canceled against each other in the subsequent derivation of the association probabilities. They will therefore have no influence on the resulting probabilities and can be viewed as a virtual model. With this in mind and using $c_1 = \left(\frac{1-P_D}{1-P_{FA}}\right)$ and $c_2 = \left(\frac{P_D V_k}{P_{FA}}\right)$, the association probabilities can be calculated as follows:

$$
\begin{aligned}
\mathrm{P}\{a_k^i\} &\propto \frac{1}{\prod_{\boldsymbol{z}_k^j \in \mathcal{G}_k} p^c(\boldsymbol{z}_k^j)} \prod_{\boldsymbol{z}_k^j \in \mathcal{N}^i} p^c(\boldsymbol{z}_k^j) \int \left(\prod_{\boldsymbol{z}_k^j \in \mathcal{T}^i} p^d(\boldsymbol{z}_k^j | \boldsymbol{x}_k) \right) p(\boldsymbol{x}_k) \mathrm{d}\boldsymbol{x}_k \\
&= \int \prod_{\boldsymbol{z}_k^j \in \mathcal{T}^i} \frac{p^d(\boldsymbol{z}_k^j | \boldsymbol{x}_k)}{p^c(\boldsymbol{z}_k^j)} p(\boldsymbol{x}_k)) \mathrm{d}\boldsymbol{x}_k \\
&= \int \left(\prod_{\boldsymbol{z}_k^j \in \mathcal{D}^i} \frac{P_D V_k}{P_{FA}} \mathcal{N}(\boldsymbol{z}_k^j; \boldsymbol{h}^{(j)}(\boldsymbol{x}_k), \sigma_r^2) \right) c_1^{\rho_k^i} p(\boldsymbol{x}_k) \mathrm{d}\boldsymbol{x}_k \\
&= c_1^{\rho_k^i} c_2^{\nu_k^i} \int \mathcal{N}(\hat{Z}_k^i; \boldsymbol{h}_i(\bar{\boldsymbol{x}}_k), \boldsymbol{R}_k^i) p(\boldsymbol{x}_k) \mathrm{d}\boldsymbol{x}_k \\
&= c_1^{\rho_k^i} c_2^{\nu_k^i} \int \mathcal{N}(\hat{Z}_k^i; \boldsymbol{h}_i(\bar{\boldsymbol{x}}_k), \boldsymbol{H}_k^i \bar{\boldsymbol{P}}_k \boldsymbol{H}_k^{i\intercal} + \boldsymbol{R}_k^i) \mathcal{N}(\boldsymbol{x}_k; \bar{\boldsymbol{x}}_k, \bar{\boldsymbol{P}}_k) \mathrm{d}\boldsymbol{x}_k \\
&= c_1^{\rho_k^i} c_2^{\nu_k^i} \mathcal{N}(\hat{Z}_k^i; \boldsymbol{h}_i(\bar{\boldsymbol{x}}_k), \boldsymbol{H}_k^i \bar{\boldsymbol{P}}_k \boldsymbol{H}_k^{i\intercal} + \boldsymbol{R}_k^i),
\end{aligned}
\tag{2.23}
$$

where ρ_k^i is the number of misdetections and ν_k^i is the number of detections.

2.4 Simulation study

A simulation study was performed, using as input the simulated output of a laser scanner with a range of 100 meters and 360° field of view. The initial surge velocity of the target was uniformly drawn from the interval [0.3m/s, 0.6m/s]. Initial values for position and heading variables was uniformly drawn from the intervals shown in Table 2.1. The intervals were chosen so that the target was likely to stay within range throughout the simulation.

2.4.1 Simulation results

In the 100 simulations, the filter successfully tracked the target in all scenarios. Figure 2.5 and 2.6 show the actual and estimated target trajectory from a simulation with initial state $\boldsymbol{x}_0 = [-43.3\ 56.7\ 0.4\ -0.1\ -0.1\ 5.0]^\intercal$. A closer inspection of the trajectories, shown in Figure 2.6 reveals a zigzag pattern that is typical for the all the estimated trajectories. The pattern arises from the assumption that the best guess for the predicted endpoint angles of the kayak is in the middle between two beams. While undesirable, it does not seem to negatively affect the overall performance of the filter.

Table 2.1: Initial condition intervals

Quadrant	x interval	y interval	ϕ interval
1	[40m, 60m]	[40m, 60m]	[170°, 190°]
			[260°, 280°]
2	[-40m, -60m]	[40m, 60m]	[−10°, 10°]
			[260°, 280°]
3	[-40m, -60m]	[-40m, -60m]	[−10°, 10°]
			[80°, 100°]
4	[40m, 60m]	[-40m, -60m]	[170°, 190°]
			[80°, 100°]

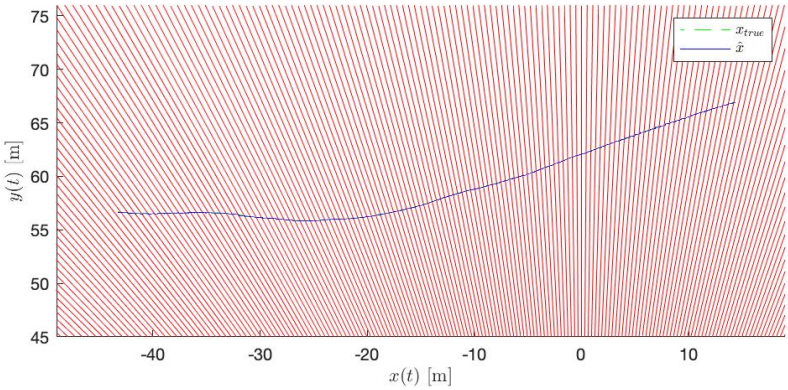

Figure 2.5: Example of true and estimated trajectory.

The consistency of the filter was evaluated by calculating the averaged normalized estimation error squared (ANEES)

$$\text{ANEES}_k = \frac{1}{n_x T} \sum_{n=1}^{M} (\hat{x}_k^n - x_k^n)^\intercal \hat{\boldsymbol{P}}_k^{n\,-1} (\hat{x}_k^n - x_k^n). \tag{2.24}$$

where n_x is the number of states, T the number of time steps and M the number of simulations. The resulting ANEES can be seen in Figure 2.7, where the 95% quantiles of the χ^2 distribution is shown in green. This indicate that the filter is somewhat underconfident. However it is clear from the figure that the filter does not diverge.

The root mean square error (RMSE) measure was also used to evaluate the

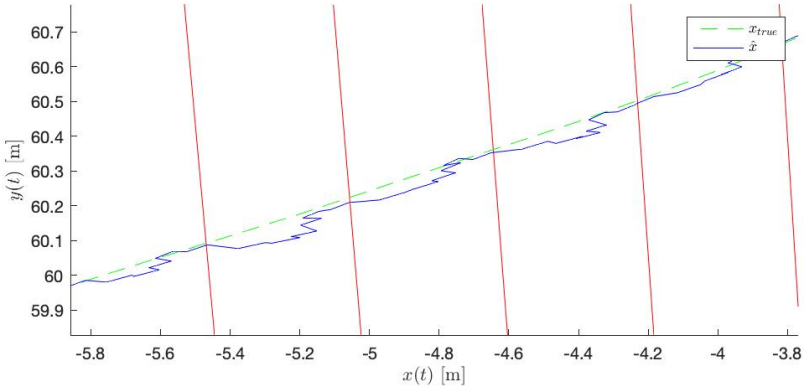

Figure 2.6: Closer view of example of trajectories from Figure 2.5

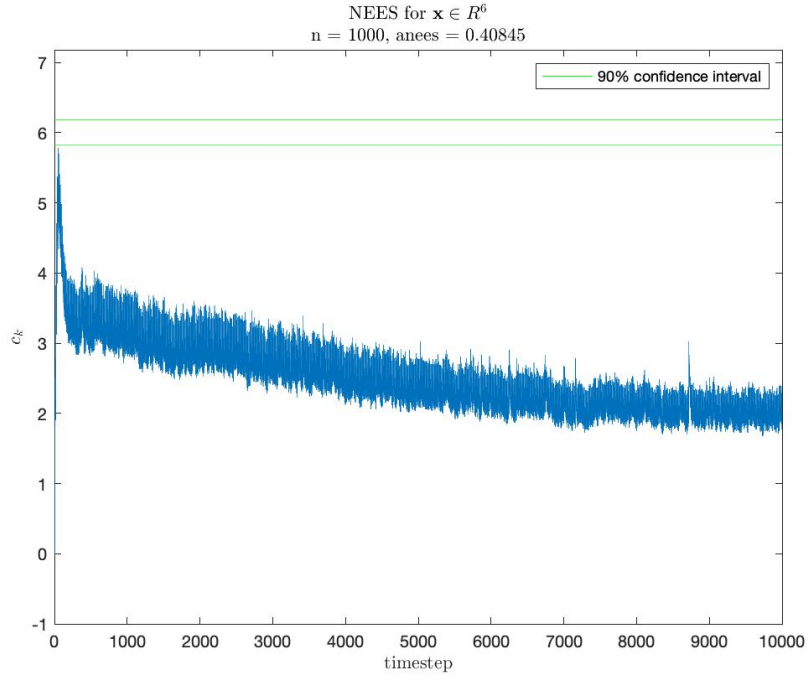

Figure 2.7: Consistency analysis

filter's performance. For a state variable x the RMSE at time step k is given by

$$\text{RMSE}_k = \sqrt{\frac{1}{M}\sum_{n=1}^{M}(\hat{x}_k^n - x_k^n)^2}, \tag{2.25}$$

where M is total number of simulations. The time averaged RMSE for the different state variables are presented in Table 2.2.

Table 2.2: Time averaged RMSE

Variable	Value	Unit
x	0.0570	m
y	0.0577	m
u	0.1210	m/s
v	0.1160	m/s
ϕ	0.0925	rad
l	0.0022	m

2.5 Real Data test

The filter was also tested on real lidar data collected with a Velodyne VLP16 lidar with specifications as seen in Table 2.3. The available data originated from an experiment where the lidar was positioned on a quay a small distance above the waterline, the setup and environment around the lidar is shown in Figure 2.8. The beams going parallel to the water was thus placed too high to detect the kayak. It was therefore decided to project the 3D measurements down to the 2D plane. Measurements from stationary objects was also filtered out before being sent to the filter.

Table 2.3: Specifications of the Velodyne VLP16 lidar sensor used for data collection.

Parameter	Value
Horizontal FOV	360°
Horizontal resolution	0.2°
Vertical FOV	+ 15.0° to -15.0°
Vertical resolution	2.0°

The results from running the filter on real data is shown in Figure 2.9. While the results seem promising, the sensor model used during simulations may be too simple as it does not include the possibility of the kayak being located between two of the vertical beam layers, i.e. that no beams will hit the kayak. This can be handled using for instance location dependent detection probability or more advanced sensor models while still preserving the essence of the model employed in this work.

Figure 2.8: Lidar setup for data collection.

2.6 Chapter Summary

This chapter has presented a direct approach for EOT using lidar measurements. The returns from each laser beam is processed directly in an EKF where data association is resolved using PDAF inspired techniques along with a RANSAC based method for hypothesis generation. We have shown that the suggested method is able to track a kayak through simulations and preliminary results for real data is also promising. Further work includes the evaluation of alternative methods such as the sample-based particle filter as a replacement for the EKF updates and the inclusion of other target models to account for non-stick shaped objects.

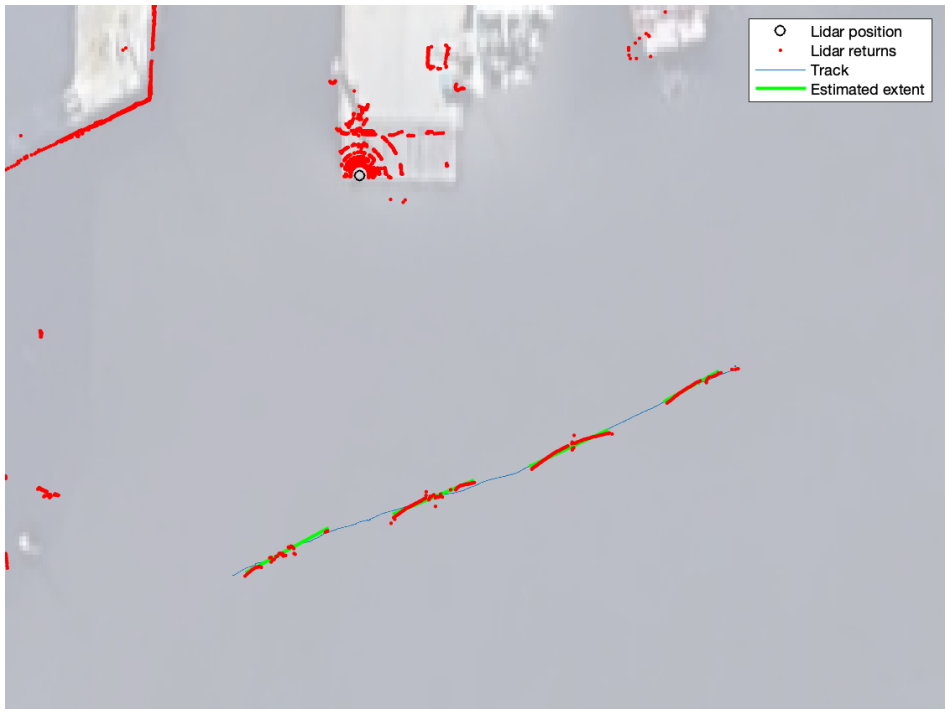

Figure 2.9: Snapshot of estimated target and received measurements along with estimated target trajectory.

Part II

Collision Avoidance

Chapter 3

Scenario-based Model Predictive Control in Marine Collision Avoidance

This chapter is based on:

[32] Inger Berge Hagen, D. Kwame Minde Kufoalor, Edmund Førland Brekke, and Tor Arne Johansen. MPC-based Collision Avoidance Strategy for Existing Marine Vessel Guidance Systems. In *IEEE International Conference on Robotics and Automation*, Brisbane, QLD, 2018.

3.1 Introduction

The existing matured technology platforms on marine vessels form an essential part of the emerging autonomous surface vehicles (ASVs). Such platforms include mission planning systems, guidance, navigation and control systems, which have several advanced capabilities such as path and trajectory tracking, dynamic weather routing, dynamic positioning (see e.g. [19]).

Important aspects of ASVs that are still at early development stages are automatic obstacle tracking and collision avoidance . The collision avoidance aspect requires the capability to make safe and reliable decisions in hazardous situations, and its success may depend immensely on how well the collision avoidance strategy incorporates the relevant components and functionalities mentioned above.

Much research has been done in the field of collision avoidance and a number of different approaches for solving this type of problems have emerged. Methods especially relevant for comparison are in this case velocity obstacle (VO) [57] and dynamic window (DW) [16], [20]. Other strategies include set-based methods [65], potential fields [51] and inevitable collision states (ICS) [62]. With many methods there is a limitation to the extent to which the dynamics of the ASV and the effect of other essential components can be incorporated into collision avoidance algorithms. The use of Model Predictive Control (MPC) allows the possibility to explicitly include models of relevant components that influences the ASV's dynamics [49]. Within this framework it is also possible to include models of the obstacles' motion,

the evolution of the dynamic environment, and different operational constraints. This introduces a design flexibility (and possibly performance gains) superior to other approaches explored in the collision avoidance literature.

A considerable amount of literature has been published on the use of MPC for collision avoidance within a range of fields: ground vehicles [50, 58, 101], aircrafts [56] and underwater vehicles [9]. Recently it has also been employed in the case of marine crafts [15, 30, 49]. MPC is a general and powerful method that can compute optimal trajectories and employ nonlinear vehicle models. Environmental forces are easily included, and risk, hazard and operational constraints along with mission objectives can be formalized in the cost function. However, computational complexity and convergence issues is a challenge for real time implementation. To evade these issues, one approach is to reduce the search space to a finite number of control behaviors. Optimization can then be reduced to evaluating the cost associated with each behavior and comparing these [50].

Although accurate vessel models can be used in predicting the effect of the autopilot, steering and propulsion systems within the MPC framework, it may neither be feasible nor convenient to replicate the numerous capabilities of existing advanced guidance systems in the collision avoidance algorithm. Moreover, discrepancies between the predicted and actual maneuvering commands generated by the guidance system may lead to an undesired behavior of the ASV. In an attempt to avoid these issues, this work investigates the option of excluding the underlying decision methods of the guidance system from the prediction model of the simulation-based MPC scheme proposed in [49]. We therefore look at the collision avoidance system as an extension to the guidance system where the decisions of the latter are used as desired setpoints to the MPC collision avoidance method.

In addition to this, we propose and discuss the use of transitional costs as part of the MPC objective for collision avoidance maneuvers that are in progress. The discussion is supported by results from a simulation study [30], where comparisons with the Velocity Obstacles (VO) method provide further insight into the performance and capabilities of our approach. To conclude the work and to verify the viability of our approach full scale experiments were conducted, and results from four key scenarios are presented.

3.2 Collision avoidance system architecture

The architectural components of the proposed collision avoidance system are shown in Figure 3.1. The architecture focuses on information flow between the collision avoidance system and the other components. We consider a mission planning system that generates a path in terms of a desired forward speed (u_p) and a set of waypoints (WPs) for the ASV to visit. These are the inputs to the guidance system that provides the necessary course (χ_c) and speed (u_c) commands to the autopilot in order to reach the waypoints and desired speed. The autopilot determines the steering and propulsion control commands (δ_r and δ_p, respectively). The result of the steering and propulsion system are forces and moments (τ) that determine the vessel's motion.

Due to disturbances and obstacles that may be detected along the vessel's

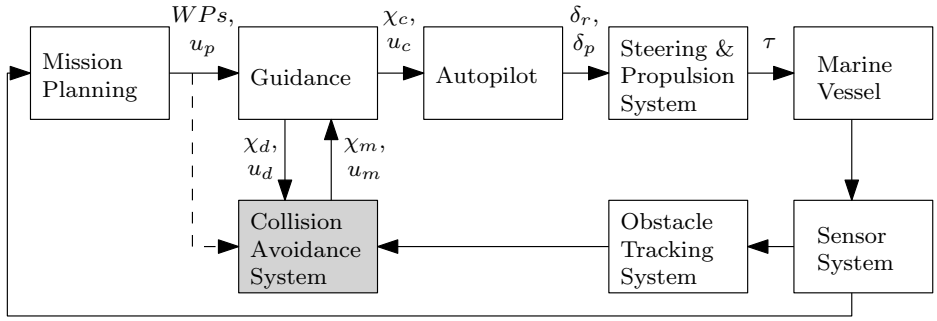

Figure 3.1: Information flow for guidance and motion control with collision avoidance (proposed architecture and parameterization).

planned path, re-planning and updates to motion control may be necessary. Such updates depend on information available from the sensor system and the capabilities of the obstacle tracking system. This chapter focuses on the collision avoidance system as an extension to the guidance system, and we propose the use of the guidance decisions (χ_d, u_d) as desired reference to the collision avoidance system. The task of the collision avoidance system is therefore to determine the amount of modification (χ_m, u_m) required in order to ensure compliance with COLREGS and thereby avoid collision.

3.3 MPC collision avoidance strategy

The MPC collision avoidance scheme presented in this thesis is based on the simulation-based control behavior selection approach of [49]. The MPC is designed according to the architecture proposed in Section 3.2. Note that the COLAV has been separated from the guidance module. This implies that the simple internal simulation model of the MPC does not include the known guidance behavior as was assumed in [49].

The main objective of the MPC is to compute modifications to the desired course (χ_d) and speed (u_d) that lead to a COLREGS-compliant ASV trajectory (cf. Figure 3.2). In this work, an obstacle's future motion is predicted as a straight-line trajectory, and we focus on a hazard minimization criterion (i.e. a cost function) that considers dynamic obstacles and COLREGS compliance. Including static obstacles is straightforward [49].

A scenario in the MPC is defined by the current state of the ASV, the trajectories of obstacles, and a control behavior candidate [49]. The set of control behaviors are chosen so that the resulting maneuvers are easily observable from other vessels (cf. COLREGS). The following set of alternative control behaviors are evaluated and assumed to be fixed on the prediction horizon:

- Course offset in degrees (χ_m):
  -90, -75, -60, -45, -30, -15, 0, 15, 30, 45, 60, 75, 90.
- Speed factor (u_m): 1, 0.5, 0
  i.e. 'keep speed', 'slow down', 'stop'

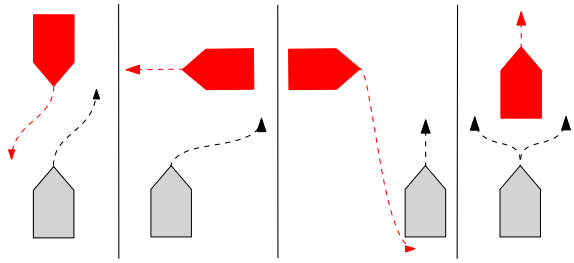

Figure 3.2: Main COLREGS scenarios and correct vessel behavior. The ASV is marked in gray and obstacle vessel in red. From left: head-on, crossing from starboard, crossing from port, overtaking. Furthermore, any action taken to avoid collision must be significant enough to be readily apparent to other vessels (cf. COLREGS, Rule 8). For a comprehensive guide to steering and sailing rules, see [13].

The modifications are in turn applied to the desired decisions (χ_d, u_d) from the guidance system to obtain a course and speed command (i.e. $\chi_c = \chi_d + \chi_m$, and $u_c = u_d \cdot u_m$). Therefore, choosing $\chi_m = 0$ and $u_m = 1$ simply recovers the desired course χ_d and speed u_d. This parametrization leads to a total of $13 \cdot 3 = 39$ possible scenarios to be simulated and evaluated. Trajectories for the obstacles must also be predicted. The computational complexity thus depend on the number of scenarios, the number of obstacles and the chosen prediction horizon. The internal model and cost function are described next.

3.3.1 Internal simulation model

A model of the ASV is necessary to generate the trajectories to be evaluated by the cost function. The limited computational resources of the target platform in our experiments require a much simpler model than the 3-degrees of freedom model used in [49]. In the experiments the ASV is only expected to perform long-range, deliberate maneuvers, this along with its relatively fast dynamics, makes the time the ASV needs to change its course/speed negligible. We therefore argue that a sufficiently accurate trajectory can be achieved using only the kinematic equation

$$\dot{\eta} = R(\chi)\upsilon, \tag{3.1}$$

where $\eta = (x, y, \chi)$ denotes the position and course in the earth-fixed frame, $\upsilon = (\upsilon_x, \upsilon_y, r)$ denotes the velocities in surge, sway, and yaw, decomposed in the body-fixed frame, and $R(\chi)$ is the rotation matrix from body-fixed to earth-fixed frame. The prediction of the ASV's trajectory is made by inserting the desired values from scenario k into the equation (3.1), ie. $\upsilon = (\upsilon_x = u_d \cdot u_m^k, \upsilon_y = 0, r = 0)$ and $R(\chi = \chi_d + \chi_m^k)$. This model implies an instant turn and it also assumes no drift due to wind and ocean current. This is clearly a very simplified model but its applicability for our experiments is confirmed by [30], where both the kinematic equation (3.1) and the full 3-DOF model were tested, producing only minor differences in the simulation results.

3.3.2 Cost function components

The cost function specifies the hazard evaluation criterion used in the collision avoidance strategy. We adopt the main components proposed in [49]. Specifically,

- a cost associated with collision with an obstacle,
- a cost for violating COLREGS,
- and a cost for the choice of maneuvering effort.

In addition, we introduce a new cost component:

- a COLREGS-transitional cost,

which penalizes control behaviors that abort a COLREGS-compliant maneuver. The new cost makes it possible to use decisions from a guidance strategy as reference to the MPC collision avoidance scheme, without including the same guidance strategy in the MPC's internal model (cf. Figure 3.1).

With the guidance strategy included in the MPC collision avoidance, as in [49], a cost penalizing the change of control behavior is sufficient to deter the abortion of COLREGS-compliant maneuvers, provided that an adequate prediction horizon has been chosen. Not including the guidance strategy in the MPC collision avoidance results in a chattering behavior appearing in overtaking and crossing scenarios, as can be seen in the simulations of [30].

The problem arises because the modification to the guidance decision is made under the assumption that the desired guidance decision is constant on the prediction horizon.

Using a LOS guidance strategy as an example, i.e. $\chi_d = \chi_{LOS}$. When a collision avoidance maneuver is initiated by a modification to the course command, the ASV will deviate from the desired path. At the next run of the MPC, χ_{LOS} points back towards the desired path. Setting $\chi_c = \chi_{LOS}$ ($\chi_m = 0$) will cause the ASV to cross the desired path and pass the obstacle on the side opposite to what was initially predicted. If this new path is collision free and COLREGS-compliant, this scenario has the lowest cost and will be chosen. This process repeats itself until another crossing would lead to a violation of the requirement of keeping well clear (cf. COLREGS, Rule 16).

Note that the complex decision process outlined above may not be straightforward to address using a simple implementation of hysteresis (see e.g. [57]) that is merely dependent on the rate at which collision avoidance decisions switch. The transitional cost systematically addresses this issue by penalizing control behaviors that will cause the ASV to pass an obstacle on a different side than what is predicted with the current control behavior. Furthermore, by ensuring that the cost of collision with an obstacle dominates the corresponding transitional cost, a change in decision that is necessary due to a high cost of collision will still be allowed.

3.3.3 Cost function details

The MPC collision avoidance objective is to evaluate the scenarios $k \in \{1, 2, \ldots, N_s\}$ for each obstacle vessel $i \in \{1, 2, \ldots, N_o\}$ at time t_0 and select the control behavior

that minimizes the cost $\mathcal{H}^k(t_0)$. Specifically,

$$k^*(t_0) = \arg\min_k \mathcal{H}^k(t_0), \tag{3.2}$$

where

$$\begin{aligned}\mathcal{H}^k(t_0) = \max_i \max_{t\in\mathcal{D}(t_0)} &\left(\mathcal{C}_i^k(t)\mathcal{R}_i^k(t) + \kappa_i \mathcal{M}_i^k(t) + \lambda_i \mathcal{T}_i^k(t)\right) \\ &+ f(u_m^k, \chi_m^k)\end{aligned} \tag{3.3}$$

The terms of the above cost function will now be defined. For the following, the definitions are as proposed in [49]:

- the cost associated with collision with obstacle i at time t in scenario k, i.e. $\mathcal{C}_i^k(t)$, and the corresponding collision risk factor, $\mathcal{R}_i^k(t)$,
- the cost for violating COLREGS, $\kappa_i \mathcal{M}_i^k(t)$, were κ_i is a tuning parameter,
- and the cost of maneuvering effort associated with scenario k, i.e. $f(u_m^k, \chi_m^k)$.

Each scenario is evaluated at discrete sample times along the horizon T using the discretization interval T_s, i.e. $\mathcal{D}(t_0) = \{t_0, t_0 + T_s, \ldots, t_0 + T\}$. The costs at a given time t are calculated based on the position, speed and course of the ASV and the obstacles at time t, obtained from the simulations of their respective trajectories (cf. Section 3.3.1).

The COLREGS-transitional cost $\lambda_i \mathcal{T}_i^k(t)$ is formulated using the binary indicator $\mathcal{T}_i^k \in \{0,\ 1\}$ and weight λ_i, which is a tuning parameter. The indicator value is specified using

$$\mathcal{T}_i^k(t) = O_i^k(t) \vee Q_i^k(t) \vee X_i^k(t), \tag{3.4}$$

where the binary indicators $O_i^k(t) = 1$, $Q_i^k(t) = 1$ and $X_i^k(t) = 1$ indicate the type of situation at time t, (the ASV is overtaking a vessel, the ASV is being overtaken and a crossing situation, respectively) and that the control behavior of scenario k will at time t cause the vessels to pass each other on the side opposite to what is predicted with the current control behavior. The following paragraphs define the indicator for each situation type.

Overtaking

If the ASV is currently overtaking obstacle i, a control behavior in scenario k at a future time t is associated with a transitional cost if the predicted location of obstacle i at time t is not on the same side of the ASV as observed at the current time t_0. That is, for $t \in \{t_0 + T_s, \ldots, t_0 + T\}$,

$$O_i^k(t) = \begin{cases} O_i(t_0) \wedge S_i^k(t) & \text{if } \neg S_i(t_0) \\ O_i(t_0) \wedge \neg S_i^k(t) & \text{if } S_i(t_0) \end{cases} \tag{3.5}$$

where $S_i(t_0) = 1$ indicates that obstacle i is currently on the ASV's starboard side, whereas $S_i^k(t) = 1$ indicates that obstacle i appears on the ASV's starboard side at the future time t in scenario k. The ASV is currently overtaking obstacle i, i.e. $O_i(t_0) = 1$, if the obstacle is considered *close, ahead*, and traveling at a *lower speed*.

If the obstacle's speed $|\vec{v}_i(t_0)|$ is not close to zero, the following condition must also hold:

$$\vec{v}(t_0) \cdot \vec{v}_i(t_0) > \cos(\phi_{ot})|\vec{v}(t_0)||\vec{v}_i(t_0)|, \tag{3.6}$$

where ϕ_{ot} is a suitable angle according to COLREGS, $\vec{v}(t_0)$ is the current velocity of the ASV, and $\vec{v}_i(t_0)$ is the current velocity of obstacle i. In the situation where the ASV is being overtaken by the obstacle, the binary indicators defined above are appropriately adapted from the perspective of the obstacle.

Crossing

If obstacle i is currently crossing the path of the ASV from starboard side, a COLREGS-compliant maneuver to starboard should result in the obstacle appearing on port side when the crossing situation is over. Therefore, an alternative control behavior in scenario k at a future time t is associated with a transitional cost if the obstacle is on starboard side at time t and the control behavior suggests a change in maneuver to port side. That is, for $t = t_0 + T_s, \ldots, t_0 + T$,

$$X_i^k(t) = X_i(t_0) \wedge S_i(t_0) \wedge S_i^k(t) \wedge \text{turn to port}. \tag{3.7}$$

The ASV is said to be currently in a crossing situation with obstacle i if the obstacle is *ahead* and

$$\vec{v}(t_0) \cdot \vec{v}_i(t_0) < \cos(\phi_{cr})|\vec{v}(t_0)||\vec{v}_i(t_0)| \wedge \neg O_i(t_0) \wedge \neg Q_i(t_0), \tag{3.8}$$

where ϕ_{cr} is a suitable angle according to COLREGS.

3.4 Experiments

3.4.1 Test setup and objectives

Experiments were performed in the Trondheimsfjord to test the performance of the proposed MPC collision avoidance scheme in realistic situations where deliberate COLREGS-compliant maneuvers are expected, more than 1 nautical mile away from a dynamic obstacle.

The ASV used is Maritime Robotics' Polar Circle 845 Sport vessel called Telemetron (Figure 3.3). Telemetron is a relatively small Rigid Bouyancy Boat (RBB) with a V-shaped hull, making it both stable and highly maneuverable. We used the Trondheim Port Authority's Munkholmen II tugboat as the obstacle vessel. Some technical specifications of the vessels are provided in Table 3.1.

The MPC collision avoidance scheme was implemented in C++ and installed on the embedded computer of the Telemetron vessel. In addition, the interface between the collision avoidance system and the existing systems was implemented according to the proposed architecture shown in Figure 3.1. We used the Automatic Identification System (AIS) as the sensor for tracking the motion of the obstacle vessel. The accuracy of AIS depends on the GPS system of the target vessel and is not a tool for precision navigation. It is however sufficient for our purposes.

Figure 3.3: The Polar Circle 845 Sport vessel Telemetron.

Table 3.1: Vessel specifications

Parameter	**Telemetron** (ASV)	**Munkholmen II** (obstacle)	Unit
Length	8.0	14.0	m
Width	3.0	6.0	m
Weight	~ 2000	–	kg
Power	225	520	hp
Max. speed	~ 34	~ 10	kn

Both the guidance system and the MPC collision avoidance extension installed on the ASV were run at a rate of 0.5Hz. However, since the AIS data received is updated at least once in 10 s, a linear prediction is used until new information about the obstacle is received. Moreover, the predicted position of the obstacle vessel is considered *close* to that of the ASV when it is 1000 m away, the safety distance used in computing the collision risk factor $\mathcal{R}_i^k$ (defined in [49]) was 200 m, and the prediction horizon T was set to 400 s, with $T_s = 5$ s discretization interval.

The experiments were performed in weather conditions that introduced significant disturbances into the dynamics of the ASV. Although no measurements of the weather condition were available during the experiments, updated weather forecast close to the time of the experiments reflect the conditions experienced: wind speeds up to 15 m/s, wave height of about 1 m, and up to 0.5 m/s currents.

3.4.2 Results

The results from different collision avoidance scenarios are shown in Figure 3.5–3.8. The figures show snap shots of the trajectories and the main variables that describe the behavior of the ASV and the obstacle vessel. An aerial photo taken during the experiments can be seen in Figure 3.4. In Figure 3.5 the ASV is the give-way vessel, and it performs a COLREGS-compliant maneuver in order to avoid

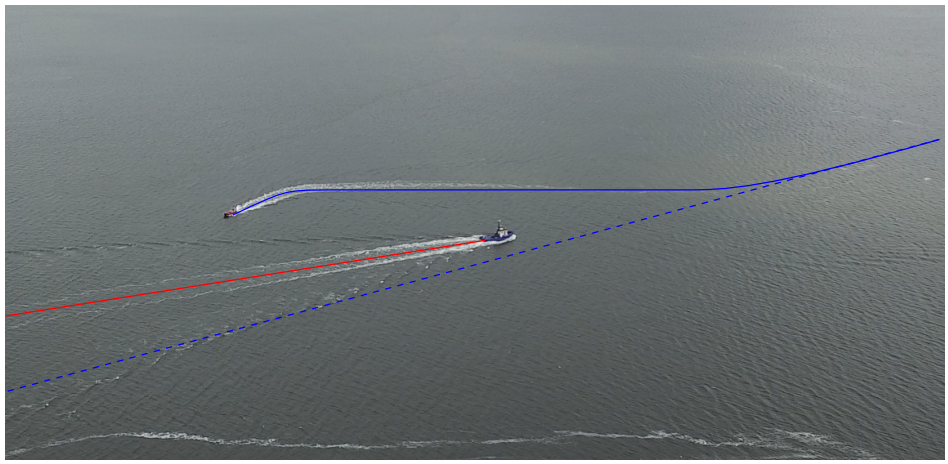

Figure 3.4: Head-on situation: Planned path of ASV (- -) and actual trajectories of ASV (—) and obstacle vessel (—).

collision. A clear deviation from the desired course from the guidance system can be seen in Figure 3.5b. The next results represent cases where both the ASV and the obstacle vessel are expected to perform COLREGS-compliant maneuvers in order to avoid collision. We examine the ASV's behavior in the case where the obstacle vessel 'stays on' (Figure 3.6) and in cases where the obstacle vessel either performs a COLREGS-compliant maneuver (Figure 3.7) or makes the situation worse through a more dangerous maneuver (Figure 3.8).

The snap shots in Figure 3.8a reveal an important property of the MPC collision avoidance method. That is, the capability to abort a COLREGS-compliant maneuver when a drastic change in situation is detected. Moreover, the collision avoidance scheme does not prevent the ASV from making necessary reactive maneuvers to its port side when in a close range situation as observed in the second snap shot of Figure 3.8a and the corresponding course modification in Figure 3.8b (between samples 220 and 280). Although the control behavior parameterization and tuning prioritize course modification, the speed is reduced in critical situations (cf. Figure 3.8b). Although the environmental disturbances are not explicitly accounted for in the collision avoidance implementation, the results confirm the viability of the SBMPC method. An important observation is that an acceptable level of robustness to disturbances is achieved due to the choice of parameterization of alternative control behaviors (χ_m, u_m) and the cost function components (see Section 3.3) that ensure that the control behavior remains unchanged unless an alternative behavior provides a significant reduction in the collision hazard.

Considering the weight and design of the ASV, the weather conditions also introduce significant uncertainty into the guidance system. Although the obstacle vessel is much heavier, it is less maneuverable at low speeds and therefore not always successful in keeping a steady course. Consequently, the experiments provide results for scenarios where the collision avoidance system's capability of predicting the obstacle's future trajectory is uncertain. The results suggest that a more

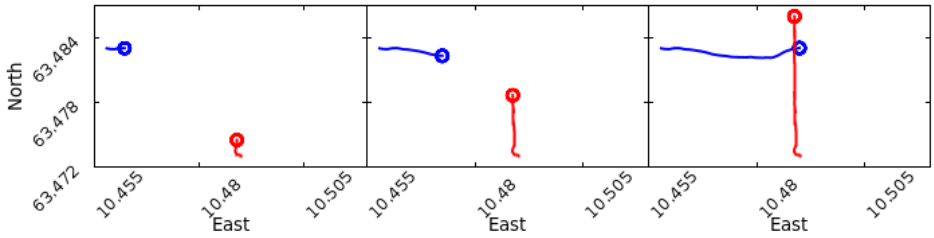

a Trajectories of the ASV (—) and the obstacle vessel (—)

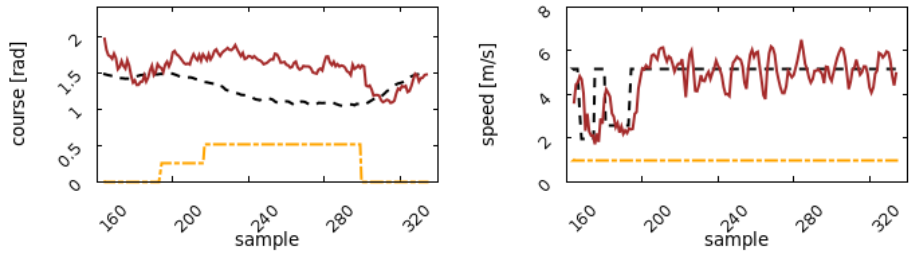

b Desired value from guidance (- -), collision avoidance modification (—·), and measured value (—)

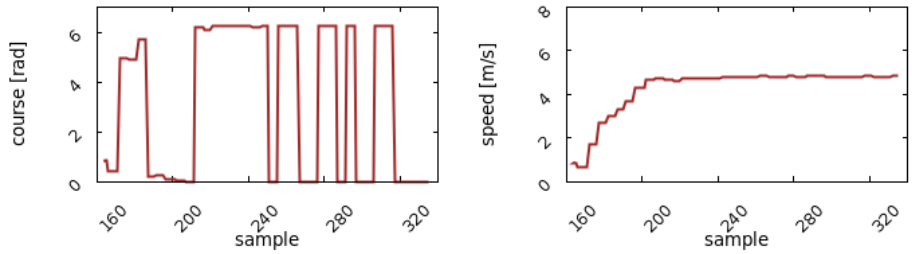

c Obstacle course and speed values from AIS

Figure 3.5: Obstacle vessel crossing from starboard.

careful tuning of the cost function weights is needed to avoid spikes in the collision avoidance modifications, see Figure 3.6b, 3.7b and 3.8b.

3.5 Chapter Summary

This chapter has presented a collision avoidance system capable of avoiding dynamic obstacles in a COLREGS-compliant manner while following a predefined path. The suggested collision avoidance system does not include a model of the ASV's guidance system and can easily be implemented in already existing guidance and control architectures, without the need for further knowledge of the guidance system's behavior. This also makes it possible to switch between different guidance strategies while the collision avoidance is running. The model of the ASV dynamics used in the experiments was a generic kinematic model.

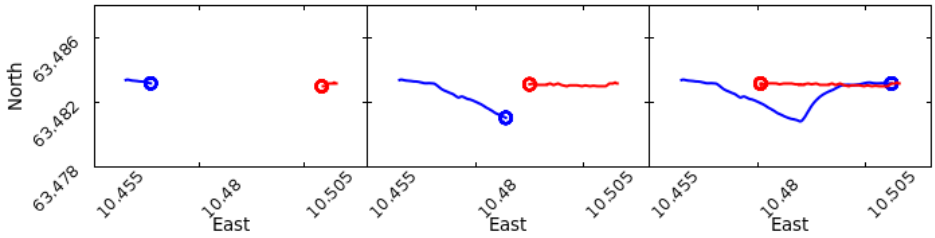

a Trajectories of the ASV (—) and the obstacle vessel (—)

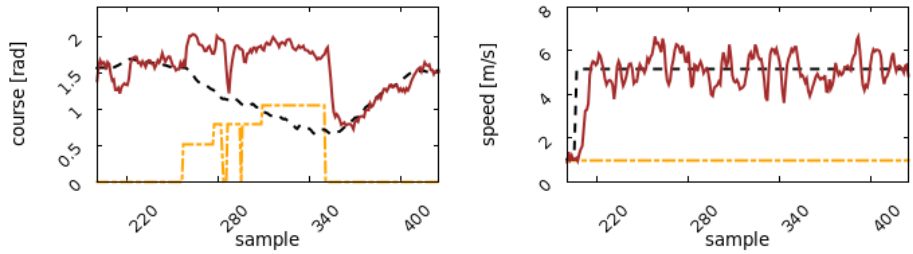

b Desired value from guidance (- -), collision avoidance modification (—·)

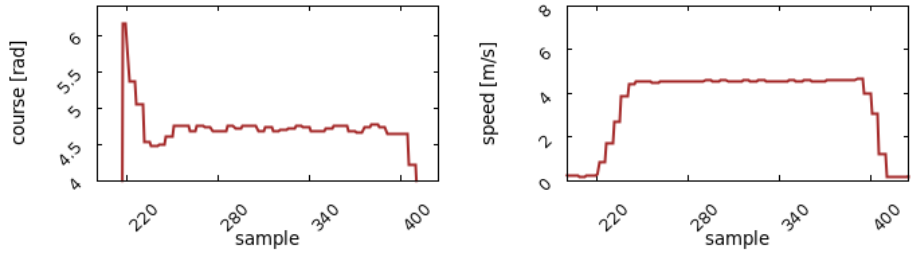

c Obstacle course and speed values from AIS

Figure 3.6: Obstacle vessel approaching head-on.The ASV performs a COLREGS compliant avoidance maneuver, before returning to its planned path.

A transitional cost was proposed to increase the incentive to continue an already started COLREGS maneuver and alleviate the oscillating behavior displayed in overtaking and crossing situations. The tests also showed that, when drastic changes in the situation are detected, it is also capable of aborting the maneuver and perform a reactive maneuver not normally sanctioned by COLREGS to avoid collision.

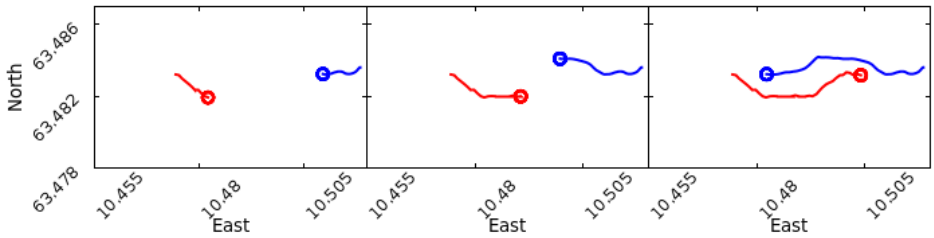

a Trajectories of the ASV (—) and the obstacle vessel (—)

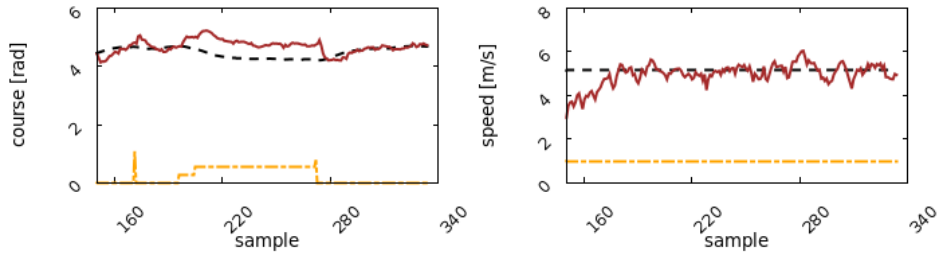

b Desired value from guidance (- -), collision avoidance modification (—·), and measured value (—)

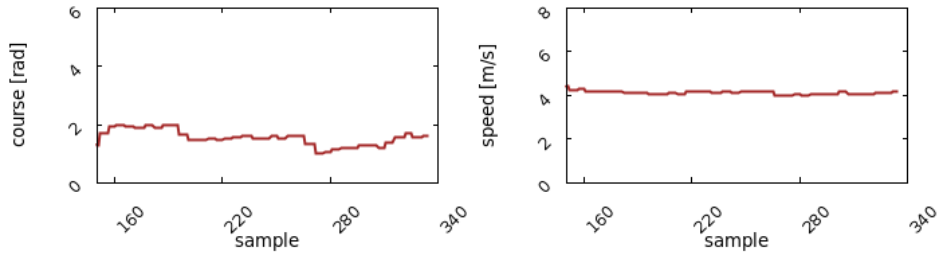

c Obstacle course and speed values from AIS

Figure 3.7: Obstacle vessel approaching head-on and turns to starboard. In this situation both vessels act according to COLREGS.

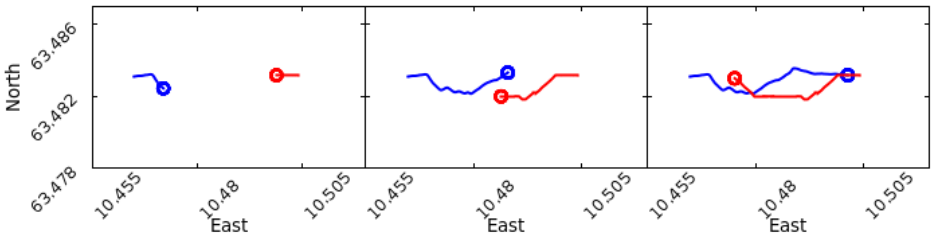

a Trajectories of the ASV (—) and the obstacle vessel (—)

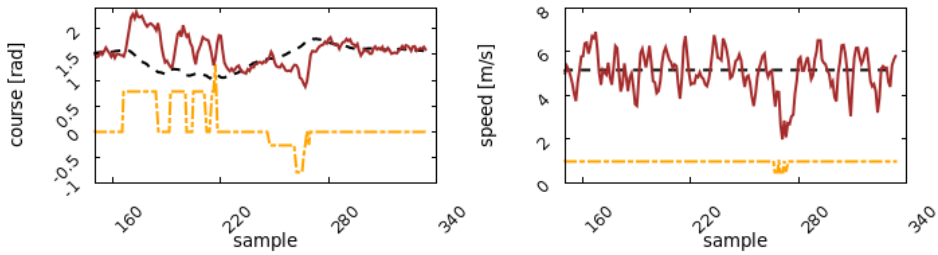

b Desired value from guidance (- -), collision avoidance modification (—·), and measured value (—)

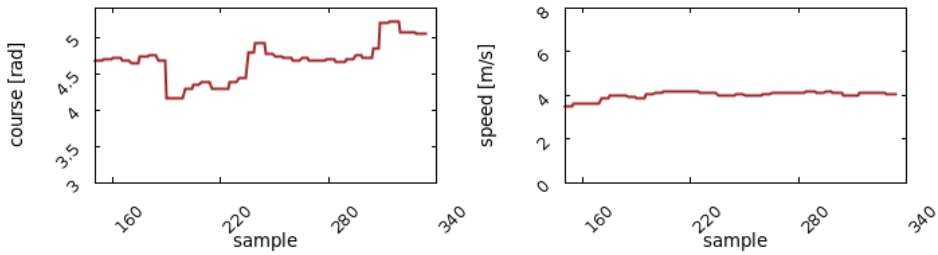

c Obstacle course and speed values from AIS

Figure 3.8: Obstacle vessel approaching head-on and turns to port, contrary to what is advised by COLREGS. The ASV then performs a necessary reactive maneuver to port.

Chapter 4

Extending the SBMPC with Additional Decision Steps

This chapter is a continuation of the work on the SBMPC method for collision avoidance, presented in the previous chapter and in [32]. The work presented here is based on the conference paper:

[34] Inger Berge Hagen, D. Kwame Minde Kufoalor, Edmund Førland Brekke, and Tor Arne Johansen. Scenario-based model predictive control with several steps for colregs compliant ship collision avoidance. In *14th IFAC Conference on Control Applications in Marine Systems, Robotics and Vehicles (CAMS)*, 2022. in press.

4.1 Introduction

Anti-collision control in compliance with the main COLREGs traffic rules at sea is essential in autonomous navigation systems that are required to realize the vision of autonomous ships. This is an active area of research, where several algorithms have been proposed in the literature. The research presented in this chapter is designed to study in more depth the so-called Scenario-Based Model Predictive Control (SBMPC) approach that was introduced in [49], and we only refer to [91] for a comprehensive review of alternative methods.

The SBMPC method considers a prediction of alternative trajectories for other ships together with a simulation-based prediction of alternative trajectories for the own ship. Scenarios are generated based on the available information about other ships behavior and the alternative control actions that can be taken by own ship, i.e. change in course or speed. By considering a finite number of scenarios, the optimal own ship control action is selected by minimizing a cost function that penalizes collision risk, COLREGs violation and deviation from the pre-planned nominal path. Optimality is evaluated on a finite time horizon into the future, where the length of this horizon corresponds to a typical encounter between ships, e.g. 10 minutes. The method has been tested in field trials in [55] and [54], and several extensions have been studied, e.g. [1, 86, 87].

Although the original SBMPC paper [49] describes that the Model Predictive Control (MPC) algorithm can switch between several control policies on the horizon, e.g. different speeds or course offsets, the current implementations are limited to single-step SBMPC [32], which is motivated by test results showing that a single-step approach is sufficient to achieve COLREGs compliance and safety in typical encounters. The main reason for this is likely that the safety cost is designed with an explicit time-dependent discounting factor that means that the closest collision risks are prioritized before more distant collision risks. Since the SBMPC re-evaluates the cost periodically based on updated information, this strategy is found to be successful also in multi-ship encounters, [54, 55]. We note that so-called move-blocking strategies that lead to control input parameterizations with a lower number of decision steps are common in MPC in order to reduce computational complexity and increase robustness, [8, 22] and it is common in industrial process control with MPC that it is implemented with only a single decision step, [74].

In this chapter we study how a multi-step SBMPC compares to a single-step SBMPC. This is motivated by the following:

- Multiple decision steps provides additional degrees of freedom for the control action on the horizon, that is in general expected to improve efficiency in utilization of the available space, time, energy and resources.
- There could be complex situations, in particular multi-ship encounters and grounding hazards, where more complex maneuvers are needed and it could be important to plan more pro-actively.
- It is helpful to visualize the complete plan to the helmsman, including the explicit plan for return to the original planned path, in order to increase trust and situational awareness. With a one-stage SBMPC the implicit assumption is that other ships that are further away, and the return to original path, will be dealt with later, which may not always provide sufficient trust.

These advantages must be weighted against increased computational complexity and evaluated also in the context of robustness to uncertainty about other ships' behaviors into the future.

We will start by giving a brief overview of the SBMPC method, a more detailed account can be found in the previous chapter, and a description of the proposed modifications. Then follows an explanation of the setup used in the simulations. The chapter finishes with a presentation of the simulation results and a discussion of these.

4.2 COLREGs compliant collision avoidance

This section describes the collision avoidance methods employed in the later simulations. First, a brief overview is given of the previous work on the SBMPC method, for more details see [49] and [32], then follows a more detailed explanation of the proposed extensions.

4.2.1 SBMPC

In essence, the SBMPC method seeks to identify the minimal maneuver producing a collision-free and safe trajectory. This is done by making a prediction of the future trajectory for each obstacle, along with a prediction for the ownship's trajectory for each alternative control behavior enumerated by the index, k, given by the finite set K. Each of the ownship's trajectories is assigned a cost and the control behavior incurring the lowest cost is applied to the vessel. Identifying this control behavior is done by solving the following optimization problem at the current time, t_0:

$$k^*(t_0) = \arg\min_k \mathcal{H}^k(t_0), \tag{4.1}$$

where the cost function calculating the cost for each control behavior is defined as

$$\mathcal{H}^k(t_0) = \max_i \max_{t \in \mathcal{T}(t_0)} \mathcal{H}_i^k(t) + f(u_m^k, \chi_m^k). \tag{4.2}$$

The function f in the above equation denotes the cost of maneuvering efforts incurred by the control behavior, and is defined by modifications to course angle (χ_m^k) and speed (u_m^k), while the cost with regards to each obstacle (i) is given by

$$\mathcal{H}_i^k(t) = c_i(u_m^k, \chi_m^k, t) + \mu_i(u_m^k, \chi_m^k, t) + \tau_i(u_m^k, \chi_m^k, t). \tag{4.3}$$

The function c_i denotes the cost of collision risk, μ_i the cost for violating the COLREGs, and τ_i is a cost on transitions between situation types, e.g., a maneuver that turns an overtaking into a crossing. These three functions are time dependent and their cost is calculated based on the predicted trajectories for each element in the set $\mathcal{T}(t_0) = \{t_0, t_0+T_s, \ldots, t_0+T\}$, where T_s is the sampling period and T is the prediction horizon. Note that the function c_i includes the mentioned discounting of future events though a factor $1/(t-t_0)^p$, where $p \geq 1/2$ is an exponent. Grounding risks can also be included in a similar manner.

The cost function $\mathcal{H}^k(t_0)$ thus calculates the cost for selecting control behavior k at time t_0. The stage cost at time $t \in \mathcal{T}(t_0)$ is based on the predicted state of the ASV and each obstacle i. For the ASV, the trajectory is predicted by simulation using a 3-degrees of freedom (DOF) model:

$$\begin{aligned} \dot{\boldsymbol{\eta}} &= \boldsymbol{R}(\psi)\boldsymbol{v}, \\ \boldsymbol{M}\dot{\boldsymbol{v}} + \boldsymbol{C}(\boldsymbol{v})\boldsymbol{v} + \boldsymbol{D}(\boldsymbol{v})\boldsymbol{v} &= \boldsymbol{\tau}_u, \end{aligned} \tag{4.4}$$

where position and heading in the Earth-fixed coordinate frame is given by $\boldsymbol{\eta} = (x, y, \psi)$ and surge, sway and yaw velocities in the body-fixed frame by $\boldsymbol{v} = (v_x, v_y, r)$. In the above equation, $\boldsymbol{R}(\psi)$ represents a rotation matrix and $\boldsymbol{M}$, $\boldsymbol{C}$ and $\boldsymbol{D}$ are the mass, Coriolis and damping matrices. The force vector $\boldsymbol{\tau}_u$ is produced by the propulsion and steering system. An autopilot takes as input command values for course and speed, which for each control behavior is given by $\chi_c(t) = \chi_r(t) + \chi_m^k$ and $u_c(t) = u_r(t) \cdot u_m^k$, where χ_r and u_r are the reference values chosen to follow the pre-planned path. The time dependency of the reference and command values are due to the inclusion of a guidance strategy, which is necessary to obtain sufficient accuracy in the predictions. The method employed in this work is the line-of-sight (LOS) guidance strategy.

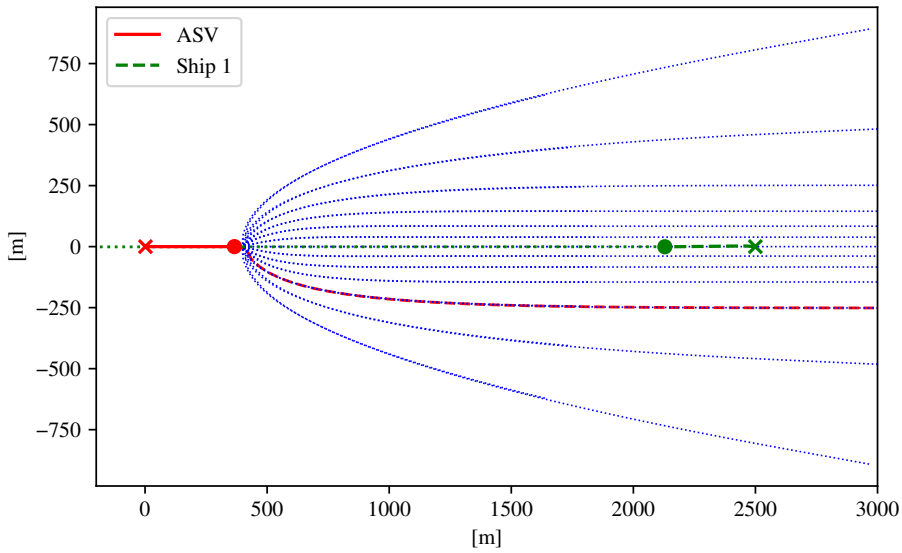

Figure 4.1: SBMPC path predictions: ASV alternative paths (···), ASV optimal path (−−) and obstacle path (···).

For each obstacle i, a kinematic model is used:

$$\dot{\boldsymbol{\eta}}_i = \boldsymbol{\eta}_i = (x_i, y_i), \ \boldsymbol{v}_i = (v_{x,i}, v_{y,i}), \tag{4.5}$$

where the position and velocity coordinates are in the Earth-fixed coordinate frame. This assumes that the obstacle will continue on a straight-line trajectory. This is suitable when the obstacle is deemed to be the stand on vessel. In cases where the obstacle is required to give way a more complex model could predict more accurately the obstacle's intended path, but this is outside the scope of this thesis.

The set K of alternative control behaviors employed is given by:

- For course: $\chi_m^k \in \{-90°, -75°, -60°, -45°, -30°, -15°, 0°, 15°, 30°, 45°, 60°, 75°, 90°\}$
- For speed: $u_m^k \in \{1, 0.5, 0\}$, which signifies 'keep speed', 'slow down' and 'stop'.

The combination of these gives $|K| = 13 \cdot 3 = 39$ alternative control behaviors. The predicted paths for these control behaviors in a head-on situation using LOS guidance is shown in Figure 4.1. The curved appearance of the paths is due to predicted changes in the course reference (χ_r) which depends on the ASV's position.

4.2.2 Multi-step SBMPC

The SBMPC algorithm contains a single decision point at the present time $t = t_0$ for the ASV's predicted paths, meaning that only one course and/or speed maneuver

is planned on the horizon. In the multi-step SBMPC, additional decision points within the prediction horizon allow for multiple planned maneuvers.

To keep the algorithm's runtime down, it is desirable to investigate whether only a limited increase in the number of possible trajectories is sufficient to improve collision avoidance behavior. The COLREGs' preference towards change of course, rather than speed, for collision avoidance maneuvers, is already reflected in the SBMPC's tuning and the investigation into possible advantages of additional decision points is therefore focused on course modifications. The following paragraphs describe the variants of the multi-step approaches that has been evaluated.

Return-to-Path Prediction

In this approach, the cost calculation for each control behavior k includes the search for a point in time where it is safe to return to the planned path. The return time is given by $t_r^* = \min \mathcal{T}_r$, where $\mathcal{T}_r = \{t | t \in \mathcal{T}(t_0), \mathcal{H}_i^k(t_r) = 0 \ \forall \ i\}$. If such a t_r^* exists for the optimal control behavior k^*, a new prediction is made for the ASV's trajectory where the control behavior k^* is applied from time step t_0 to t_r^* and $\chi_m^k = 0$ and $u_m^k = 1$ from t_r^* to T. An example of such a path can be seen in Figure 4.2. If the return does not incur any cost for collision risk or COLREGs violations, i.e. $\mathcal{H}_i^k(t) = 0 \ \forall \ t > t_r^*$, the return behavior is deemed optimal.

Note that with the current implementation and typical tuning, the maneuvering cost, $f(u_m^k, \chi_m^k)$, is at its minimum when $\chi_m^k = 0$ and $u_m^k = 1$. This means that when an obstacle is passed, and the maneuvering costs are the only concern, the ASV will return to its planned path regardless of earlier predictions. For this reason, maneuvering costs due to the return are not included in the cost of control behavior k^*

Additional Decision Points

This approach gives the possibility of further modifying the course and speed at given points on the prediction horizon. The alternative control behavior modifications are defined by the set J, the elements of which must be coherent with the alternative course modifications already defined for the decision point at t_0 in the set K. With the current implementation they must for instance be divisible by 15, i.e., the increment between the angular values in K for the predicted paths to be viable.

The position of each additional decision point is given by a sample index (s) on the prediction horizon. For a set S of indices containing $N = |S|$ additional decision points, the possible course modifications for each path is given by $\boldsymbol{\chi}_m^{k,\boldsymbol{j}} = [\chi_m^k, \ \chi_m^{j_1}, \ \ldots, \ \chi_m^{j_N}]$, where $\chi_m^{j_n} \in J$, $n = 1 \ldots N$. An example showing predicted paths for $N = 1$ additional decision points, $\chi_m^{j_n} \in \{15°, 0°, -15°\}$, $u_m^k \in [1, \ 0.5, \ 0]$ and $S = \{100\}$ is shown in Figure 4.3 and 4.4.

The increased number of decision points necessitates some changes in the optimization problem and cost function. Notably, the cost must be evaluated with regards to all obstacles for additional course changes to affect the cost. This can be achieved by replacing the maximization of obstacle cost with a sum. In addi-

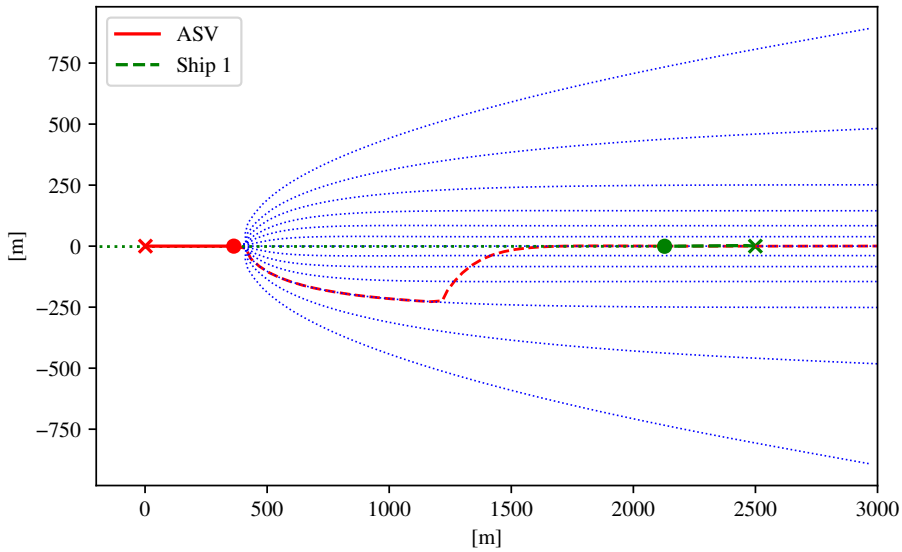

Figure 4.2: Multi-step SBMPC return-to-path predictions: ASV alternative paths (···), ASV optimal path (--) and obstacle path (···).

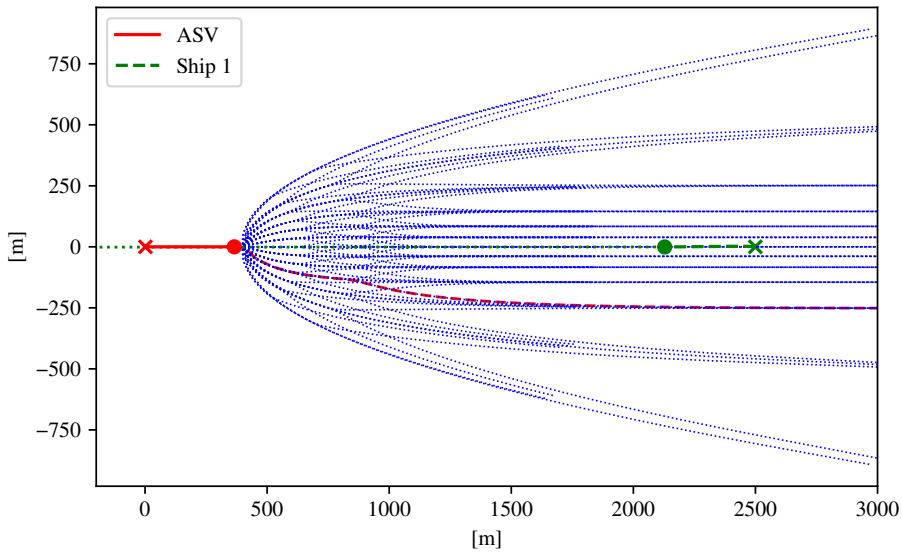

Figure 4.3: Predicted paths (···) using SBMPC with additional decision point at time index 100 with $\chi_m^{j_n} \in \{15°, 0°, -15°\}$, along with optimal path (···).

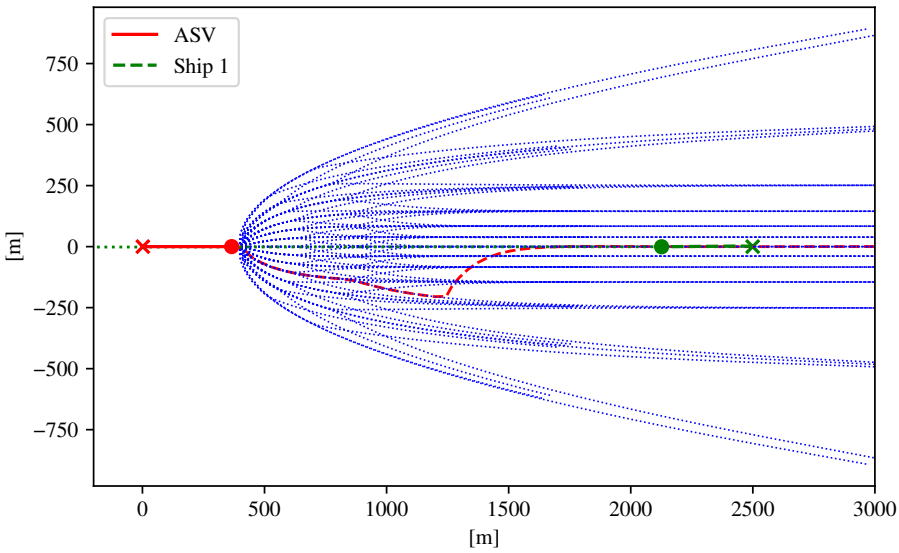

Figure 4.4: Predicted paths (···) using SBMPC with additional decision point at time index 100 with $\chi_m^{j_n} \in \{15°, 0°, -15°\}$ and return to path, along with optimal path (···).

tion, the optimization must be extended to include the maneuvering decision at all points, giving the optimization problem

$$(k^*(t_0), \boldsymbol{j}^*(t_0)) = \arg\min_{k,\boldsymbol{j}} \hat{\mathcal{H}}^{k,\boldsymbol{j}}(t_0) \tag{4.6}$$

with the modified cost function

$$\begin{aligned} \hat{\mathcal{H}}^{k,\boldsymbol{j}}(t_0) = \sum_i \max_{t \in \mathcal{T}(t_0)} \big(& c_i(u_m^k, \boldsymbol{\chi}_m^{k,\boldsymbol{j}}, t) + \mu_i(u_m^k, \boldsymbol{\chi}_m^{k,\boldsymbol{j}}, t) \\ & + \tau_i(u_m^k, \boldsymbol{\chi}_m^{k,\boldsymbol{j}}, t) \big) + f(u_m^k, \boldsymbol{\chi}_m^{k,\boldsymbol{j}}) \\ & + e(u_m^k, \boldsymbol{\chi}_m^{k,\boldsymbol{j}}). \end{aligned} \tag{4.7}$$

Note that to avoid restricting the use of decision points, no maneuvering cost is imposed on the use of these, instead the term e was added. This term gives a penalty on distance from the planned path at the prediction's endpoint, which was done to benefit decision point modifications that brings the vessel back toward it's planned path.

In the case where $\boldsymbol{j}^*$ contains maneuvers, at the next iteration of the multi-step SBMPC a path prediction is also performed with the optimal maneuvers from the previous iteration. If no other control behavior produces a lower cost, this will be considered optimal.

Table 4.1: Overview of the number (n_{cp}) and position (p_{cp}) of additional change points used in each simulation (#).

n_{cp}	#	p_{cp}				
1	1	50	100	150	200	300
2	1	50	150	100	200	–
	2	100	150	200	300	–
3	1	50	100	150	–	–
	2	100	150	200	–	–
	3	150	200	300	–	–

4.3 Simulation setup

To examine the value of the extensions described in the previous section, different scenarios were designed to demonstrate their effect. Simulations were then performed for the following variations of the SBMPC method:

1. Original SBMPC
2. SBMPC with modified cost function
3. Multi-step SBMPC (return to path)
4. Multi-step SBMPC (additional decision points)

For method 4, the number of additional decision points (n_{cp}), the points' time index on the prediction horizon (p_{cp}) and the set of alternative control behaviors (J) must be specified. Simulations were run two sets of possible modifications, $J = \{\pm 15^\circ\}$ and $J = \{\pm 30^\circ\}$, with configurations of number and positions of decision points as shown in table 4.1. We note that this limited selection is chosen since we have primarily considered head-on and overtaking scenarios, while crossing scenarios would likely benefit from a wider selection of behaviors.

4.4 Results

Results from the different modifications are presented in the following sections.

4.4.1 Cost-function modification

The modified cost function, equation (4.7), allows all obstacles to be taken into consideration when solving the optimization problem. This is an advantage in multi-vessel encounters such as the one seen in Figure 4.5, where the SBMPC is run using the modified cost function and a single decision step at $t = t_0$. In this scenario, the original formulation of the cost function, equation (4.2), will produce a chattering behavior starting with a starboard maneuver to avoid Ship 3, followed by a port maneuver to avoid Ship 1 or Ship 2, depending on which vessel incurring the highest cost. This behavior continues until the cost of moving closer to either of the obstacles is equally high and an equilibrium is reached. It is difficult to identify a tuning that completely removes this behavior and the modified cost function,

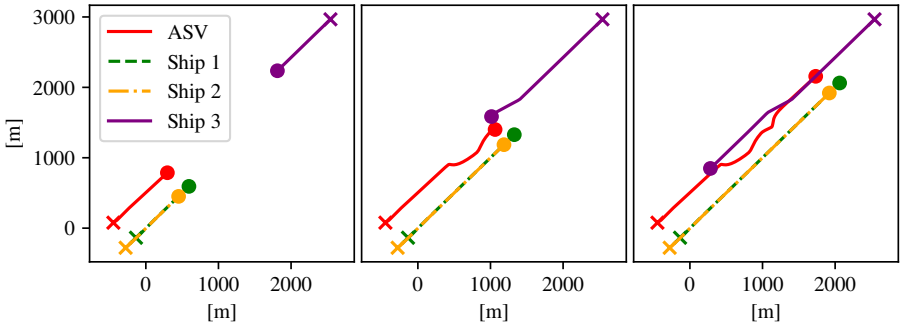

a SBMPC with modified cost function: Trajectory snap-shots. Starting position is marked with (✕).

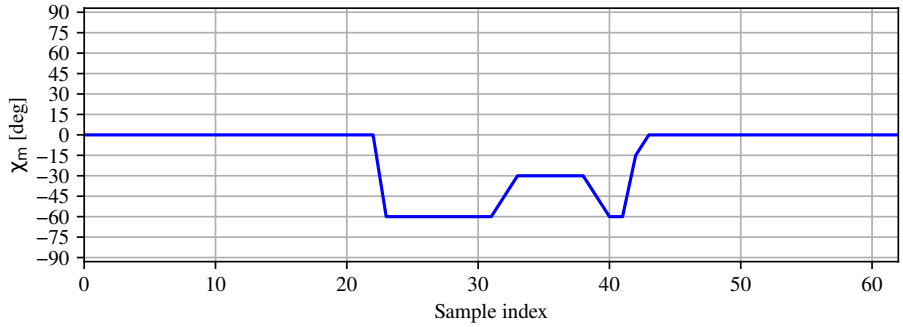

b SBMPC with modified cost function: Course modifications

Figure 4.5: Scenario demonstrating the effect of the modified cost function 4.7 in a multi-vessel encounter.

which includes the cost with regards to all vessels in the total cost for each control behavior, provides a simple solution that does not affect the behavior in encounters with only two vessels involved.

From the offsets shown in Figure 4.5b we see four distinct maneuvers. The first is intended to avoid collision with Ship 3 while maintaining a safe distance to Ship 1 and Ship 2. The second and third course modification changes are reactions to Ship 3's evasive maneuver and its subsequent return to the original course. The fourth occurs when Ship 3 is past, and allows the ASV to return to its planned path. While the second and third maneuver may seem excessive, they do demonstrate the SBMPC's ability to adjust according to the behavior of other vessels in situations with limited maneuvering space.

4.4.2 Return to path

As there is no cost for the return trajectory, this addition does not affect the solution of the optimization problem nor the resulting trajectory of the ASV. However, it

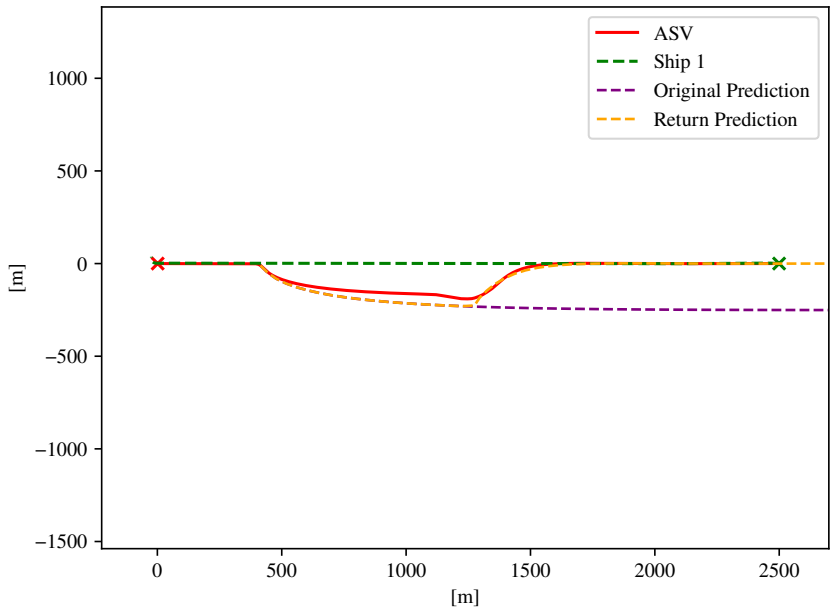

Figure 4.6: Difference between predictions with and without return to path prediction in a head-on encounter, compared to the resulting trajectory.

does provide a more accurate prediction of the trajectory, see Figure 4.6, which must be seen as a clear advantage by anyone charged with monitoring the vessel or using it for decision support.

4.4.3 Additional decision points

While several scenarios were extensively considered and tested, it did prove difficult to identify many realistic situations where the additional decision points would significantly influence the behavior of the ASV. Nevertheless, one scenario in which they were relevant is shown in Figure 4.7, where the ASV is in a head on situation with Ship 3 while traveling parallel to two other vessels, Ship 1 and Ship 2. Both for the original and modified SBMPC the situation leads to a starboard course maneuver of 60 degrees, along with a 50 % speed reduction. The simulation employing additional decision points was run with $n_{cp} = 1$ and $p_{cp} = 150$, which allows the ASV to plan to straighten it's course at an earlier point in time as seen in Fig, 4.7a. We note that the speed reductions leads to further separation of the ships, an effect that is not visualized in Figure 4.7

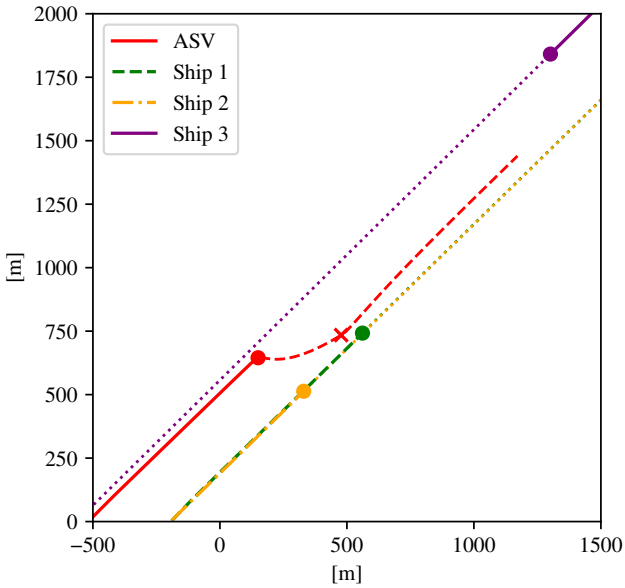

a Snapshot of SBMPC with additional decision point at prediction index 150 (×).

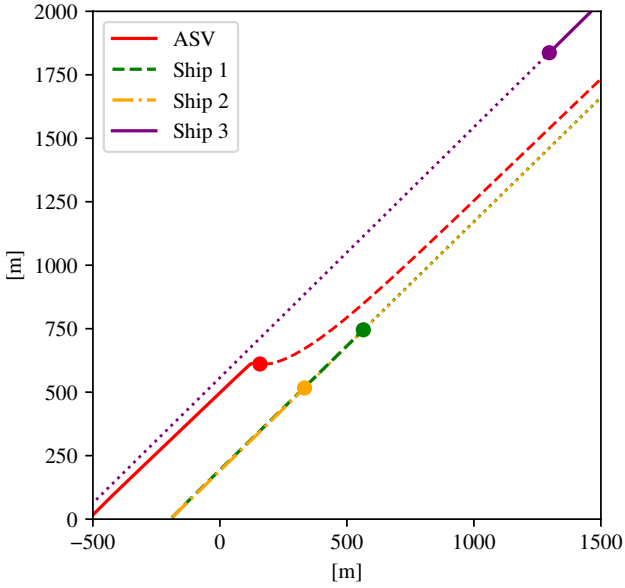

b Snapshot of original SBMPC.

Figure 4.7: Scenario demonstrating the effect of additional decision points in a multi-vessel encounter.

4.5 Discussion

Modifying the cost function to include all obstacles in the cost calculation for each trajectory is an advantage in multi-vessel encounters as it reduces course oscillations that can occur with the original cost function. The trajectory thereby becomes more predictable to other vessels involved in the encounter, an important characteristic to any collision avoidance scheme.

Including the search for a possible return to the planned path does improve the prediction's accuracy, but does not affect the resulting trajectory. However, this is a useful feature with regards to monitoring of the ASV's behavior, as it provides a more complete view of the encounter, which is important when using the method as a tool for decision support. It should be noted that in situations where the course modification is large at the point of return, e.g. 90°, the subsequent course change may appear quite abrupt if the LOS path following strategy is tuned with a short lookahead distance. While clearly fulfilling the COLREGs requirement of being readily observable to other vessels, it should be considered whether a long lookahead distance is desirable or another return strategy is more appropriate.

With regards to the additional decision points it can be argued that the difficulties in creating scenarios where course modifications were triggered, along with the relatively small effect they have on the resulting trajectories can be seen as an indication of robustness in the original SBMPC. It also highlights the problem of how to best place the decision points on the prediction horizon, as this is likely to vary between encounters and will also depend on parameter values used in the SBMPC. It therefore seems unlikely that additional decision points can significantly improve behavior without a more adaptive method for discretizing the candidate control behaviors and a notable increase in runtime. On the other hand, the introduction of multiple decision-points may still be useful in future extensions that consider coordinated collision avoidance control enabled by frequent route exchange and negotiation between vessels [1], possibly also including conflict resolution from traffic control centrals.

4.6 Chapter Summary

A modified version of the SBMPC method implemented in [32] has been presented. A simulation study where the original and modified algorithms have been run with the same tuning on different collision avoidance scenarios was performed. The sum of vessel related costs for all vessels in the modified cost function reduces chattering behavior in multi-vessel scenarios, and the prediction of a return path improves the accuracy of the predictions. The results with regards to additional decision points showed a slightly improved behavior in only very few scenarios. This indicates that the existing SBMPC is effective.

Part III

Evaluation

Chapter 5

Evaluation of Safety and COLREGs Compliance in Collision Avoidance Situations

This chapter is based on:

[36] Inger Berge Hagen, Olav Vassbotn, Morten Skogvold, Tor Arne Johansen, and Edmund Førland Brekke. Safety and COLREGS Evaluation for Marine Collision Avoidance Algorithms. *Ocean Engineering*, 2022. unpublished/under revision.

5.1 Introduction

Preventing collisions is crucial for safe navigation at sea. An important action in this regard was the 1972 adoption of the COLREGs [42] as a convention by the IMO, providing a set of rules regulating traffic at sea. Since then, navigational aids such as the AIS, automatic radar plotting aid (ARPA) and ECDIS have become commonplace, further assisting vessels navigate increasingly congested waterways. However, a report by European Maritime Safety Agency (EMSA) [18] shows that human action remain a significant cause of casualties or incidents at sea, with 54% of analyzed accident events being attributed to human action. Over the period 2014-2019, a total of 13204 incidents with a ship were reported, out of which 44% were classified as navigational, i.e., collision, contact and grounding or stranding. Reducing these numbers by increasing the autonomy level of marine vessels is one of the main objectives for research into collision avoidance methods. Removing or reducing the need for personnel onboard could also have the additional gain of reducing the human consequences of marine accidents which, according to the same report [18], amounted to 496 fatalities and 6210 persons injured within the same period.

However, a major problem facing anyone who wish to implement a COLREGs compliant collision avoidance algorithm is the rules' intentional vagueness with regards to the prescribed actions in vessel encounters. The rules were developed for manned vessels and leave room for interpretation and the use of judgment, as

seen in this example from Rule 8(a): "Any action to avoid collision shall be ... made in ample time and with due regard to the observance of good seamanship." Work on how to regulate the behavior of autonomous vessels is underway and the IMO recently announced the completion of a scoping exercise [46] analyzing its ship safety treaties in this regard. Still, the outcome of the exercise [61] underlines that the COLREGs should remain the reference point and that as much as possible of its current content should be retained. This conclusion provides a rationale for further research into methods that seek to include the COLREGs.

A considerable amount of literature has been published on the topic of marine collision avoidance and several review articles are available, giving an overview of the development over the years. While some articles, such as [83, 85], treat the subject as a means for supporting human operators, others, for instance [10, 59, 71] see it as a component in the development of ASVs. This distinction was remarked upon in [41] which seeks to find common grounds where research advances with regards to one objective could benefit the other. The methods considered are compared in terms of motion prediction, conflict detection and resolution and their strengths and weaknesses highlighted. A more recent review paper [92], that also views collision avoidance in the ASV perspective, focus on clarifying terminology, analyze existing regulatory framework and suggest a classification scheme for path-planning[1] algorithms. The work is supported by the accompanying paper [91] where 45 collision avoidance algorithms were compared based on eight properties from the literature. While such reviews give an overview over methods, trends and developments within collision avoidance research, it is remarked in [91] that when comparing algorithms "the comparison of the considered properties only gives a partial understanding of the performance".

The trajectories produced by collision avoidance algorithms can be evaluated in terms of different properties such as time, length, smoothness, energy consumption and safety. Many algorithms also claim compliance with the COLREGs, but as noted in [91], exactly what this entails varies. Although it should be assumed that when discussing collision avoidance algorithms exclusively, rather than autonomous vessels as a whole, compliance only relates to rules concerning steering and navigation as opposed to the complete rule set. It therefore seems pertinent to identify methods for evaluating vessel behavior in terms of COLREGs-compliance. Based on the conclusions of [91] an evaluation simulator platform using multi-objective optimization (MOO) was proposed in [90], assessing performance in terms of path fitness and safety. While COLREGs-compliance and seamanship is not yet included in the evaluation, it is clear that it is considered by the author as a crucial point for further research.

One example where evaluation of COLREGs compliance was attempted is [72], where a neural network was employed to create scenarios likely to challenge the collision avoidance algorithms being tested. While scenario generation is the main focus, the metrics used to measure the difficulty levels of the generated scenario, namely the risk of collision and the degree of COLREGs noncompliance give an impression of the performance of the algorithms. The degree of compliance is given as the percentage of simulation steps where the vessel is behaving in accordance

[1] The article labels collision avoidance as local (reactive) path-planning.

with the COLREGs. For a single simulation step, lack of compliance is defined as a give-way vessel in a crossing or head on situation not making a starboard maneuver, or as a stand-on vessel in a crossing situation making a starboard maneuver. The importance of scenario selection was also brought forward in [89], which proposes a methodology for automatic simulation-based testing of ASVs using a Gaussian process (GP) model to guide the scenario selection. The method is demonstrated by two case studies, where requirements for safety, mission compliance and COLREGs compliance for give-way vessels are formulated in the formal specification language signal temporal logic (STL).

While the evaluation of COLREGs compliance is limited in the above mentioned works, it was the main topic of a thesis by Woerner [96], which presents an exhaustive method for objective evaluation of COLREGs compliance. The method was included in the proposition of a test framework for ASVs in [98], and further developed in [97] and [99]. The assessment method is based on trajectory data and can be performed either in real time or post mission. A score is assigned to each vessel based on a set of metrics that evaluate the degree of safety and COLREGs compliance in an encounter, notably with regards to Rules 8 and 13-17. Its ability to detect violations of these is validated in the thesis by statistics from an extensive simulation study along with a survey of how well self-identified ship masters agree with the algorithm's rule and blame assignment in near-miss or collision scenarios. The metrics have since served as an inspiration for the evaluation methods in [38, 53, 64, 82] and [69]. It was also suggested in [90] that they may be used as a basis for further extension of the evaluation simulator platform.

The fact that the COLREGs were written for human operators and are vague enough to allow for the use of common sense is reflected in Woerner's works by the number of parameters that are left to be decided by the evaluator. The values may depend on for instance the type of encounter or present environmental conditions. This leads to the question of what value these parameters should take on for the evaluation algorithm's scores to conform with the human notion of good seamanship as prescribed by the COLREGs. To get some insight into how the COLREGs is practiced at sea and how that translates into the parameters of the evaluation algorithm this chapter presents two case studies based on AIS-data collected from vessels in normal operation.

The purpose of this chapter is to provide a comprehensive system for the evaluation of vessel behavior with regards to compliance with COLREGs Rule 8a, 8b and 13-17. The algorithm presented in the following sections is founded on the method developed by Woerner, presented in [99] and [96], and includes several improvements of the evaluation algorithm itself along with a detailed description of the complete evaluation process. This also covers implementation details that were omitted in the presentation of Woerner's method.

It is desirable to test the algorithm's performance on realistic encounters to shed light on whether the scores reflect human interpretation of the COLREGs. To highlight the connection between vessel behavior and the resulting scores, several scenarios have been evaluated and are presented along with their corresponding scores and the parameter values used in the evaluation.

In short the main contributions of this chapter are: a) providing an algorithm for maneuver detection, b) mathematical expressions for all the metrics employed,

c) tentative values for parameters and weights used in the calculations, and d) results showing trajectories along with the resulting scores and penalties from both simulated and real life encounters. The overreaching objective being to provide a tool for the development of COLREGs compliant collision avoidance (COLAV) algorithms that can also act as a starting point for a more complete performance evaluation of autonomous vessels.

The remainder of this chapter starts with a presentation of the method used for maneuver detection followed by a description of the metrics employed in the performance evaluation. Next is a complete overview of the tuning parameters of the method, this includes both a description of each parameter and the numerical value used in this work. Then follows a presentation of evaluation results for both simulated and real-life encounters. The chapter concludes with a discussion of the results and a short summary

5.2 Method

One of the first questions that must be addressed when discussing collision avoidance is how to define an encounter. A useful concept in this context is the ship domain, which is the area around a vessel that the navigator would like to keep free of other vessels or objects. Several different shapes for this area have been proposed [85]. The size of the ship domain will also vary according to factors such as the type of area where the encounter occurs, the traffic density in the area, the own ship's length and its speed. Independent of the ship domain's shape and size, action must be taken before the domain is breached if infringement is to be avoided. This leads to the definition of a larger domain that, when entered, requires the navigator to consider evasive maneuvers. Providing a detailed definition of such an area is outside the scope of this paper, instead four stages are defined such that different definitions of the ship domain can be accommodated. Stage 1 include vessels that have been detected but are at a distance that does not require any actions to be considered. In Stage 2 the type of encounter must be decided and evasive maneuvers must be considered. Stage 3 and 4 is only relevant for stand-on vessels and will be further explained in Section 5.2.5. This definition implies that an encounter occurs when two vessels enter Stage 2 range and ends when the vessels re-enter Stage 1. These instances thus define the start and end point of the trajectories that are to be evaluated. In the case of multiple encounters within the same period of time, each vessel's behavior is evaluated with regards to each of the other vessels encountered. The evaluation results in a total score which is calculated based on different scores and penalties depending on the encounter type. Scores are denoted $\mathcal{S} \in [0, 1]$ where 1 is the best score and penalties are denoted $\mathcal{P} \in [0, 1]$, where 1 is the highest penalty. The relation between a penalty and its corresponding score is such that $\mathcal{S} = 1 - \mathcal{P}$. When a score is calculated from multiple penalties, weights are used to balance their importance, these are denoted $\gamma \in [0, 1]$.

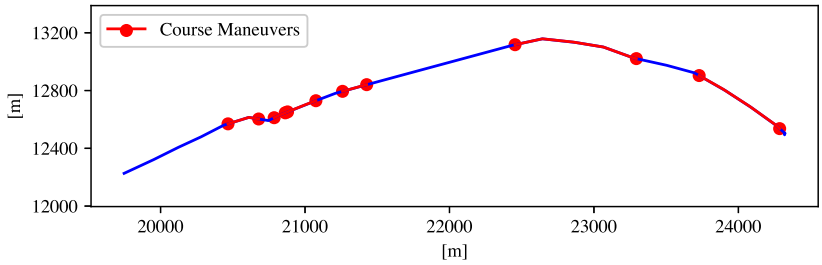

a Detected course maneuvers.

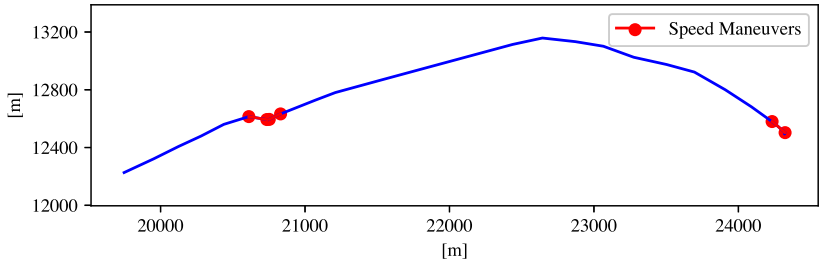

b Detected speed maneuvers.

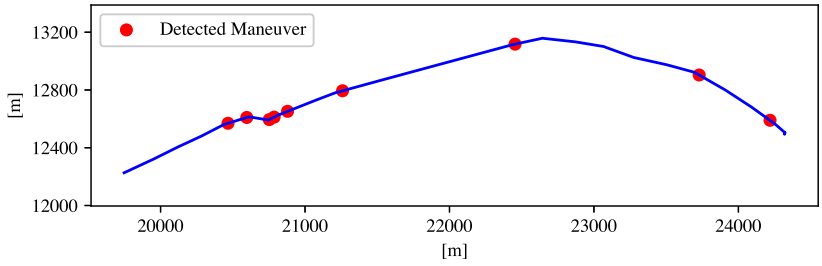

c Start point of detected maneuvers.

Figure 5.1: Example of maneuver detection in AIS data. The vessel is moving from left to right.

5.2.1 Maneuver detection

Pre-processing

The method for identifying maneuvers in vessel trajectories is identical for data produced in simulations or ship automation systems and data gathered from AIS. However, as the update frequency of AIS messages can vary both between vessels and depending on the current speed of a vessel some pre-processing is necessary before the evaluation is performed.

The simulation outputs are trajectories in the form of timestamped states in a local North-East-Down (NED) frame containing position $(x,\ y)$, speed $(u,\ v)$ and course angle (χ), from which the speed over ground (SOG) can easily be obtained. The timestamped AIS messages contains position in the form of latitude and longitude, along with course over ground (COG) and SOG. The first step in the

pre-processing is to remove any undefined (NaN) values and transform the messages into a local NED frame with positions in meters and velocities in meters per second. Constant sample frequency is then achieved by applying one-dimensional linear interpolation to each trajectory.

Detection

Maneuvers can be marked by a change in course or speed. The approach employed here to detect these changes is based on the derivatives of the course and speed. Before the derivatives are calculated, a Gaussian filter is applied to both the course angle values and the speed values to assure smoothness. The derivatives are then found by central finite difference. The maneuver detection method is illustrated by Figures 5.1, 5.2 and 5.3 which display example data gathered from AIS messages over a thirty minute period.

A course change maneuver is detected when the following conditions are fulfilled:

$$\begin{aligned} |U| &\geq \epsilon_U \\ |\dot{\chi}| &\geq \epsilon_{\dot{\chi}}. \end{aligned} \tag{5.1}$$

Meaning that the vessel must be classified as moving and the first course derivatives must be above the given thresholds, see Figure 5.2b. The maneuver lasts until $\dot{\chi} = 0$ or $|U| < \epsilon_U$. The course maneuvers detected in the example data marked on the trajectory can be seen in Figure 5.1a.

When it comes to speed changes, crossing the threshold $|U| \geq \epsilon_U$ will signify the vessel starting or stopping, see Figure 5.3a, and will thus mark either the start or end of a maneuver. If the vessel is moving, maneuver detection is triggered when acceleration exceeds the threshold $|\dot{U}| \geq \epsilon_{\dot{U}}$. The maneuver lasts until the acceleration again falls beneath the threshold or the vessel stop moving, see example in Figure. 5.3.

5.2.2 Safety score

The safety score (S_{safety}) is determined at the time of closest point of approach (CPA), i.e., when the range between vessels is at its smallest, and is calculated based on the score for pose (S_Θ) and the score for range (S_r). Woerner [99] proposes several possible expressions for this score, the formulation presented below is an alternative to these which increases the importance of the pose as the range between the vessels decreases.

$$\mathcal{S}_{safety} = \begin{cases} 0, & \mathcal{S}_r = 0 \\ 1, & \mathcal{S}_r = 1 \\ (1 - \mathcal{S}_r)\mathcal{S}_\Theta + \mathcal{S}_r, & otherwise. \end{cases} \tag{5.2}$$

The first case signifies that the vessels are at a distance small enough to be considered a collision and the vessel is awarded a zero score, independent of pose. In the second case, the range between the vessels at CPA is equal to or larger than the preferred range, and the pose is again disregarded. If the range at CPA

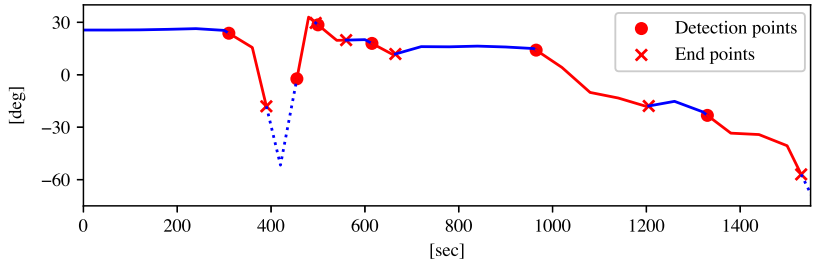

a Maneuver detection: Course.

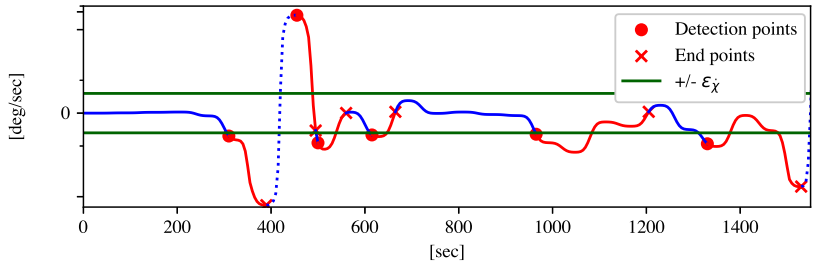

b Maneuver detection: First derivative of course.

Figure 5.2: Detection of course changes in AIS data. Sections marked in red (—) are registered as maneuvers. Dotted sections denote that the vessel is static.

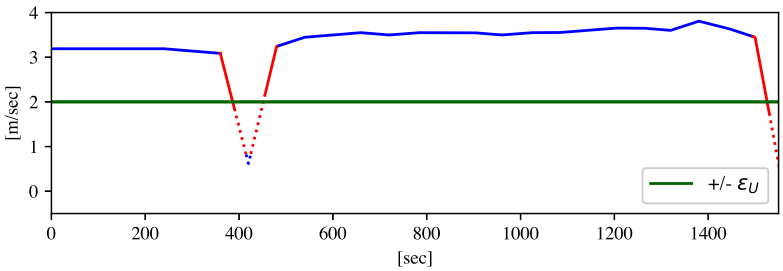

a Speed: A vessel moving slower than ϵ_U is considered static (dotted line).

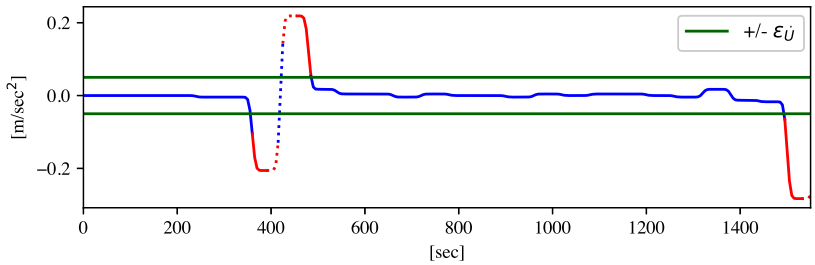

b Acceleration: Speed maneuvers are registered when the acceleration is larger than $\epsilon_{\dot{U}}$.

Figure 5.3: Detection of speed changes in AIS data. Sections marked in red (—) are registered as maneuvers. A dotted line signifies that the vessel is considered as static.

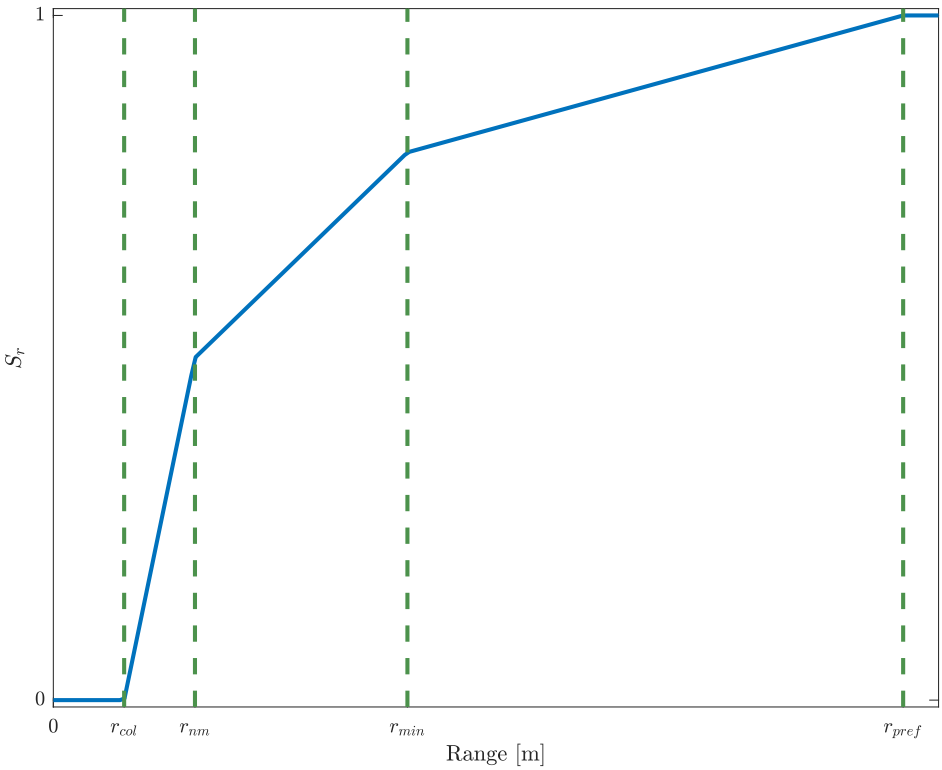

Figure 5.4: Scoring function for range, S_r, along with range parameters r_{col}, r_{nm}, r_{min} and r_{pref} (--).

is somewhere in between collision and preferred range, the score is a weighted combination of the two.

The safety score with regards to range ($\mathcal{S}_r$) is defined as a piece-wise continuous function of the range at CPA (r_{cpa}) and depends on a set of range parameters defining the preferred (r_{pref}), minimum acceptable (r_{min}), near-miss (r_{nm}) and collision (r_{col}) range. The function is given by

$$\mathcal{S}_r = \begin{cases} 1, & r_{pref} \leq r_{cpa} \\ 1 - \gamma_{min}\left(\frac{r_{pref} - r_{cpa}}{r_{pref} - r_{min}}\right), & r_{min} \leq r_{cpa} < r_{pref} \\ 1 - \gamma_{min} - \gamma_{nm}\left(\frac{r_{pref} - r_{cpa}}{r_{pref} - r_{nm}}\right), & r_{nm} \leq r_{cpa} < r_{min} \\ 1 - \gamma_{min} - \gamma_{nm} - \gamma_{col}\left(\frac{r_{nm} - r_{cpa}}{r_{nm} - r_{col}}\right), & r_{col} \leq r_{cpa} < r_{nm} \\ 0, & \text{otherwise,} \end{cases} \tag{5.3}$$

with the condition $\gamma_{min} + \gamma_{nm} + \gamma_{col} = 1$.

The safety score with regards to pose at CPA ($\mathcal{S}_\Theta$) is a weighted combination of contact angle score ($\mathcal{S}_\alpha$) and relative bearing score ($\mathcal{S}_\beta$), and is given by

$$\mathcal{S}_\Theta = \gamma_\alpha \mathcal{S}_\alpha + \gamma_\beta \mathcal{S}_\beta. \tag{5.4}$$

The weights must fulfill the condition $\gamma_\beta + \gamma_\alpha = 1$, but can be adjusted to place more importance on the own ship's pose by setting $\gamma_\beta > \gamma_\alpha$. The contact angle $\alpha \in [-180°, 180°)$, and the relative bearing $\beta \in [0°, 360°)$ are defined as the angle between course and LOS to the other vessel as seen from the obstacle and the own ship's point of view respectively. The importance of α_{cpa} and β_{cpa} with regards to the safety of a passing is illustrated by the situations shown in Figure 5.6. The calculation of $\mathcal{S}_\alpha$ and $\mathcal{S}_\beta$ is shown in Equations (5.5) and (5.6), where the values for the cut-off angles α_{cut}, β_{cut}^{min} and β_{cut}^{max} can be chosen to reward beam and stern contact, see Table 5.4. Plots of these functions can be seen in Figure 5.5.

$$\mathcal{S}_\alpha = \begin{cases} \frac{1-\cos(\alpha_{cpa})}{1-\cos(\alpha_{cut})}, & |\alpha_{cpa}| < \alpha_{cut} \\ 1, & \text{otherwise} \end{cases} \tag{5.5}$$

$$\mathcal{S}_\beta = \begin{cases} \frac{1-\cos(\beta_{cpa})}{1-\cos(\beta_{cut}^{min})}, & \beta_{cpa} < \beta_{cut}^{min} \\ \frac{1-\cos(\beta_{cpa})}{1-\cos(\beta_{cut}^{max})}, & \beta_{cpa} > \beta_{cut}^{max} \\ 1 - \cos(\beta_{cut}^{min}), & \text{otherwise} \end{cases} \tag{5.6}$$

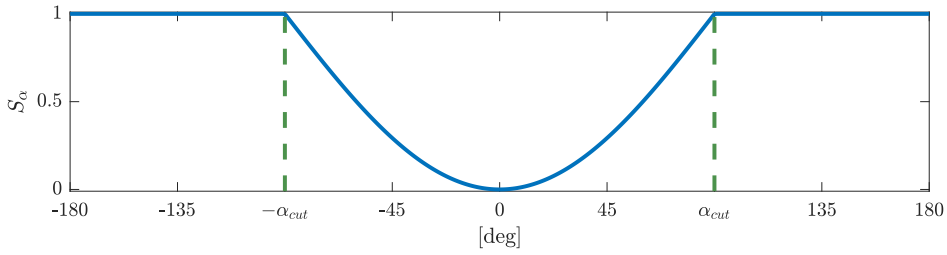

a Scoring function for contact angle at CPA, S_α.

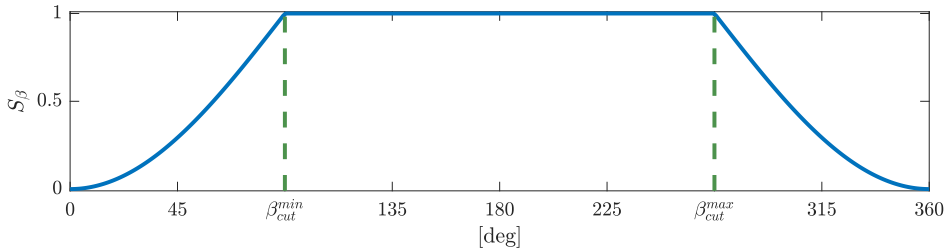

b Scoring function for relative bearing at CPA, S_β.

Figure 5.5: Scoring functions used for vessel pose at time of CPA, along with cut-off angles (--).

5.2.3 Encounter Classification

The COLREGs specify the required actions for vessels in head-on situations and for the give-way and stand-on vessels in crossing and overtaking situations, see Figure 5.7. The method used for determining which rule to apply in a given situation follows Woerner's entry criteria [99], but is outlined here for completeness. The

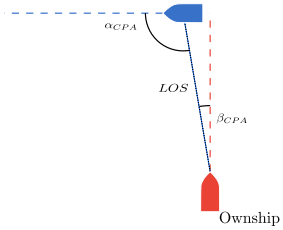

a Near perpendicular pose at CPA, $\mathcal{S}_\alpha \approx 1$ and $\mathcal{S}_\beta \approx 0.1$.

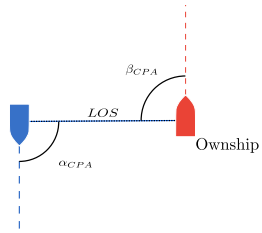

b Parallel pose at CPA, $\mathcal{S}_\alpha \approx 1$ and $\mathcal{S}_\beta \approx 1$.

Figure 5.6: The relative bearing angle (β) and contact angle (α) at CPA convey the difference in risk between two encounters with equal range at CPA.

a Head-on: Both vessels should alter their course to starboard.

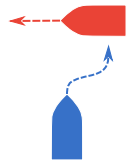

b Crossing: The vessel which has the other on its starboard side should keep out of the way and preferably avoid passing ahead of the other vessel.

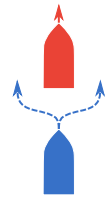

c Overtaking: The vessel doing the overtaking should keep out of the way of the vessel being overtaken.

Figure 5.7: Qualitative behavior as prescribed by the COLREGs.

applicable rule is predominantly determined by the relative poses of the vessels involved at entry time into Stage 2, illustrated in Fig.5.8. The COLREGs does in general not use numerical values in its definitions, the exception is overtaking situations where a vessel is said to be overtaking another when it approaches from a direction more than 22.5° abaft from her beam. For the vessel being overtaken this corresponds to a relative bearing of $\beta \in (\theta^{15}_{min}, \theta^{15}_{max})$, where $\theta^{15}_{min} = 112.5°$ and $\theta^{15}_{max} = 247.5°$. To assure that the other vessel is approaching, a limit has also been set on the contact angle $\alpha \in (-\theta^{13}_{crit}, \theta^{13}_{crit})$ and it has been added that the overtaking vessel must keep a higher speed than the own ship.

Rule 13 also fixes one side of the limits for crossing situations. When a vessel is approaching from port the lower limit is set to zero such that $\beta \in (0°, \theta^{15}_{min})$, for a vessel approaching from starboard the limits are $\beta_{180} \in (-\theta^{15}_{min}, \theta^{15}_{crit})$, where $\beta_{180} : [0°, 360°) \to [-180°, 180°)$. The corresponding limits for the contact angles are reciprocate of the relative bearing for these two situations. Note that the sector defining a crossing from starboard, i.e., a give-way situation, is larger than the crossing from port section. For head-on situations the limits for both the relative bearing and contact angle have been set to $\alpha, \beta_{180} \in (-\theta^{14}_{crit}, \theta^{14}_{crit})$.

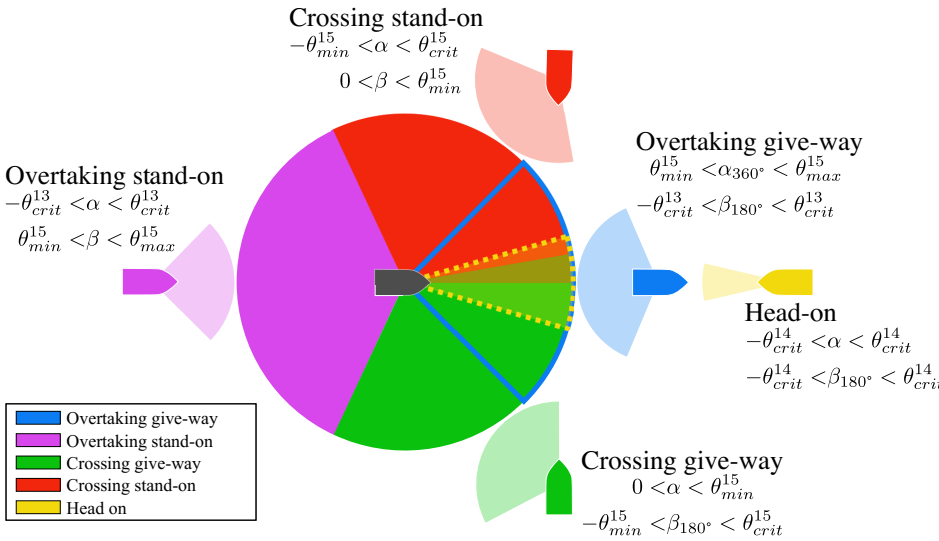

Figure 5.8: Situation classification from the own ship's viewpoint. The mappings $\alpha_{360} : [-180°, 180°) \to [0°, 360°)$ and $\beta_{180} : [0°, 360°) \to [-180°, 180°)$ are used to better display the inherent symmetry in the situation classification.

5.2.4 Rule 16 - Give way

Rule 16 concerns the behavior of vessels that have give-way responsibilities towards another vessel. The give-way vessel must then keep well clear by taking early and substantial action. As suggested by Woerner in [99], the behavior is evaluated by penalizing late and not-readily apparent maneuvers. The formulation of the give-way score is given by

$$\mathcal{S}_{16} = \mathcal{S}_{safety}\mathcal{S}^{ap}_{\Delta}(1 - \mathcal{P}_{delay}), \tag{5.7}$$

where the penalty $\mathcal{P}_{delay}$ is based on the timeliness of the action and the score $\mathcal{S}^{ap}_{\Delta}$ on how readily apparent the maneuver is, both are explained in the following sections. The chosen formulation for $\mathcal{S}_{16}$ places equal importance on the different factors and requires that all factors are high for a good overall score. In his thesis Woerner [96] also applies a penalty for hindrance of stand-on vessel, i.e., the failure to stay well clear, but does not present a definition for this penalty. As Rule 16 applies in both crossing and overtaking situations that have quite different vessel configurations this penalty is in our work included in the scores for the specific situations.

Delayed Action

Maneuvers to avoid collision should be made in ample time, failing to do so is a breach of both Rule 16 and 8a. In this implementation the parameter r_{detect}, used in [99] and signifying the range at time of detection, has been exchanged with r_{entry} which signifies the range when the vessels enter Stage 2. The reason is in part that the time of detection is not known in the cases where data originates from

AIS, but also that common marine radars can detect vessels at ranges far beyond what would be a reasonable distance for collision avoidance maneuvers. In addition, late maneuvers are only penalized if the range at CPA is less than preferred, i.e., $r_{cpa} < r_{pref}$. The range r_{man} signifies the range at the time of detection of the first maneuver after the vessels enter Stage 2.

$$\mathcal{P}_{delay} = \begin{cases} 0, & r_{cpa} > r_{pref} \\ \frac{r_{entry} - r_{man}}{r_{entry}}, & r_{entry} > r_{man} > r_{cpa}, \end{cases} \tag{5.8}$$

Non-apparent Maneuver

Rule 16 also prescribes that maneuvers should, if possible, be substantial. This is clarified by Rule 8b which states that a change in course or speed should be large enough to be readily apparent to another vessel observing, either visually or by radar. The score consists of a course component $\mathcal{P}_{\Delta\chi}^{\neg ap}$ and a speed component $\mathcal{P}_{\Delta U}^{\neg ap}$ and is calculated by the following equation:

$$\mathcal{S}_{\Delta}^{ap} = 1 - (\gamma_{\Delta\chi}^{\neg ap}\mathcal{P}_{\Delta\chi}^{\neg ap} + \gamma_{\Delta U}^{\neg ap}\mathcal{P}_{\Delta U}^{\neg ap}), \tag{5.9}$$

where the weights $\gamma_{\Delta\chi}^{\neg ap}$ and $\gamma_{\Delta U}^{\neg ap}$ must be chosen so that $\gamma_{\Delta\chi}^{\neg ap} + \gamma_{\Delta U}^{\neg ap} = 1$. This deviates from the penalty function presented in [99] by also penalizing non-apparent speed changes when there are no penalty due to course changes. Using a weighted addition instead of multiplication also makes it possible to achieve the minimum score if the vessel is given the maximum penalty for both course and speed changes.

The penalty for non-apparent course change ($\mathcal{P}_{\Delta\chi}^{\neg ap}$) is based on the maximum course change ($\Delta\chi$) between the time of entry into Stage 2, denoted t_0, and the time of CPA, denoted t_{cpa}.

$$\begin{aligned} \Delta\chi = \max(&|\chi(t_0) - \chi(t_1)|,\ |\chi(t_0) - \chi(t_2)|, \\ &\ldots, |\chi(t_0) - \chi(t_{cpa-1})|,\ |\chi(t_0) - \chi(t_{cpa})|) \end{aligned} \tag{5.10}$$

The penalty is applied if $\Delta\chi$ is above the threshold for minimum detectable course change ($\Delta\chi_{md}$), and below the threshold of what is considered readily apparent ($\Delta\chi_{ap}$). The penalty is given by

$$\mathcal{P}_{\Delta\chi}^{\neg ap} = \begin{cases} 1 - \left(\frac{|\Delta\chi| - \Delta\chi_{md}}{\Delta\chi_{ap} - \Delta\chi_{md}}\right)^2, & \Delta\chi_{md} < |\Delta\chi| < \Delta\chi_{ap} \\ 0, & \text{otherwise}, \end{cases} \tag{5.11}$$

which is a slightly stricter penalty function than Woerner's [99]. A plot of the penalty as a function of course change can be seen in Figure 5.10.

The penalty for non-apparent speed change ($\mathcal{P}_{\Delta U}^{\neg ap}$) is based on the relative speed reduction ($\Delta U_{\downarrow}^{rel}$) which is given by

$$\Delta U_{\downarrow}^{rel} = |\Delta U_{\downarrow}|/U(t_0) \tag{5.12}$$

where

$$\begin{aligned} \Delta U_{\downarrow} = \max(&U(t_0) - U(t_1),\ U(t_0) - U(t_2), \\ &\ldots, U(t_0) - U(t_{cpa-1}),\ U(t_0) - U(t_{cpa})). \end{aligned} \tag{5.13}$$

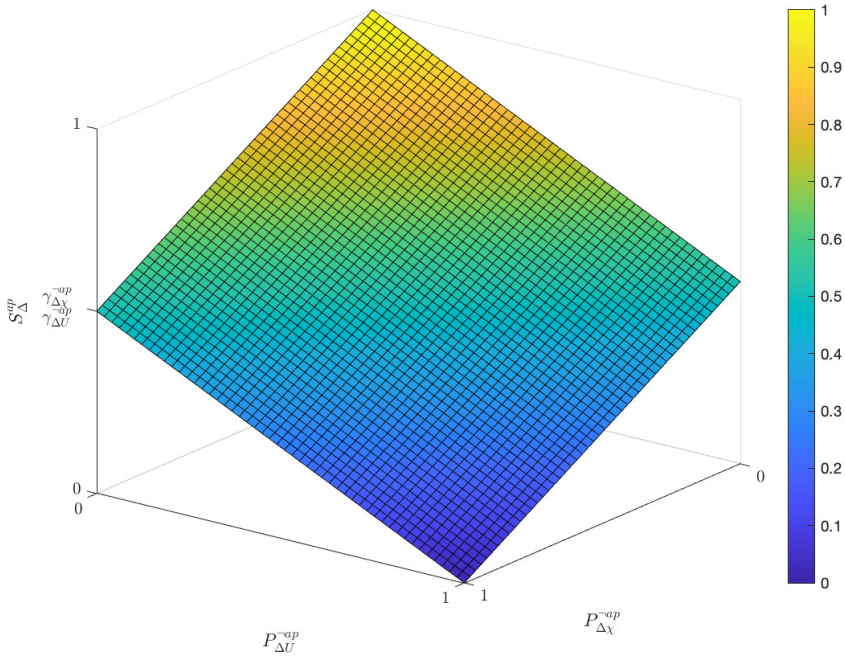

Figure 5.9: Apparent maneuver score, $\mathcal{S}_\Delta^{ap}$, as a function of the penalties for non-apparent course change, $\mathcal{P}_{\Delta\chi}^{\neg ap}$, and non-apparent speed change,$\mathcal{P}_{\Delta U}^{\neg ap}$. Weights are $\gamma_{\Delta\chi}^{\neg ap} = \gamma_{\Delta U}^{\neg ap} = 0.5$.

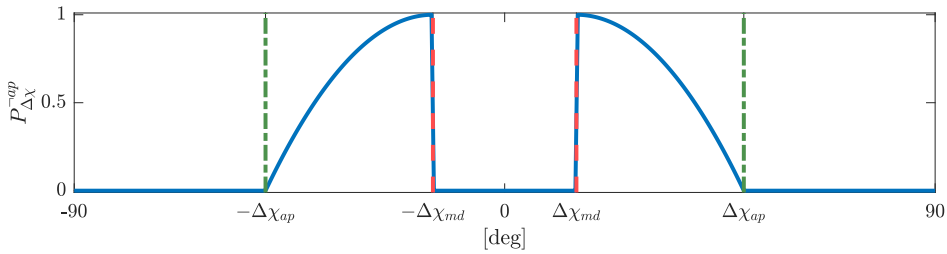

Figure 5.10: Penalty function for non-apparent course changes, $\mathcal{P}_{\Delta\chi}^{\neg ap}$ (—), along with the limits for minimum detectable course change, $\Delta\chi_{md}$ (--), and readily apparent course change, $\Delta\chi_{ap}$ (-·).

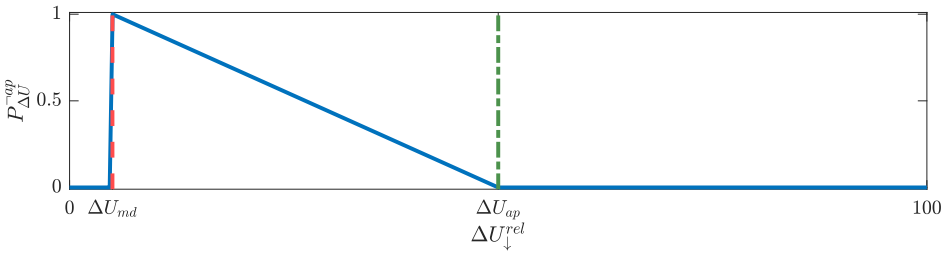

Figure 5.11: Penalty function for non-apparent speed changes, $\mathcal{P}_{\Delta U}^{\neg ap}$ (—), as a function of the relative speed reduction, $\Delta U_{\downarrow}^{rel}$, along with the limits for minimum detectable speed change, ΔU_{md} (--), and readily apparent speed change, ΔU_{ap} (--).

The penalty is applied if $\Delta U_{\downarrow}^{rel}$ lies between the thresholds for minimum detectable (ΔU_{md}^{rel}) and readily apparent (ΔU_{ap}^{rel}) speed changes, and is given by

$$\mathcal{P}_{\Delta U}^{\neg ap} = \begin{cases} \frac{\Delta U_{ap}^{rel} - \Delta U_{\downarrow}^{rel}}{\Delta U_{ap}^{rel} - \Delta U_{md}^{rel}}, & \Delta U_{md}^{rel} < \Delta U_{\downarrow}^{rel} < \Delta U_{ap}^{rel} \\ 0, & \text{otherwise.} \end{cases} \tag{5.14}$$

This formulation is equal to Woerner's [99] apart from the addition of the lower threshold ΔU_{md}^{rel}. This was added to avoid putting heavy penalties on very small speed changes that will neither be noticed, nor affect the situation in any significant manner. A plot of this penalty as a function of the relative speed reduction can be seen in Figure 5.11. As in the original formulation, only non-apparent speed reductions are penalized. The reasoning behind this was not explained, but for give-way vessels in overtaking or crossing situations, where this penalty is applicable, it appears that an additional penalty for non-apparent speed increase is superfluous. With regards to overtaking situations, a small speed increase by the give-way vessel is unlikely to have negative effects, as it will only reduce the duration of the encounter. In crossing situations, the give-way vessel is expected to pass behind the stand-on vessel. Any negative effect in the form of a less than preferred range at CPA will then be penalized by the range safety score, see Equation (5.3). On the other hand, passing ahead of the stand-on vessel will incur its own penalty, see Section 5.2.8, possibly in conjunction with a reduced safety range score.

5.2.5 Rule 17 - Stand on

Rule 17 is concerned with vessels that have stand-on responsibilities to another vessel and implicitly defines four zones or stages for stand-on vessel responsibilities based on range between vessels. The circular representation of these stages, used in this work, is shown in Figure 5.12. However more complex shapes where the stage-defining ranges vary according to relative bearing and vessel speed can also be applied. While vessels in Stage 1 are considered too distant for the COLREGs to apply, a stand-on vessel in Stage 2 is required to maintain its course and speed. However, if the give-way vessel fails to take appropriate action the vessels enter Stage 3 where the stand-on vessel may take action to avoid collision. Further, if it becomes apparent that collision can not be avoided by the actions of the give-way

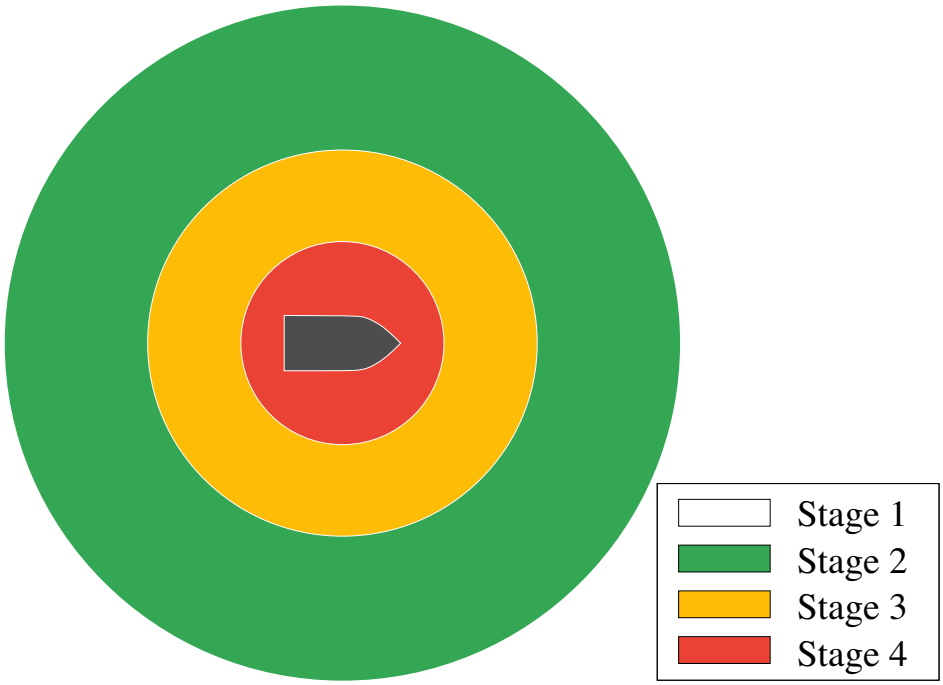

Figure 5.12: Circular representation of the different stages in an encounter. Vessels Stage 1 are detected, but at a distance that does not require further action to be taken. If a vessel enters Stage 2 the navigators must consider evasive maneuvers. Stage 3 and 4 only concerns stand-on vessels.

vessel alone, the vessels enter Stage 4 where the stand-on vessel must take action to avoid collision. Even so, she should, as far as the situation allows avoid turning port for a vessel on her port side. The total score for rule 17 is thus determined by any penalties accumulated in Stage 2 ($\mathcal{P}_2$) and 3 ($\mathcal{P}_3$), along with the penalty on port turns from Stage 4 ($\mathcal{P}_{pt}$) and is given by:

$$\mathcal{S}_{17} = \mathcal{S}_{safety}\mathcal{S}_{s2}\mathcal{S}_{s3}\mathcal{S}_{pt}. \tag{5.15}$$

This formulation places equal importance in the different scores and require high scores in all stages for a good total score. Note that if a stage is not entered during an encounter, the vessel will receive a score of 1 in this stage. While Woerner [99] does not include an equivalent of Stage, 3 his definition of *in extremis* corresponds to our Stage 4.

Stage penalties

The penalty for port turns in Stage 4 is only applied if the give-way vessel is on the port side of own ship when entering Stage 4, i.e., the contact angle $\alpha < 0°$ and the relative bearing $\beta < 180°$. A port turn is defined as present if the stand on vessel moves more than two ship widths to port between the time of entry into Stage 4

and time of CPA. Such a penalty is also included in [99], but its definition is not presented. The definition used in this paper is given by

$$\mathcal{P}_{pt} = \begin{cases} 1, & \alpha < 0^\circ,\ \beta < 180^\circ, \text{ and port turn} \\ 0, & \text{otherwise.} \end{cases} \tag{5.16}$$

The calculation of $\mathcal{P}_x$, $x \in \{2, 3\}$ is based on the penalties for course change ($\mathcal{P}_{x,\Delta\chi}$), speed increase ($\mathcal{P}_{x,\Delta U\uparrow}$) and speed decrease ($\mathcal{P}_{x,\Delta U\downarrow}$) from the respective stages. A give-way compensation ($C_{x,gw}$) will be given in situations where the stand-on vessel has give-way responsibilities to another vessel. For both stages, the penalty is calculated as follows:

$$\begin{aligned} \mathcal{P}_x = \min(1, (&\gamma_{\Delta\chi}\mathcal{P}_{x,\Delta\chi} + \gamma_{\Delta U\uparrow}\mathcal{P}_{x,\Delta U\uparrow} \\ &+ \gamma_{\Delta U\downarrow}\mathcal{P}_{x,\Delta U\downarrow})(1 + C_{x,gw})). \end{aligned} \tag{5.17}$$

Give-way compensation

In Woerner's [99] algorithm, vessels are compensated for all maneuvers required of normal navigation, but the method for calculating the compensation is not presented. While such maneuvers may be ascribed to many things, e.g., grounding hazards, sea marks, shipping lanes, this paper is limited to open water encounters with no such restrictions. Compensation is therefore only given if the stand-on vessel finds itself in a multi-vessel encounter where it has give-way responsibilities to other vessels. The compensation given is

$$\mathcal{C}_{x,gw} = \begin{cases} \gamma_c, & \text{if give-way responsibilities} \\ 0, & \text{otherwise.} \end{cases} \tag{5.18}$$

Course change penalty for Stage 2 and 3

For each course measurement within the stage, the angular difference with regards to the course at the time of entry is calculated. The largest of these values, denoted $\Delta\chi_{max}$, is then used for the calculation of the penalty ($P_{\Delta\chi}$), in the following expression:

$$\mathcal{P}_{\Delta\chi} = \begin{cases} \min\left(1, \ \frac{|\Delta\chi_{max}| - \Delta\chi_{md}}{\Delta\chi_{ap} - \Delta\chi_{md}}\right), & \Delta\chi_{max} > \Delta\chi_{md} \\ 0, & \text{otherwise.} \end{cases} \tag{5.19}$$

As in the calculation of penalties for non-apparent course changes (see Section 5.2.4), course changes above $\Delta\chi_{ap}$ are considered readily apparent and will in this case receive the full penalty, while changes smaller than $\Delta\chi_{md}$ are considered insignificant. A plot of the function can be seen is Figure 5.13.

Speed change penalties

The calculations for speed change penalties for Stage 2 and 3 based are based on the relative speed increase and decrease within each stage, given by

$$\begin{aligned} \Delta U_{\uparrow}^{rel} &= \Delta U_{\uparrow}/U(t_0) \\ \Delta U_{\downarrow}^{rel} &= \Delta U_{\downarrow}/U(t_0), \end{aligned} \tag{5.20}$$

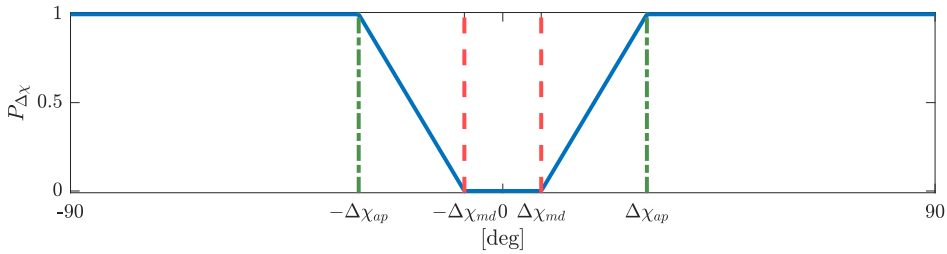

Figure 5.13: Penalty function for course change, $P_{\Delta\chi}$ (—), along with limits for minimum detectable course change, $\Delta\chi_{md}$ (--), and readily apparent course change, $\Delta\chi_{app}$ (-·).

where t_0 denotes time of entry into the respective stage. For each stage the speed increase ($\Delta U_\uparrow$) and the speed decrease ($\Delta U_\downarrow$) are given by

$$\begin{aligned}\Delta U_\uparrow = \max(&U(t_1) - U(t_0),\ U(t_2) - (t_0), \ldots, \\ &U(t_{end-1}) - U(t_0)),\ U(t_{end}) - U(t_0))\end{aligned} \tag{5.21}$$

$$\begin{aligned}\Delta U_\downarrow = \max(&U(t_0) - U(t_1),\ U(t_0) - U(t_2), \ldots, \\ &U(t_0) - U(t_{end-1}),\ U(t_0) - U(t_{end})),\end{aligned} \tag{5.22}$$

where t_{end} denotes either time of exit from the stage, or time of CPA, depending on which event occurs first. Both increasing and decreasing the speed can be penalized if the relative change is above the threshold for minimum detectable speed change (ΔU_{md}^{rel}). The penalties are given by Equations (5.23) and (5.24), the plots of which can be seen in Figure 5.14.

$$\mathcal{P}_{\Delta U\uparrow} = \begin{cases} 0, & \Delta U_\uparrow^{rel} < \Delta U_{md}^{rel} \\ 1 - \frac{\Delta U_{ap}^{rel} - \Delta U_\uparrow^{rel}}{\Delta U_{ap}^{rel} - \Delta U_{md}^{rel}}, & \Delta U_{md}^{rel} < \Delta U_\uparrow^{rel} < \Delta U_{ap}^{rel} \\ 1, & \text{otherwise,} \end{cases} \tag{5.23}$$

and

$$\mathcal{P}_{\Delta U\downarrow} = \begin{cases} 0, & \Delta U_\downarrow^{rel} < \Delta U_{md}^{rel} \\ 1 - \frac{\Delta U_{ap}^{rel} - \Delta U_\downarrow^{rel}}{\Delta U_{ap}^{rel} - \Delta U_{md}^{rel}}, & \Delta U_{md}^{rel} < \Delta U_\downarrow^{rel} < \Delta U_{ap}^{rel} \\ 1, & \text{otherwise,} \end{cases} \tag{5.24}$$

5.2.6 Rule 13 - Overtaking

In overtaking situations, the COLREGs deem the vessel being overtaken as the stand-on vessel, she is required to keep her course and speed, while the overtaking vessel must keep out of the way until she is past and clear. The score calculation for this rule thus contains two cases and is given by the following expression

$$\mathcal{S}_{13} = \begin{cases} \mathcal{S}_{16} - \gamma_{ah13}\mathcal{P}_{ah13}, & \text{if give-way} \\ \mathcal{S}_{17}, & \text{if stand-on,} \end{cases} \tag{5.25}$$

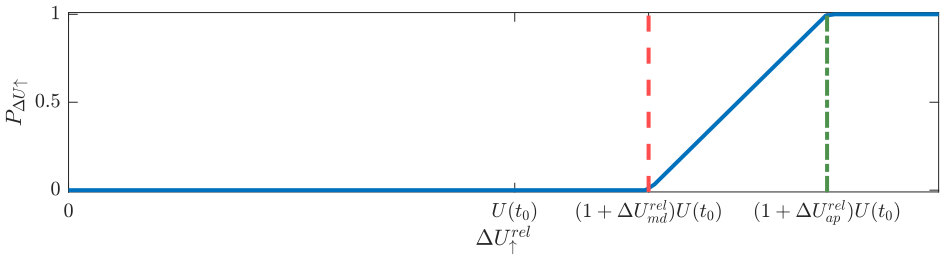

a Penalty function for speed increase, $P_{\Delta U\uparrow}$ (—).

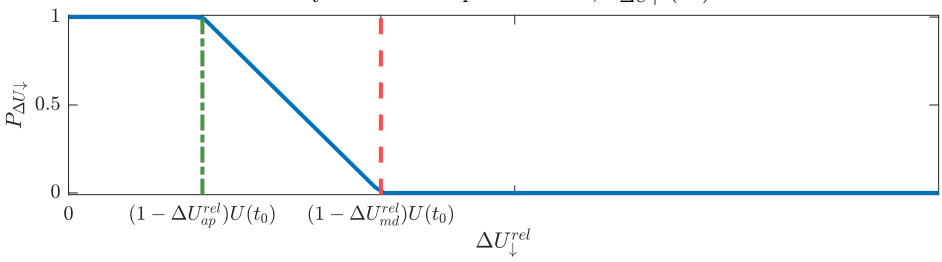

b Penalty function for speed decrease, $P_{\Delta U\downarrow}$ (—).

Figure 5.14: Penalties for speed change as functions of relative speed change along with limits for minimum detectable speed change, ΔU^{rel}_{md} (--), and readily apparent speed change, ΔU^{rel}_{app} (-·).

where $\mathcal{P}_{ah13}$ is a penalty for passing ahead of, and thus being a hindrance to the stand-on vessel, and γ_{ah13} the weight deciding the influence of this penalty on the total score. This penalty, though left undefined, is also used in Woerner's algorithm [99], where it is included in the give-way score $\mathcal{S}_{16}$. Our definition of the penalty is based on the pose of the give-way vessel and is given by:

$$\mathcal{P}_{ah13} = \begin{cases} 1, & |\alpha_{cpa}| < \alpha_{ah13} \\ 0, & \text{otherwise,} \end{cases} \tag{5.26}$$

where α_{ah13} marks the limits for the undesired contact angles.

5.2.7 Rule 14 - Head on

In head on situations, both vessels have equal responsibility for avoiding collision by changing their course to starboard, and pass on the port side of each other. The maneuver must be made in ample time and be readily apparent to the other vessel. Applicable penalties for head on situations are therefore a penalty for non-starboard turns ($\mathcal{P}_{nsb}$), a penalty for starboard-to-starboard passing ($\mathcal{P}_{sts}$) and a non-apparent course change penalty ($\mathcal{P}^{\neg ap}_{\Delta\chi}$) in combination with the penalty for delayed action ($\mathcal{P}_{delay}$) , see Sections 5.2.4 and 5.2.4. The score is calculated using the following expression

$$\begin{aligned} \mathcal{S}_{14} =& (1-\gamma_{nsb}\mathcal{P}_{nsb}-\gamma_{sts}\mathcal{P}_{sts})(1-\mathcal{P}^{\neg ap}_{\Delta\chi}) \\ & (1-\mathcal{P}_{delay}), \end{aligned} \tag{5.27}$$

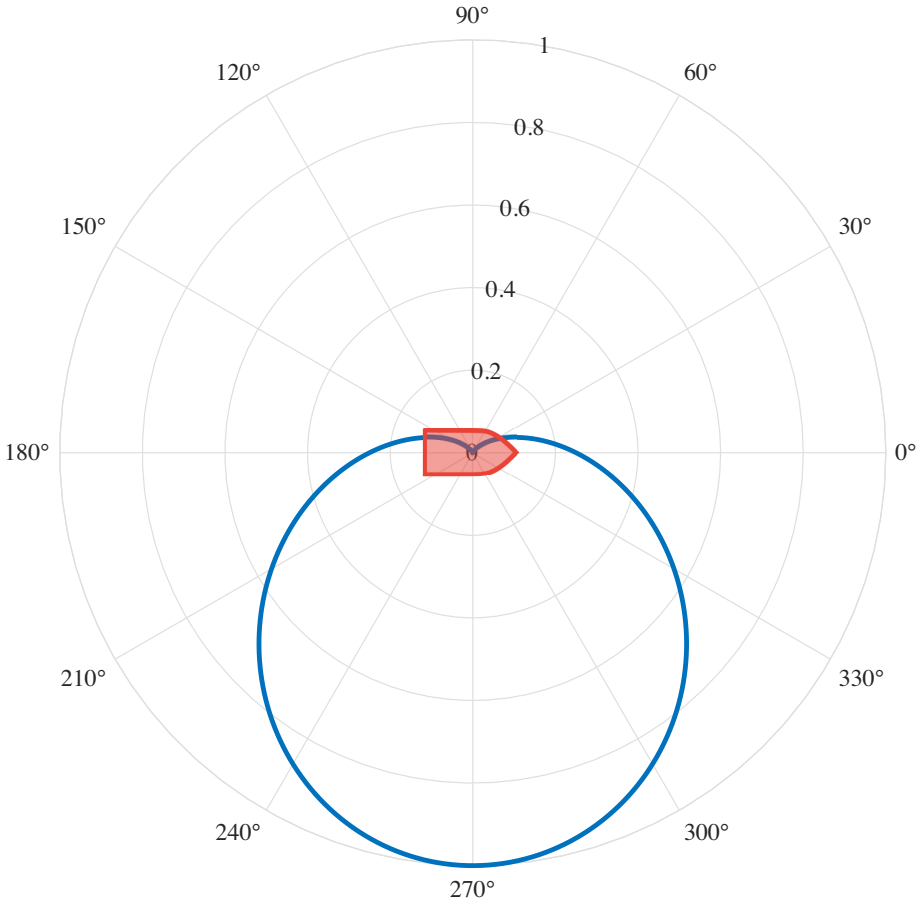

Figure 5.15: Polar plot of $\left(\frac{\sin(\theta)-1}{2}\right)^2$ (—), used in Equation (5.28) to penalize starboard-to-starboard poses at CPA.

where γ_{nsb} and γ_{sts} are weights and should be chosen so that $\gamma_{nsb} + \gamma_{sts} = 1$

The penalty for a starboard-to-starboard passing is based on the involved vessels' pose at CPA, see Figure 5.15, and is given by

$$\mathcal{P}_{sts} = 1 - \left(\frac{\sin(\alpha_{cpa}) - 1}{2}\right)^2 \left(\frac{\sin(\beta_{cpa}) - 1}{2}\right)^2, \tag{5.28}$$

which is the same expression as used in Woerner's evaluation [99], except formulated as a penalty.

The penalty for non-starboard turns ($\mathcal{P}_{nsb}$) is based on the starboard course change ($\Delta\chi_{sb}$), which is given by

$$\begin{aligned}\Delta\chi_{sb} = \max(&\chi(t_1) - \chi(t_0),\ \chi(t_2) - \chi(t_0),\\ &\ldots, \chi(t_{cpa-1}) - \chi(t_0),\ \chi(t_{cpa}) - \chi(t_0)),\end{aligned} \tag{5.29}$$

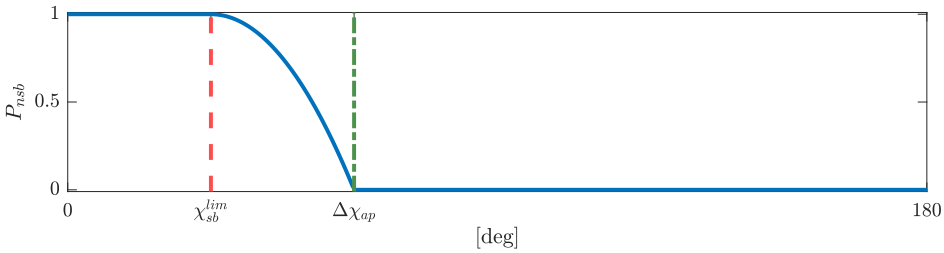

Figure 5.16: Non-starboard turn penalty, $\mathcal{P}_{nsb}$ (—), as a function of course change along with limits for what is considered a starboard turn, χ_{sb}^{lim} (--), and readily apparent speed change, ΔU_{app} (-·).

assuming that starboard course changes are defined as positive. A full penalty is given if the course change is less than the limit χ_{sb}^{lim} and no penalty is given if the starboard course change is readily apparent. The penalty is given by

$$\mathcal{P}_{nsb} = \begin{cases} 1, & \Delta\chi_{sb} < \chi_{sb}^{lim} \\ 0, & \Delta\chi_{sb} > \Delta\chi_{ap} \\ 1 - \left(\frac{\Delta\chi_{sb} - \chi_{sb}^{lim}}{\Delta\chi_{ap} - \chi_{sb}^{lim}}\right)^2, & \text{otherwise.} \end{cases} \tag{5.30}$$

5.2.8 Rule 15 - Crossing

In crossing situations the vessel that has the other on her port side is required to stand on, while the other must give way and keep well clear. The score is thus dependent on the vessel's give-way or stand-on behavior, the evaluation of which is described in Section 5.2.4 and 5.2.5 respectively. As in the case of overtaking situations a penalty is applied if the give-way vessel crosses in front of the stand-on vessel. The score is given by the following

$$\mathcal{S}_{15} = \begin{cases} \mathcal{S}_{16} - \gamma_{ah15}\mathcal{P}_{ah15}, & \text{if give way} \\ \mathcal{S}_{17}, & \text{if stand on,} \end{cases} \tag{5.31}$$

where γ_{ah15} is a weight defining the importance of the crossing ahead penalty ($\mathcal{P}_{ah15}$), which is given by

$$\mathcal{P}_{ah15} = \begin{cases} 1, & \alpha_{ah15}^{min} < \alpha_{cpa} < \alpha_{ah15}^{max} \\ 0, & \text{otherwise.} \end{cases} \tag{5.32}$$

5.3 Parameter Values

The COLREGs rely on the experience and judgment of sailors, and contains few guidelines when it comes to quantifying the required actions. A thorough investigation into quantification of the COLREGs is outside the scope of this article but values used for parameters and weights are included here for completeness. Note

that the default values have been adapted to relatively large vessels in open water encounters in calm weather, but is based on limited data and is accompanied by a high degree of uncertainty.

The set of parameters can be divided into four subsets. The first, containing range parameters that are likely to vary according to situation specific factors, has been classified as adjustable parameters. The list of these along with descriptions of their meaning and default values used for evaluating encounters in open waters are displayed in Table 5.1.

Table 5.1: Adjustable range parameters

Parameter	Value	Unit	Description
r_{Stage2}	3500	m	Range at which two vessels are considered in an encounter.
r_{Stage3}	2000	m	Range at which the stand-on vessel may take action if the give-way vessel fails to do so.
r_{Stage4}	700	m	Range at which the stand-on vessel must take action to avoid collision.
r_{pref}	1200	m	Preferred range between two vessels at CPA.
r_{min}	500	m	Minimum acceptable range between two vessels at CPA.
r_{nm}	200	m	Range between two vessels at CPA considered as a near-miss.
r_{col}	100	m	Range between two vessels at CPA considered as a collision.

The second set contains angular values used for classifying an encounter as either head-on, crossing (stand-on or give-way) or overtaking (stand-on or give-way) and can be found in Table 5.2. The values chosen for θ^{15}_{min} and θ^{15}_{max} have their basis in COLREGs Rule 13.

Table 5.2: Situation classification parameters

Parameter	Value	Unit	Description
θ^{13}_{crit}	45.0°	deg	Angle defining an overtaking situation.
θ^{14}_{crit}	13.0°	deg	Angle defining a head-on situation.
θ^{15}_{min}	112.5°	deg	Angle used in definition of crossing and overtaking situations.
θ^{15}_{max}	247.5°	deg	Angle used in defining of crossing and overtaking situations.
θ^{15}_{crit}	10.0°	deg	Angle used in defining of crossing situation.

Third, the set of parameters used for maneuver detection are displayed in Table 5.3.

Table 5.3: Maneuver detection parameters

Parameter	Value	Unit	Description
ϵ_U	2.0	m/s	Minimum speed for vessel to be considered as moving.
$\epsilon_{\dot{U}}$	0.05	m/s^2	Acceleration threshold.
$\epsilon_{\dot{\chi}}$	0.6	deg/s	Course change threshold.

Last comes the rule specific parameters, see Table 5.4. All depend on the evaluator's interpretation of the COLREGs, and while the presented values provide a basic tuning for the algorithm, they should not be viewed as the final answer. For instance, the combination of visual observations and heavy fog may require a much larger course change for the maneuver to be readily apparent than the $\Delta\chi_{ap} = 30°$ used here.

The weights, balancing the importance of different scores or penalties, can be found in Table 5.5.

5.4 Results

The following sections present the evaluation scores for three test cases. This was chosen over the alternative option of presenting statistics from multiple evaluations as it better demonstrates how the evaluation works and how the scores are influenced by the choice of parameter values.

The first case presented shows the results from a simulated encounter, where one of the vessels is running the SBMPC collision avoidance algorithm from [32]. For this scenario the range parameters were adjusted to fit those of the algorithm. This approach is useful for testing if an algorithm produces the expected behavior, or for comparing two algorithms with the same tuning.

The second and third test case display the behavior of vessels in normal operation. The behavior displayed by these vessels will therefore reflect how the COLREGs are interpreted by professional mariners. For these cases, the parameters influencing the range score at CPA have been adjusted according to the displayed behavior. This is justified by neither vessel making an effort to increase the distance. The remaining parameters are left at their default value.

5.4.1 Simulation Results

Simulated Scenario 1

While encounters between multiple vessels are relatively rare in open waters, it is nevertheless important to be able to evaluate such situations in a sensible manner. The situation shown in Figure 5.17 consists of a head on encounter between ships 1 and 2 while ship 0, the own ship, is in a crossing encounter with both vessels.

Table 5.4: Rule specific parameters

Parameter	Value	Unit	Description
α_{cut}	90°	deg	Cut-off angle, used in contact angle score $\mathcal{S}_{\alpha_{cpa}}$, Eq. 5.5.
β_{cut}^{min}	90°	deg	Minimum cut-off angle, used in relative bearing score $\mathcal{S}_{\beta_{cpa}}$, Eq. 5.6.
β_{cut}^{max}	270°	deg	Maximum cut-off angle, used in relative bearing score $\mathcal{S}_{\beta_{cpa}}$, Eq. 5.6.
$\Delta\chi_{md}$	2°	deg	Minimum detectable course change, used in course change penalty $\mathcal{P}_{\Delta\chi}$, Eq. 5.19.
$\Delta\chi_{ap}$	30°	deg	Minimum course change considered readily apparent, used in course change penalty $\mathcal{P}_{\Delta\chi}$, Eq. 5.19.
ΔU_{md}^{rel}	0.2	–	Minimum detectable relative speed change, used in speed change penalties $\mathcal{P}_{\Delta U\uparrow}$, Eq. 5.23, and $\mathcal{P}_{\Delta U\downarrow}$, Eq. 5.24.
ΔU_{ap}^{rel}	5	–	Minimum relative speed change considered readily apparent, used in speed change penalties $\mathcal{P}_{\Delta U\uparrow}$, Eq. 5.23, and $\mathcal{P}_{\Delta U\downarrow}$, Eq. 5.24.
α_{ah13}	45°	deg	Contact angle defining an ahead passing in overtaking situations, Eq. 5.26.
$\Delta\chi_{sb}^{lim}$	10°	deg	Minimum course change considered a starboard maneuver .
α_{ah15}^{min}	$-25°$	deg	Minimum contact angle defining an ahead passing in a crossing situation.
α_{ah15}^{max}	165°	deg	Maximum contact angle defining an ahead passing in a crossing situation.
α_{ah13}	45°	deg	Contact angle defining an ahead passing in an overtaking situation.

In this setup, the vessels are following preset waypoints, but ship 0 is also running a collision avoidance algorithm. The COLREGs only concerns itself with encounters between two vessels, therefore the evaluation algorithm gives each vessel an independent score with regards to each other vessel encountered. The only consideration made for multi-vessel encounters is the give-way compensations ($\mathcal{C}_{x,gw}$) that can be given if a vessel has contradicting responsibilities. Note that for this case the range parameters (see Table 5.1) have been adjusted to the corresponding values used in a collision avoidance algorithm running on Ship 0 to test if the algorithm performs as expected. The adjusted parameter values can be seen in Table 5.6. Ship 0 enters Stage 2 with regards to both the other vessels shortly after the

Table 5.5: Weights used in calculations of scores and penalties.

Parameter	Value	Description
γ_{min}	0.20	Weight on minimum acceptable range in score for range safety $\mathcal{S}_r$, Eq.5.3.
γ_{nm}	0.30	Weight on near miss range in score for range safety $\mathcal{S}_r$, Eq. 5.3.
γ_{col}	0.50	Weight on collision range in score for range safety $\mathcal{S}_r$, Eq. 5.3.
γ_{α}	0.25	Weight on contact angle in pose score $\mathcal{S}_{\Theta_{cpa}}$, Eq. 5.4.
γ_{β}	0.75	Weight on relative bearing in pose score $\mathcal{S}_{\Theta_{cpa}}$, Eq. 5.4.
$\gamma_{\Delta\chi}^{\neg ap}$	0.50	Weight on non-apparent course changes in score for apparent maneuvers $\mathcal{S}_{\Delta}^{\neg ap}$, Eq. 5.9.
$\gamma_{\Delta U}^{\neg ap}$	0.50	Weight on non-apparent speed changes in score for apparent maneuvers $\mathcal{S}_{\Delta}^{\neg ap}$, Eq. 5.9
$\gamma_{\Delta\chi}$	0.50	Weight on penalties for course changes in stage penalties $\mathcal{P}_x$, Eq. 5.17.
$\gamma_{\Delta U\uparrow}$	0.25	Weight on penalties for speed increase in stage penalties $\mathcal{P}_x$, Eq. 5.17.
$\gamma_{\Delta U\downarrow}$	0.25	Weight on penalties for speed decrease in stage penalties $\mathcal{P}_x$, Eq. 5.17.
γ_c	0.20	Weight on give-way compensation n stage penalties $\mathcal{P}_x$, Eq. 5.17.
γ_{ah13}	0.30	Weight on penalty for passing ahead in overtaking score $\mathcal{S}_{13}$, Eq. 5.25.
γ_{nsb}	0.30	Weight on penalty for non-starboard turns in head-on score $\mathcal{S}_{14}$, Eq. 5.27.
γ_{sts}	0.40	Weight on penalty for starboard-to-starboard passing in head-on score $\mathcal{S}_{14}$, Eq. 5.27.
γ_{ah15}	0.50	Weight on penalty for give-way vessel passing ahead in crossing score $\mathcal{S}_{15}$, Eq. 5.31.

simulation is started, while Ship 1 and 2 do not enter Stage 2 until after ship 1 has finished her give-way maneuver for ship 0.

From the trajectory plot (Figure 5.17) it appears that Ship 0 has prioritized her give-way responsibilities to ship 1 over her stand-on responsibilities to ship 2. This is reflected in the resulting scores, see Table 5.7a and 5.7b.

Ship 2, which is the give-way vessel in the crossing situation with ship 0, makes

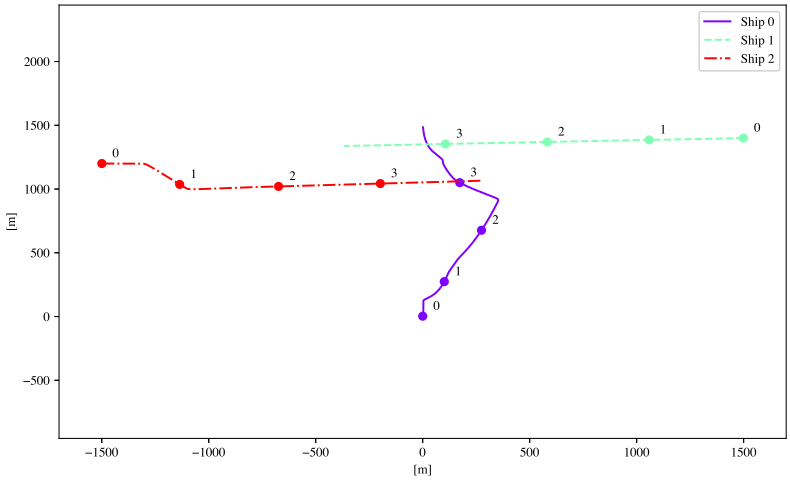

Figure 5.17: Simulated scenario 1, multi-vessel encounter. The positions of the vessels are marked at four instances during the encounter.

Table 5.6: Parameters used for simulated scenario 1

Parameter	Value	Unit
r_{Stage2}	1900	m
r_{Stage3}	700	m
r_{Stage4}	200	m

Parameter	Value	Unit
r_{pref}	200	m
r_{min}	100	m
r_{nm}	50	m
r_{col}	35	m

a large starboard turn to pass behind, but receives a small penalty for delayed action ($\mathcal{P}_{delay}$). The scores for this situation is shown in Table 5.9a.

In the head-on situation between ship 1 and ship 2, both vessels receive full scores (see Table 5.8b and 5.9b) despite not making any avoidance maneuvers. This is because the range at CPA is larger than the preferred range (r_{pref}).

Ship 1 keeps constant course and speed throughout the simulation and therefore receives a full score for her stand-on behavior in the crossing situation with ship 0, see Table 5.8a.

5.4.2 On-Water Results

The trajectories used for testing the evaluation method with regards to human behavior was extracted from AIS data gathered by AIS Norway, a network consisting of about 90 base stations, established by the Norwegian Coastal Administration

Table 5.7: Scores and Penalties for ship 0 in simulated scenario 1

Score/Penalty	Value
$\mathcal{S}_{15}$	0.96
$\mathcal{P}_{ahead15}$	0.00
$\mathcal{S}_{16}$	0.96
$\mathcal{S}_{safety}$	1.00
$\mathcal{S}_{\Theta}$	0.52
$\mathcal{S}_{r}$	1.00
$\mathcal{P}_{delay}$	0.00
$\mathcal{P}_{\Delta}^{\neg ap}$	0.04
$\mathcal{P}_{\Delta U}^{\neg ap}$	0.07
$\mathcal{P}_{\Delta \chi}^{\neg ap}$	0.00

a Ship 0: Give-way crossing with regards to ship 1.

Score/Penalty	Value	
$\mathcal{S}_{15}$	0.35	
$\mathcal{S}_{safety}$	1.00	
$\mathcal{S}_{\Theta}$	0.83	
$\mathcal{S}_{r}$	0.99	
$\mathcal{S}_{17}$	0.35	
$\mathcal{P}_{pt}$	0.00	
	Stage 2	Stage 3
$\mathcal{P}_{x}$	0.42	0.40
$\mathcal{P}_{x,\Delta\chi}$	1.00	1.00
$\mathcal{P}_{x,\Delta U\uparrow}$	0.05	0.00
$\mathcal{P}_{x,\Delta U\downarrow}$	0.02	0.00
$\mathcal{C}_{x,gw}$	0.20	0.20

b Ship 0: Stand-on crossing with regards to ship 2.

[88] and covers an area stretching from the Norwegian baseline to 40-60 nautical miles from the coast.

AIS is a transceiver/receiver system for tracking and monitoring of vessels at sea. The fitting of an AIS transceiver is required by the SOLAS [45] for all vessels of 300 gross tonnage and above traveling internationally and above 500 gross tonnage not traveling internationally, and on all passenger vessels. In addition, many non-SOLAS vessels are fitted with the simpler and less expensive Class B transceivers that provide much of the same functionality including the publication of the vessel's position, speed, unique id (Maritime Mobile Service Identity (MMSI)), type and dimensions. Recorded AIS can be useful for extracting information about the behavior of human operated vessels.

AIS Scenario 1

The head-on encounter shown in Figure 5.18 is between two relatively large vessels, a passenger ship (ship 25) and a cargo ship (ship 29). When the distance between the vessels is 3079 meters the cargo ship makes a starboard maneuver of 10°, and at 2410 meters the passenger ship one of 25.5°. At the time of CPA each vessel has the other on their port side at a distance of 235 meters.

The parameters used for the evaluation of this encounter can be found in Table 5.10 and the resulting scores in Table 5.11. As the distance between the vessels at the CPA is larger than the preferred distance, no penalty has been given for delayed action ($\mathcal{P}_{delay}$). It is safe port-to-port passing leading to a negligible penalty for

Table 5.8: Scores and Penalties for ship 1 in simulated scenario 1

Score/Penalty	Value	
$\mathcal{S}_{15}$	1.00	
$\mathcal{S}_{safety}$	1.00	
$\mathcal{S}_{\Theta}$	0.84	
$\mathcal{S}_{r}$	1.00	
$\mathcal{S}_{17}$	1.00	
$\mathcal{P}_{pt}$	0.00	
	Stage 2	Stage 3
$\mathcal{P}_{x}$	0.00	0.00
$\mathcal{P}_{x,\Delta\chi}$	0.00	0.00
$\mathcal{P}_{x,\Delta U\uparrow}$	0.00	0.00
$\mathcal{P}_{x,\Delta U\downarrow}$	0.00	0.00
$\mathcal{C}_{x,gw}$	0.20	0.20

a Ship 1: Stand-on crossing with regards to ship 0.

Score/Penalty	Value
$\mathcal{S}_{14}$	1.00
$\mathcal{P}_{sts}$	0.00
$\mathcal{P}_{nsb}$	0.00
$\mathcal{P}_{\Delta\chi}^{\neg ap}$	0.00
$\mathcal{P}_{delay}$	0.00

b Ship 1: Head-on with regards to ship 2.

Table 5.9: Scores and Penalties for ship 2 in simulated scenario 1

Score/Penalty	Value
$\mathcal{S}_{15}$	0.89
$\mathcal{P}_{ahead15}$	0.00
$\mathcal{S}_{16}$	0.89
$\mathcal{S}_{safety}$	0.99
$\mathcal{S}_{\Theta}$	0.49
$\mathcal{S}_{r}$	0.99
$\mathcal{P}_{delay}$	0.10
$\mathcal{P}_{\Delta}^{\neg ap}$	0.00
$\mathcal{P}_{\Delta U}^{\neg ap}$	0.00
$\mathcal{P}_{\Delta\chi}^{\neg ap}$	0.00

a Ship 2: Give-way crossing with regards to ship 0.

Score/Penalty	Value
$\mathcal{S}_{14}$	1.00
$\mathcal{P}_{sts}$	0.00
$\mathcal{P}_{nsb}$	0.00
$\mathcal{P}_{\Delta\chi}^{\neg ap}$	0.00
$\mathcal{P}_{delay}$	0.00

b Ship 2: Head-on with regards to ship 1.

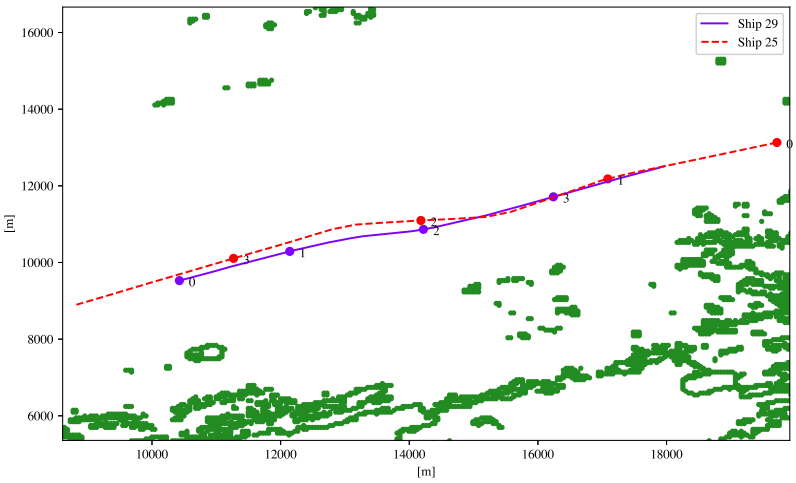

Figure 5.18: AIS scenario 1, head-on. The positions of the vessels are marked at four instances during the encounter.

the vessels' pose at the CPA ($\mathcal{P}_{sts}$). As neither vessel makes a port maneuver no penalty is given for non starboard maneuvers ($\mathcal{P}_{nsb}$). However, both vessels receive a penalty for non-apparent maneuver ($\mathcal{P}_{\Delta\chi}^{\neg ap}$) as the maneuvers made are below the threshold for what is considered readily apparent ($\Delta\chi_{app}$). The difference in the magnitude of the maneuvers is reflected in both the penalty and the total score for this encounter ($\mathcal{S}_{14}$). While this one head-on situation may be an exception, the fact that both vessels are penalized for making non-apparent maneuvers may indicate that the threshold is set too high. Lowering this limit from $\Delta\chi_{app} = 30°$ to $\Delta\chi_{app} = 25°$ results in a total score of $\mathcal{S}_{14} = 0.99$ for ship 25, and a total score of $\mathcal{S}_{14} = 0.20$ for ship 29 and highlights the importance of selecting appropriate parameter values.

Table 5.10: Parameters used for AIS scenario 1

Parameter	Value	Unit
r_{Stage2}	3500	m
r_{Stage3}	2000	m
r_{Stage4}	700	m

Parameter	Value	Unit
r_{pref}	200	m
r_{min}	100	m
r_{nm}	50	m
r_{col}	35	m

Table 5.11: Scores and Penalties for AIS scenario 1

Score/Penalty	Value
$\mathcal{S}_{14}$	0.77
$\mathcal{P}_{sts}$	0.01
$\mathcal{P}_{nsb}$	0.00
$\mathcal{P}_{\Delta\chi}^{\neg ap}$	0.23
$\mathcal{P}_{delay}$	0.00

a Ship 25

Score/Penalty	Value
$\mathcal{S}_{14}$	0.13
$\mathcal{P}_{sts}$	0.01
$\mathcal{P}_{nsb}$	0.00
$\mathcal{P}_{\Delta\chi}^{\neg ap}$	0.87
$\mathcal{P}_{delay}$	0.00

b Ship 29

Table 5.12: Parameters used for AIS scenario 2

Parameter	Value	Unit
r_{Stage2}	3500	m
r_{Stage3}	2000	m
r_{Stage4}	700	m

Parameter	Value	Unit
r_{pref}	1200	m
r_{min}	1000	m
r_{nm}	800	m
r_{col}	200	m

AIS Scenario 2

The crossing encounter shown in Figure 5.19 is between a bulk carrier (Ship 0) and an offshore supply ship (Ship 1) . These are again relatively large vessels and the encounter takes place in open waters which is reflected in the range parameters used in the evaluation, see Table 5.12. When the distance between the vessels is 2157 meters the carrier makes a starboard maneuver of 35° allowing the supply ship to pass ahead with the range at CPA being 1218 meters, the carrier then returns to its original course. The supply ship keeps constant course and speed throughout the duration of the encounter.

The behavior of both vessels are in line with the COLREGs which is reflected in the scores in Table 5.13. The give-way vessel (Ship 0) makes a substantial maneuver in good time which is rewarded by a zero penalty for non-apparent maneuver ($\mathcal{P}_{\Delta}^{\neg ap}$) and delayed action ($\mathcal{P}_{delay}$). It then passes behind the other vessel, thus the penalty for passing ahead ($\mathcal{P}_{ah15}$) is also zero. This behavior allows the stand-on vessel (Ship 1) to keep constant course and speed leading to no maneuvering penalties in Stage 2 or 3 ($\mathcal{P}_{x}$). The penalty for port-turns in Stage 4 remains zero as the vessels never enter this stage. Both vessels do however receive a penalty for their pose at time of CPA, but as the distance between them is larger than the preferred range this is not included in the total safety score ($\mathcal{S}_{safety}$). They thus receive the maximum total score ($\mathcal{S}_{15}$) for this encounter.

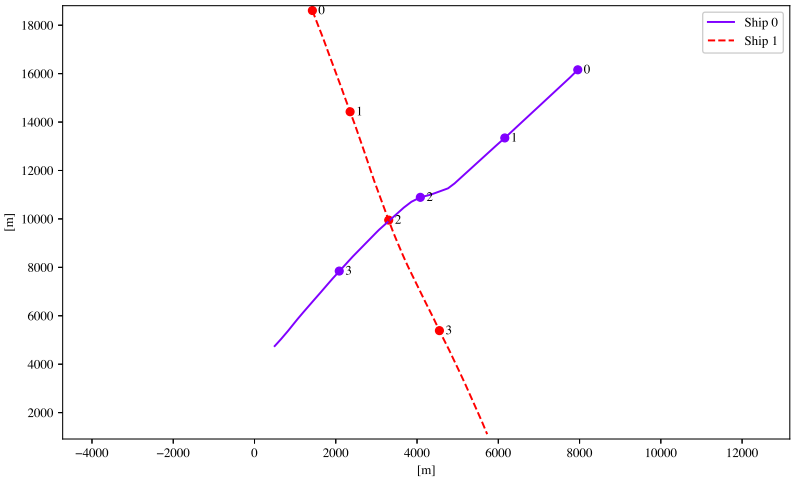

Figure 5.19: AIS scenario 2, crossing. The positions of the vessels are marked at four instances during the encounter.

Table 5.13: Scores and Penalties for AIS scenario 2

Score/Penalty	Value
$\mathcal{S}_{15}$	1.00
$\mathcal{P}_{ahead15}$	0.00
$\mathcal{S}_{16}$	1.00
$\mathcal{S}_{safety}$	1.00
$\mathcal{S}_{\Theta}$	0.31
$\mathcal{S}_{r}$	1.00
$\mathcal{P}_{delay}$	0.00
$\mathcal{P}_{\Delta}^{\neg ap}$	0.00
$\mathcal{P}_{\Delta U}^{\neg ap}$	0.00
$\mathcal{P}_{\Delta \chi}^{\neg ap}$	0.00

a Ship 0

Score/Penalty	Value	
$\mathcal{S}_{15}$	1.00	
$\mathcal{S}_{safety}$	1.00	
$\mathcal{S}_{\Theta}$	0.77	
$\mathcal{S}_{r}$	1.00	
$\mathcal{S}_{17}$	1.00	
$\mathcal{P}_{pt}$	0.00	
	Stage 2	Stage 3
$\mathcal{P}_{x}$	0.00	0.00
$\mathcal{P}_{x,\Delta\chi}$	0.00	0.00
$\mathcal{P}_{x,\Delta U\uparrow}$	0.00	0.00
$\mathcal{P}_{x,\Delta U\downarrow}$	0.00	0.00
$\mathcal{C}_{x,gw}$	0.00	0.00

b Ship 1

5.5 Discussion

The presented method is only concerned with a subset of the COLREGs and is limited to test a finite number of scenarios. As such, it will never definitively prove that a collision avoidance algorithm is safe or abiding by the COLREGs. If used for verification purposes, it must be implemented as a part of a framework capable of assuring sufficient coverage of the test space. This includes the implementation of a systematic method for generating test cases. The evaluation method can however, be used on its own to identify issues in the behavior produced by COLAV algorithms and compare the performance of different COLAV algorithms or the behavior produced by algorithms with that of human operators.

Note that one should show caution when comparing scores produced by the evaluation algorithm, as these depend completely on the parameters used for the evaluation, which can be tuned to favor the evaluator's preferences. More research is needed concerning the behavior of human-controlled vessels and how the COLREGs are interpreted in different situations before parameter values can be finally agreed upon. As an example, the range parameters are likely dependent on factors such as the type, size and speed of the vessels, but also on the type of encounter, and geographical and meteorological factors, thus one set of parameters may not be suitable for all situations.

The algorithm is, as mentioned above, not an exhaustive test for COLREGs compliance. It could easily be extended to include COLREGs rule 18 by incorporating navigational status (fishing, sailing, etc.) in the situation classification, but a thorough discussion around how to include a larger part of the COLREGs in evaluation algorithms can be found in Woerner's paper [99]. Other objectives, such as temporal efficiency and energy efficiency, could also be included to provide a more comprehensive evaluation scheme.

Further work also includes the quantification of COLREGs in terms such as angles, velocities and distances, along with the identification of their dependencies on encounter specific factors. The implementation of these within the evaluation method will enable useful comparisons between autonomous and human collision avoidance behavior.

5.6 Chapter Summary

A method for evaluation of COLAV behavior with regards to safety and compliance with the COLREGs Rules 8(a, b), 13, 14, 15, 16 and 17 has been presented, including the method used for maneuver detection and all assessment metrics employed. Values for all tunable parameters and weights have also been suggested. Results from three case studies have been included to provide more insight into the evaluation process, and highlight the effect of tuning choices. The presented method allows for unbiased evaluation and comparison of COLAV algorithms and can help identify issues with the behaviors produced by said algorithms.

Chapter 6

Grounding Hazard Considerations in Collision Avoidance Evaluation

This chapter is a continuation of the work presented in the previous chapter and in [36], and is based on:

[35] Inger Berge Hagen, Martin Navarsete Murvold, Tor Arne Johansen, and Edmund Førland Brekke. Grounding Hazard Considerations in Evaluation of COLREGS Collision Avoidance Algorithms. *IEEE Transactions on Intelligent Transportation Systems*, 2022. unpublished/under revision.

6.1 Introduction

Technology is pushing society towards the use of systems with increasing levels of autonomy. This has generated considerable interest from the maritime sector, where higher levels of autonomy is envisioned to reduce both operational costs and human exposure to hazardous environments. Anti-collision control is a critical component in any autonomous transport system, also at sea, and while earlier works on the topic, [12, 40, 84] focus mainly on maintaining the distance between vessels, more recent works, e.g. [32, 57], also aim to incorporate the internationally agreed upon traffic rules, COLREGs [42].

As collision avoidance methods become more advanced, extended to consider multiple factors in addition to the vessel's position, course and speed, it becomes increasingly difficult to provide an unbiased evaluation of the methods' performance and efficiency. This issue has brought forth the need for automated evaluation for testing and verification purposes which, as clearly stated in [69], is essential for any future deployment of autonomous vessels. The application of automatic evaluation for verification purposes is demonstrated in [89], where a methodology for automatic simulation-based testing is proposed. The methodology is demonstrated through a case study where STL requirements are formulated for safety distance, mission compliance and basic COLREGs compliance for give-way vessels.

A more complete technique for COLREGs evaluation, but without the verification framework, was presented by Woerner [96], where several of the steering and sailing rules are included. The work was continued in [97] and [99], and has

inspired several others [36, 38, 64], the latter forming the foundation for the work presented in this chapter. The above mentioned works checks for compliance with COLREGs' rules 8 and 13-17, but are limited to encounters taking place in open waters. The novel contribution in this work is that we show how grounding hazards can be included for automatic evaluation of marine collision avoidance algorithms for safety and COLREGs compliance. This is motivated by the following:

- Grounding hazards pose a serous threat to marine vessels and must be considered when collision avoidance maneuvers are performed. Evaluation methods should therefore be capable of identifying algorithms that fail to do so properly.
- Situations may occur where grounding hazards limit the available maneuvering space and a compromise must be made between avoiding grounding and compliance with the COLREGs. The ability to make such compromises should be reflected in the evaluation scores.

The remainder of this chapter is organized as follows. First, a brief description of the evaluation algorithm that is the subject for the proposed extensions is presented. Then follows an explanation of which considerations have been made with regards to grounding hazards and how these have been implemented into the existing framework. Comparisons of evaluation results with and without these considerations are then presented, followed by a short discussion and summary of the chapter.

6.2 Safety and COLREGs Evaluation

This work is an extension to the safety and COLREGs evaluation algorithm presented in [36], from here on referred to as EvalTool. This section offers a brief overview of this method, which enables objective evaluation of trajectory data obtained from either simulations, experiments or from vessels in normal operation.

The evaluation is encounter-based, with an encounter being defined as the period where two vessels find themselves in such a configuration of position, course and speed that one of the COLREGs rules apply. For each encounter, the evaluation returns one score ($\mathcal{S}_{sit} \in [0, 1]$) per vessel, indicating the vessel's performance with regards to safety and COLREGs compliance with respect to the applicable Rules. The score is calculated based on metrics characterizing the vessels' trajectory during the encounter. The behavioral traits described by these metrics are awarded scores or penalties depending on whether the behavior is desired or not according to the applicable rule. These scores and penalties are then combined to form the vessel's encounter score. Scores are denoted $\mathcal{S} \in [0, 1]$, and penalties $\mathcal{P} \in [0, 1]$, and for a given metric, the associated score and penalty are related as follows: $\mathcal{S}_{metric} = 1 - \mathcal{P}_{\neg metric}$. An overview of the EvalTool's scores and penalties is given in Table 6.1, where Stage 2-4 are defined later.

Rule 13-15 of the COLREGs define a vessel's responsibility in an encounter between two vessels. In overtaking (Rule 13) and crossing (Rule 15) situations, one vessel is assigned the role as give-way vessel, while the other is assigned to be the stand-on vessel. In head-on (Rule 14) situations, both vessels must give way by altering their course to starboard. Rules 16 and 17 describe the required action by

Table 6.1: Scores and penalties employed in EvalTool

Name	Description
$\mathcal{S}_{13}$	Score for overtaking situation.
$\mathcal{S}_{14}$	Score for head-on situation.
$\mathcal{S}_{15}$	Score for crossing situation.
$\mathcal{S}_{16}$	Total score for give-way behavior.
$\mathcal{S}_{17}$	Total score for stand-on behavior.
$\mathcal{S}_{safety}$	Score for pose and range safety at CPA.
$\mathcal{S}_{r}$	Score for range safety at CPA.
$\mathcal{S}_{\Theta}$	Score for pose safety at CPA.
$\mathcal{S}_{\alpha}$	Score for contact angle safety at CPA.
$\mathcal{S}_{\beta}$	Score for relative bearing safety at CPA.
$\mathcal{S}_{s2}$	Score for stand-on behavior during Stage 2.
$\mathcal{S}_{s3}$	Score for stand-on behavior during Stage 3.
$\mathcal{S}_{pt}$	Score for stand-on behavior during Stage 4.
$\mathcal{P}_{\Delta U\uparrow}$	Penalty on speed increase by stand-on vessel.
$\mathcal{P}_{\Delta U\downarrow}$	Penalty on speed decrease by stand-on vessel.
$\mathcal{P}_{delay}$	Penalty delayed action by give-way vessel.
$\mathcal{P}_{nsb}$	Penalty on making a non-starboard turn in head-on situations.
$\mathcal{P}_{sts}$	Penalty on starboard-to-starboard passing in head-on situations.
$\mathcal{S}_{\Delta}^{ap}$	Score for apparentness of maneuver by give-way vessel.
$\mathcal{S}_{\Delta\chi}^{ap}$	Score for apparentness of course change by give-way vessel.
$\mathcal{S}_{\Delta U}^{ap}$	Score for apparentness of speed change by give-way vessel.
$\mathcal{P}_{ah13}$	Penalty on the give-way vessel crossing ahead of the stand-on vessel in overtaking situations.
$\mathcal{P}_{ah15}$	Penalty on the give-way vessel crossing ahead of the stand-on vessel in crossing situations.

the give-way and stand-on vessel, respectively. While the give-way vessel must aim to take early and substantial action to keep well clear, the stand-on vessel should maintain her course and speed. However, she may take action if the give-way vessel fails to do so. If it becomes apparent that action by the give-way vessel alone is not sufficient to avoid collision she is required to take action but should avoid port maneuvers for vessels on her port side. Rule 8 further details the actions to be performed, notably a preference towards changes in course rather than in speed

Table 6.2: Applicable rules according to situation type

Situation	Main rule	Specifying Rule		General Rule
Overtaking	13	stay-on	17	8
		give-way	16	8
Crossing	15	stay-on	17	8
		give-way	16	8
Head-on	14	–	–	8

and that maneuvers should be readily apparent to other vessels and be made at an appropriate time. The relation between these rules and the different situation types is summarized in Table 6.2.

6.3 Grounding Hazard Considerations

The addition of grounding considerations have been included in the EvalTool by performing rule specific tests when undesired behavior is detected in the form of a penalty. Our implementation of these tests employ methods from the open source ENC visualization and manipulation API Seacharts [5], which is also used for the situation visualizations in this chapter. If the tests determine that grounding hazards are indeed influencing the vessel's behavior, a compensation $C \in [0, 1]$ is calculated and applied. The following sections describe the tests and the situations in which they are applicable. Note that due to being the preferred action for collision avoidance, only course changes have been considered in the tests.

6.3.1 All situations

The first novel element to the evaluation is a grounding check which simply checks for intersections between a vessel's trajectory and unsafe depths. If an intersection point is found, the grounding penalty ($\mathcal{P}_{gr}$) is set to one, otherwise it is set to zero. Contrary to other penalties and scores, which are calculated based on only the segment of trajectory marked as an encounter, the grounding check is performed on the entire trajectory available. Grounding detection is assumed to be more relevant to the evaluation of simulated trajectories, than to those obtained from real-life vessels, where a grounding incident is not likely to go unnoticed. The grounding penalty can therefore be seen as somewhat separate to the penalties on the different behavioral traits and has not been incorporated into the situation score but is kept as a separate indicators.

6.3.2 Give-way

For vessels in head-on situations or having give-way responsibilities in crossing or overtaking situations, taking the early and substantial action required may be impossible due to the location of grounding hazards. If the magnitude of the action is below the threshold for what is considered readily apparent, the EvalTool

evaluation will give a penalty for not making an apparent maneuver ($\mathcal{P}_{\Delta}^{\neg ap}$). To decide whether a compensation should be given for this penalty, a set of alternative trajectories circumventing the obstacle vessel are constructed to determine whether the size of the course change was indeed restricted by grounding hazards. Note that, while feasible, these trajectories are not to be confused with an attempt at prescribing an optimal behavior but only used for testing if a larger deviation from the original path is feasible. For convenience they will still be referred to as trajectories for the remainder of this work.

The alternative trajectories run along ellipses constructed around the obstacle vessel's position at the closest point of approach (CPA) ($x_{cpa}^{obst},\ y_{cpa}^{obst}$). The radii of the major and minor axes are given by $R_x = \tau U_{cpa}^{os}$ and $R_y = 0.5R_x$, respectively. The τ parameter is a scaling factor given in seconds, and U_{cpa}^{os} is the own ship's speed at CPA. The radii of the ellipsis is thus the distance traveled by the vessel during the time periods specified by the elements in τ. Both the number of ellipsis (n_{ell}) and the scaling factor's elements are tunable parameters. As an example, the ellipses in Figure 6.1 were constructed with $n_{ell} = 4$ and $\tau = [60,\ 120,\ 180,\ 240]$. The ellipses are oriented according to the own ship's heading at CPA (χ_{cpa}^{os}), which in parametric form gives the following equation for the ellipses:

$$\begin{aligned} x(\theta) &= R_x \cos\chi_{cpa}^{os} \cos\theta - R_y \sin\chi_{cpa}^{os} \sin\theta + x_{cpa}^{obst}, \\ y(\theta) &= R_x \sin\chi_{cpa}^{os} \cos\theta - R_y \cos\chi_{cpa}^{os} \sin\theta + y_{cpa}^{obst}, \end{aligned} \tag{6.1}$$

where $0 \leq \theta \leq 2\pi$.

The shortest path along the ellipses between intersection points with the original path is used for the creation of alternative paths. Arc segments from circles with a diameter equal to five times the own ship's length, c.f. the maximum tactical diameter in the standards for ship maneuverability [66], create the transitions between the original path and the ellipses, similar to the so-called Dubins paths [14].

The alternative paths are then given an index in the range 1 to n_{ell} according to increasing size and checked in reverse order for intersection points with depths less than the own ship's draft. The index of the largest path not traversing an unsafe depth, marked in green in Figure 6.1, sets the variable $i_{acccept}$, if no paths are accepted it is set to zero. The resulting compensation is calculated as follows:

$$\mathcal{C}_{gw}^{gr} = \frac{n_{ell} - i_{accept}}{n_{ell}}, \tag{6.2}$$

and incorporated into the penalty for non-apparent maneuver by:

$$\mathcal{P}_{\Delta}^{\neg ap} \leftarrow \mathcal{P}_{\Delta}^{\neg ap} \cdot (1 - \mathcal{C}_{gw}^{gr}). \tag{6.3}$$

6.3.3 Stand-on

A stand-on vessel is required to maintain its course and speed during the encounter, however, it may take action if the give-way vessel neglects to make an appropriate maneuver. If it later becomes evident that actions by the give-way vessel alone is not enough to avoid collision, the stand-on vessel is required to take action.

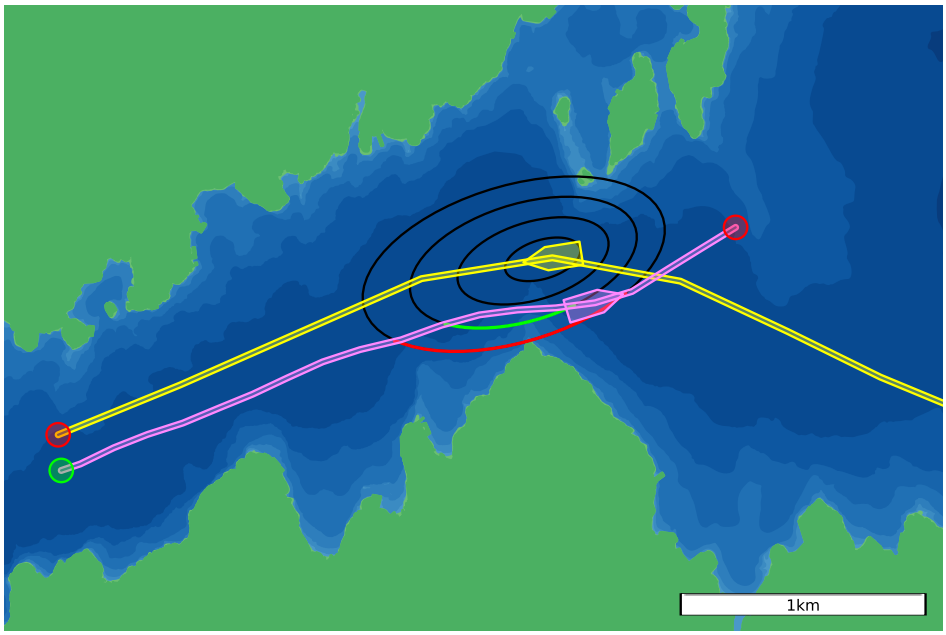

Figure 6.1: Alternative paths for the give-way vessel, marked in pink, in a crossing situation. Rejected paths are marked in red, the accepted path in green.

In the EvalTool evaluation, this is dealt with by segmenting the vessel's trajectory according to four stages defined by the distance between the vessels, see Figure 6.2. For two vessels on collision course, Stage 1 signifies that the distance between them is large enough that no action is required. As the vessels approach each other, they move into Stage 2, where action is required by the give-way vessel. If no action is taken, the vessels move into Stage 3 where action may be taken by the stand-on vessel. At this point, if neither of the vessels perform an evasive maneuver, Stage 4 commences when it becomes apparent that both vessels must take action to avoid collision.

Penalties on changes in course and speed by the stand-on vessel is therefore only given in Stage 2 and 3, and with a lower penalty on maneuvers in Stage 3. These are then combined into a joint maneuvering penalty for each stage ($\mathcal{P}_2$ and $\mathcal{P}_3$). However, if the penalized maneuvers are necessary to avoid grounding hazards, a compensation should be given.

Thus, if a maneuvering penalty has been applied for a stage, a search is performed to locate potential grounding hazards. The search area is created based on three points, where the first is either the starting point of the maneuver or, if it is a maneuver continued from an earlier stage, the starting point of the stage. The own ship's position at this point is denoted $\mathbf{p}_0^{os} = (x_0^{os},\ y_0^{os})$, and its heading by ψ_0^{os}. The second point, $\mathbf{p}_1^{os} = (x_1^{os},\ y_1^{os})$, is either the endpoint of the own ship's trajectory or the point where the vessels exit Stage 2 and move back into Stage 1. The third point can then found in the following manner:

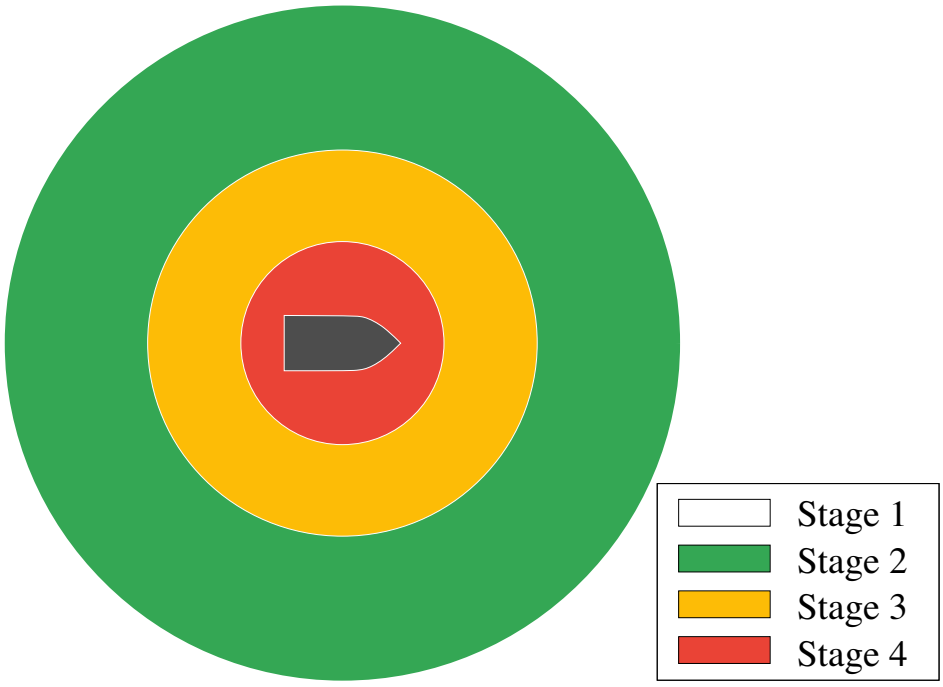

Figure 6.2: Encounter stages for stand-on vessels.

$$\hat{\mathbf{p}}_1^{os} = \mathbf{p}_0^{os} + r_{S2} \cdot [\sin(\psi_0^{os}),\ \cos(\psi_0^{os})]^T, \tag{6.4}$$

where r_{S2} is the distance defining the entry of Stage 2. The resulting search area is formed by the original trajectory and the straight lines between $\mathbf{p}_0^{os}$ and $\mathbf{p}_1^{os}$, and $\mathbf{p}_1^{os}$ and $\hat{\mathbf{p}}_1^{os}$, an example of such areas can be seen in Figure 6.3.

If the search area intersects with areas of unacceptable depths, a compensation is calculated as follows:

$$\mathcal{C}_{so}^{gr} = \begin{cases} 1, & d_{gr} \leq l_{os}^{td} \\ \frac{\gamma l_{os}^{td} - d_{gr}}{\gamma l_{os}^{td} - l_{os}^{td}}, & l_{os}^{td} < d_{gr} \leq \gamma l_{os}^{td} \\ 0 & otherwise, \end{cases} \tag{6.5}$$

where d_{gr} is the minimum distance between $\mathbf{p}_0^{os}$ and the grounding hazards and l_{os}^{td} is the tactical diameter of the vessel. This assures that full compensation is given if the distance to the hazard is less than the tactical diameter of the vessel. For the evaluations presented in this chapter, the scaling parameter γ has been set to two, i.e., compensation is given for a distance twice the tactical diameter. The compensation is incorporated into each of the penalties for course changes in Stage 2 and 3 in the following manner:

$$\mathcal{P}_{\Delta\chi} = \mathcal{P}_{\Delta\chi} \cdot (1 - \mathcal{C}_{so}^{gr}). \tag{6.6}$$

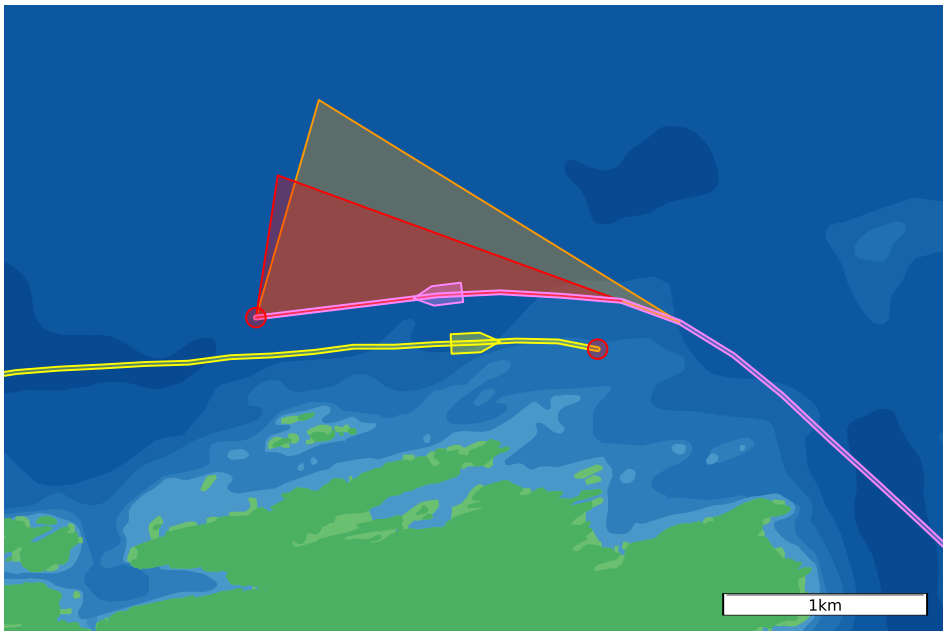

Figure 6.3: Stand-on vessel (pink) grounding hazard search areas for Stage 2 (orange) and Stage 3 (red).

6.4 Results

The scenarios presented in this section are extracted from AIS data collected off the Norwegian coast by AIS Norway and made available by The Norwegian Coastal Administration (Kystverket). The bathymetry data needed for visualization and grounding evaluation were obtained from the Norwegian Mapping Authority (Kartverket). Information regarding vessel dimensions were drawn from the static AIS data or, if not available, from the online resource Marine Traffic [60].

For each scenario in this section, the EvalTool's tuning was adjusted according to the situation. This is necessary when working with data recording real life encounters as the vessels' behavior is not controlled by preset parameters but varies according to a range of factors, such as the type of situation, the (relative) size of the vessels, closeness to land, and so on [33]. For give-way situations the number of alternative paths used in the grounding evaluation is four. While a higher number of alternative paths would give more accurate results, a lower number is better suited for visualization purposes and is sufficient for demonstrating the effect of the compensation.

6.4.1 Grounding check

The grounding check was tested by manually changing the draft parameter of a vessel from 5 to 25 meters, effectively causing parts of the vessel's original trajectory

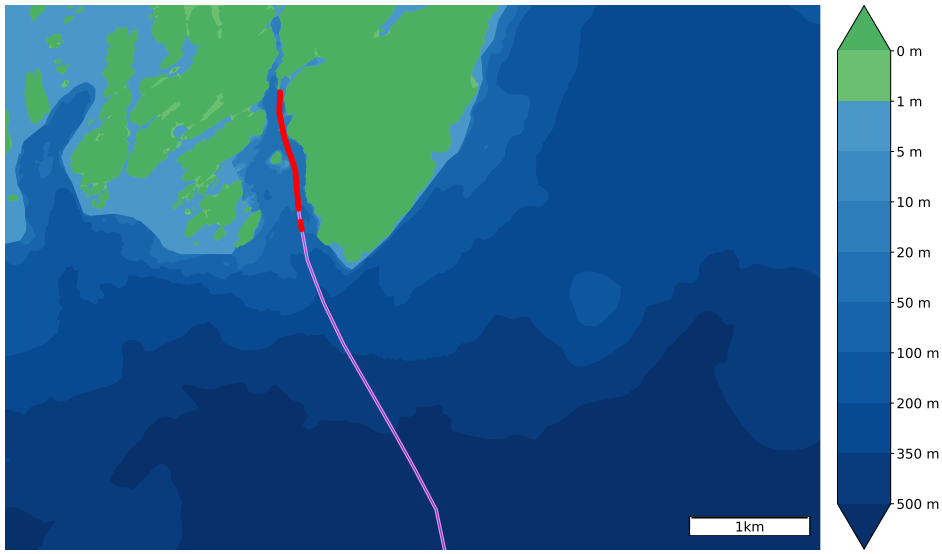

Figure 6.4: Grounding check for vessel trajectory with minimum depth adjusted from 5 to 25 meters, for illustration purposes. Segments traversing unacceptable depths are marked in red.

to pass through areas of unacceptable depths. The test is visualized in Figure 6.4, where the unsafe trajectory segments are marked in red. The test results in a grounding penalty ($\mathcal{P}_{gr}$) of one, which does not affect the vessel's situation score but as mentioned is logged as a separate indicator.

6.4.2 Give-way

This section contains comparisons of the evaluation scores of give-way vessels' behavior with and without compensation for grounding hazards. For all give-way situations presented, the limit for what is considered a readily apparent maneuver is set to 10 degrees, the number of ellipses used for creating alternative trajectories is four and the scaling parameter $\tau = [60,\ 120,\ 180,\ 249]$.

Case 1

The first example scenario, shown in Figure 6.1, is a crossing situation where the give-way vessel is required to make a starboard maneuver to keep clear of the stand-on vessel approaching from its starboard side. A comparison of relevant scores for this vessel with and without grounding considerations included is shown in Table 6.3. It shows that when grounding hazards are not considered, the give-way vessel receives a penalty for not making a readily apparent maneuver ($\mathcal{P}_{\Delta}^{\neg ap}$) of 0.32. When grounding hazards are considered, a compensation of 0.25 is given. This reduces the penalty to 0.24 and thereby increases the give-way behavior score ($\mathcal{S}_{16}$) from 0.58 to 0.69.

Table 6.3: Score comparison with and without grounding hazard compensation for the give-way vessel in Figure 6.1

Score/Penalty	Without compensation	With compensation
$\mathcal{S}_{15}$	0.58	0.69
$\mathcal{S}_{16}$	0.58	0 .69
$\mathcal{P}_{\Delta}^{\neg ap}$	0.32	0.24
$\mathcal{C}_{gw}^{gr}$	NA	0.25
$\mathcal{P}_{gr}$	NA	0

In this scenario, the give-way vessel makes a starboard maneuver, resulting in a distance at CPA of 264 meters. Still, the change in course angle is only 5.2 degrees. This is well below the limit for what is considered readily apparent in the evaluation, and the given penalty therefore appears appropriate. The vessel is however restricted in its movements by a landmass on it's starboard side, which produces a compensation of 0.25 when grounding hazards are considered.

The draft of this vessel was not available but as it is a relatively small vessel (12 by 3 meters), it is likely to lie quite shallow in the water and it's draft was set to 5 meters. While the entire accepted trajectory alternative lies within areas deeper than the vessel's draft, no additional safety margins have been added.

Case 2

The second encounter, see Figure 6.5, occurs in a narrow passage between several islands. Whether this encounter should be classified as a crossing situation, where one vessel is required to keep her course and speed while the other vessel must give way, or a head-on situation, where both vessels are required to make starboard turns, depends on the start point definition of the encounter, i.e., the entry distance of Stage 2. However, it is clear that if both vessels are to pass through the passage, they will meet head on. It was therefore chosen to tune the EvalTool to consider this as a head-on situation. While acceptable for demonstration purposes, manual tuning is not a reasonable solution for automatic evaluation and more research is needed to identify appropriate values for tuning parameters according to the situation.

The alternative trajectories used for calculating the grounding compensation for the south-going vessel is also plotted in Figure 6.5, clearly showing that the maneuvering space is very restricted. However, it would be possible for the vessel to delay its return to the original path thereby increasing the distance at CPA, originally 88 meters. The relevant scores and penalties, with and without grounding compensation, are compared in Table 6.4 and shows that the penalty for non-apparent maneuver has been reduced from 0.18 to 0.14 when grounding hazards are taken into consideration. While this may seem like a negligible difference, it is proportional to the penalty given and its effect on the total score (a increase from 0.75 to 0.82) is noticeable.

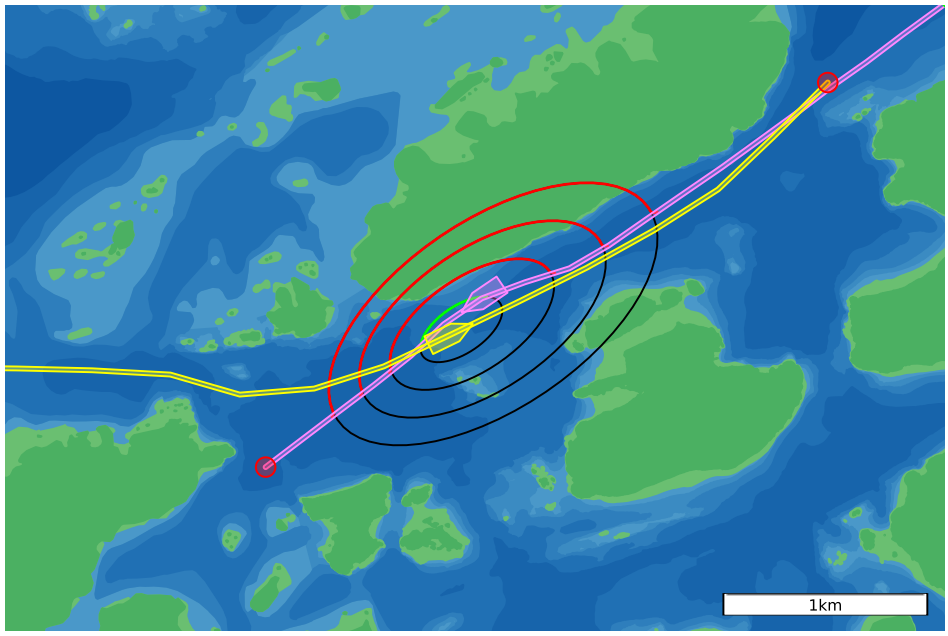

Figure 6.5: Grounding evaluation of alternative trajectories in head-on situation for south-going vessel (pink). The accepted trajectory alternative is marked in green and the rejected ones in red.

Table 6.4: Score comparison with and without grounding hazard compensation for south-going vessel in head-on situation, Figure 6.5.

Score/Penalty	Without compensation	With compensation
$\mathcal{S}_{14}$	0.75	0.82
$\mathcal{P}_{\Delta\chi}^{\neg ap}$	0.18	0.14
$\mathcal{C}_{gw}^{gr}$	NA	0.75
$\mathcal{P}_{gr}$	NA	0

Table 6.5: Score comparison with and without grounding hazard compensation for north-going vessel in head-on situation, Figure 6.5

Score/Penalty	Without compensation	With compensation
$\mathcal{S}_{14}$	0.00	0
$\mathcal{P}_{\Delta\chi}^{\neg ap}$	0	0
$\mathcal{P}_{delay}$	1	1
$\mathcal{C}_{gw}^{gr}$	NA	NA
$\mathcal{P}_{gr}$	NA	0

Case 3

With regards to the second vessel in the previous case, again see Figure 6.5, it does not make any attempt at giving way to the other vessel. While this does not carry a penalty for non-apparent maneuver (as no maneuver is made), it does lead to a full penalty for delayed action ($\mathcal{P}_{delay}$). This leads to a situation score ($\mathcal{S}_{14}$) of zero, as shown in Table 6.5. It should be noted that the reason for the lack of action is likely related to the difference in size of the two vessels. The larger vessel (70 meters), not making a maneuver, being more than six times the length of the smaller vessel (11 meters). Whether or not such behavior should also be compensated within the evaluation is outside the scope of this work but it is a common feature in the encounters extracted from the AIS data. It is therefore an important point to consider when developing collision avoidance for autonomous vessels intended to operate among human controlled vessels.

6.4.3 Stand-on

For the stand-on evaluation considering grounding hazards the γ parameter has been set to two, meaning that compensation is given if the distance between the stand-on vessel and land is less than twice the vessel's tactical diameter at the time of calculation.

Case 4

The crossing situation in Figure 6.6 takes place in a fjord. The shape of the fjord makes it necessary for the stand-on vessel to make a port turn in order to reach its destination. Such a maneuver also means turning towards the other vessel. It would therefore be prudent to delay this action for as long as possible without causing a significant increase in the risk of grounding.

The stand-on vessel in question is relatively large with a length of 170 meters, while the give-way is a smaller vessel of 12 meters. As previously mentioned, when the difference in size between meeting vessels is large, the smaller vessel will often give-way irrespective of the behavior prescribed by the COLREGs. The expectation of such behavior can be a contributing factor to the decision by the stand-on vessel of starting the maneuver early. It must also be considered that an early start

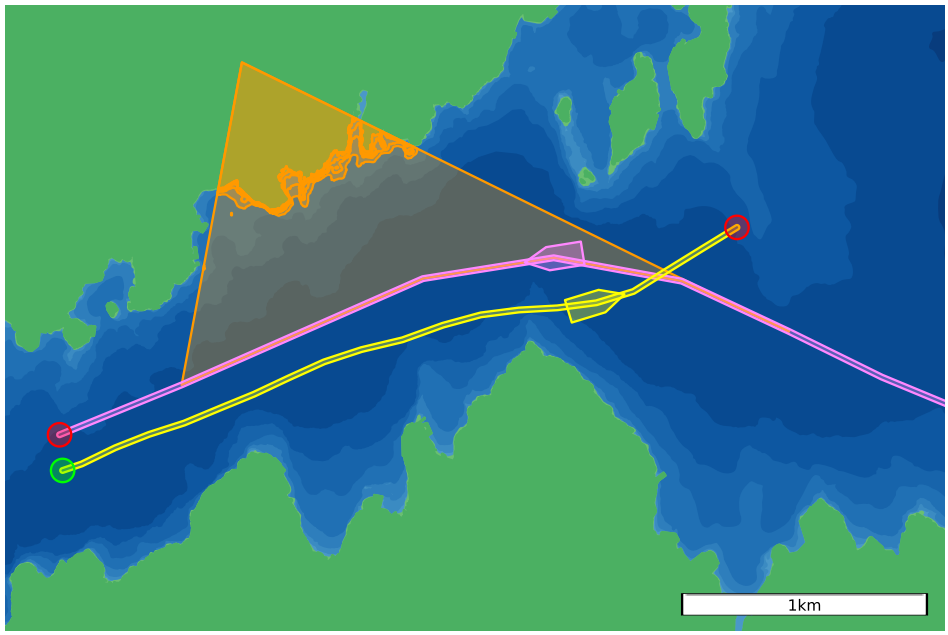

Figure 6.6: Grounding considerations for stand-on vessel (pink) in a crossing situation. A maneuver is detected in Stage 2 and the grounding hazard search area is shown in orange.

allows for a lower turn rate and shortens the traveled distance, thus economic considerations may also influence this decision.

As shown in Table 6.6, the stand-on vessel is penalized (0.59) for its port maneuver. Because the maneuver is initiated at a point where the distance to land (1762 meters) is still more than twice the vessel's tactical diameter ($5 \cdot 170 = 850$ meters), no compensation is given. This is appropriate with regards to the evaluation of COLREGs compliance, as the maneuvering space available is sufficient for a later maneuver. Other considerations, such as economy, should be dealt with separately outside the EvalTool framework.

Case 5

Another crossing situation is shown in Figure 6.3, in this scenario the stand-on vessel is moving out into open water from a passage between two islands, then making a port turn to continue westwards along the coast. This maneuver is continuous throughout Stage 2 and 3, and a maneuver penalty ($\mathcal{P}_{\Delta\chi}$) is therefore given for each stage, see Table 6.7. The change in course angle in Stage 2 is 12 degrees and 18 degrees in Stage 3. Due to the formulation of the COLREGs, the course change in Stage 3 incurs a smaller penalty than the one in Stage 2.

The continuous maneuver causes the check for grounding hazards to be performed for both stages, but as no hazards are located, compensation is not given. This is clearly a correct with regards to the absence of grounding hazards in the

Table 6.6: Score comparison with and without grounding hazard compensation for crossing situation in Figure 6.6

Score/Penalty	Without compensation		With compensation	
$\mathcal{S}_{15}$	0.55		0.98	
	Stage 2	Stage 3	Stage 2	Stage 3
$\mathcal{S}_{17}$	0.69	1	0.69	1
$\mathcal{P}_{\Delta\chi}$	0.59	0	0.59	0
$\mathcal{C}_{so}^{gr}$	NA	NA	0.0	0
$\mathcal{P}_{gr}$	NA	NA	0	0

Table 6.7: Score comparison with and without grounding hazard compensation for crossing situation in Figure 6.3

Score/Penalty	Without compensation		With compensation	
$\mathcal{S}_{15}$	0.40		0.40	
	Stage 2	Stage 3	Stage 2	Stage 3
$\mathcal{S}_{17}$	0.73	0.56	0.73	0.56
$\mathcal{P}_{\Delta\chi}$	0.55	0.89	0.55	0.89
$\mathcal{C}_{so}^{gr}$	NA	NA	0	0
$\mathcal{P}_{gr}$	NA	NA	0	0

vicinity. Nevertheless, the low situation score ($\mathcal{S}_{15} = 0.40$) highlights the difficulty of evaluating vessel behavior with regards to the COLREGs in scenarios where the behavior is influenced by geographical restrictions and pre-planned routes.

Case 6

The encounter shown in Figure 6.7 is an obvious overtaking situation, where the southernmost vessel has stand-on responsibilities. The vessels are traveling in an area with several islands where they both need to perform a starboard maneuver to continue through a passage. The vessels involved are large; the stand-on vessel is 90 meters long and the give-way vessel 124 meters. Their average speeds during the encounter are 5.5 meters/second and 7.9 meters/second respectively.

Vessels involved in overtaking situations are moving on near parallel trajectories. The duration of such encounters will therefore be longer than if the same vessels met in a crossing or head-on situation. This is especially true when the difference between the vessels' speeds is small and will lead to a larger distance traveled during the encounter. As the grounding compensations for stand-on vessels are calculated based on the vessel's position at the time of entry into a new stage and the distance traveled while in the stage is longer than for other encounter

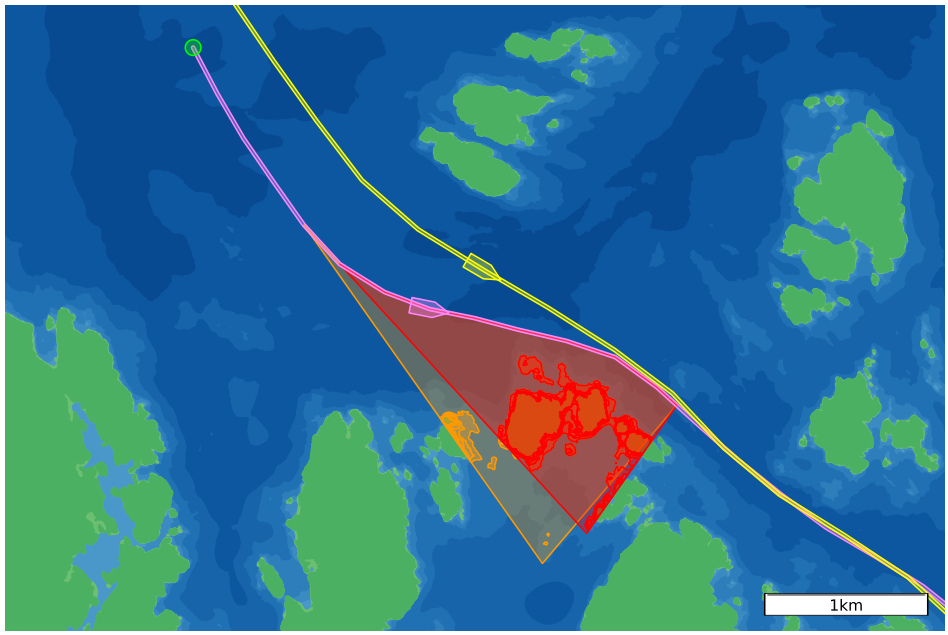

Figure 6.7: Grounding considerations for stand-on vessel (pink) in an overtaking situation. A maneuver is detected in both Stage 2 and Stage 3, the respective grounding hazard search areas are shown in orange and red.

types, it is reasonable to increase the maximum distance to a grounding hazard where compensation will be given. This was done by increasing the value of the γ variable in Equation 6.5 from two to four.

In this case, the give-way vessel makes a port turn of 25.5 degrees and therefore receives no penalty for non-apparent maneuver, but its safety score ($\mathcal{S}_{safety}$) is reduced due to its pose at CPA. For reference, the give-way vessel's total score for the encounter ($\mathcal{S}_{13}$) is 0.78. With regards to the stand-on vessel, the change in course angle during Stage 2 is 14 degrees and 23 degrees during Stage 3, both values that incur a full penalty for their relative stages when not considering grounding, see Table 6.8, this also triggers the grounding hazard checks. At the start of Stage 2 the distance between the vessel and the closest grounding hazard within the zone is 1504 meters and in Stage 3 this distance is 1299 meters. The difference is reflected in the compensation given, 0.22 in Stage 2 and 0.37 in Stage 3. This leads to an increase in the total score ($\mathcal{S}_{13}$), from 0.25 to 0.42.

While the compensations significantly increase the total score they are still quite low if the behavior displayed by the stand-on vessel is to be considered acceptable based on the location of grounding hazards in its surroundings. It therefore seems evident that the γ variable should be adjusted according to the situation type. For overtaking situations, its value should be further increased for encounters where the difference between the vessels' speeds is small and the encounter duration is long.

Another factor, also mentioned in Case 3, that may have affected the stand-

Table 6.8: Score comparison with and without grounding hazard compensation for overtaking situation in Figure 6.7

Score/Penalty	Without compensation		With compensation	
$\mathcal{S}_{13}$	0.25		0.42	
	Stage 2	Stage 3	Stage 2	Stage 3
$\mathcal{S}_{17}$	0.50	0.50	0.61	0.69
$\mathcal{P}_{\Delta\chi}$	1	1	0.78	0.63
$\mathcal{C}_{so}^{gr}$	NA	NA	0.22	0.37
$\mathcal{P}_{gr}$	NA	NA	0	0

on vessel's behavior is its large size. This makes it likely that low turn rates are preferred, thereby requiring an early initiation of course changes. However, as previously discussed this does not necessarily mandate a larger compensation. Other influencing factors outside the scope of safety and COLREGs evaluation are disinclinations to deviate from a pre-planned route, the availability of safety related information such as time to closest point of approach (TCPA) and distance to CPA (DCPA), and possible communications between the vessels.

6.5 Discussion

The results presented in the previous section show that the additional grounding considerations function as described, but that the compensations given are heavily dependent on the EvalTool's tuning. If the goal is to evaluate vessel behavior with respect to how the COLREGs are currently practiced by professional sailors, it seems evident that additional factors must be considered both in the evaluation and the tuning, notably the type of situation along with vessel size and speed.

The methods presented in this chapter are based on identifying intersections between areas representing different depths and trajectories or zones. A natural next step would be to extend the limits of the dangerous areas and thus create a safety margin around them. This can also be used as a way to include environmental forces such as wind or current by placing an additional margin on the side of the area facing the wind/current. This would yield compensations in situation where it is preferable for vessels to keep a greater distance to grounding hazards on the side where environmental forces are pushing the vessel towards the hazard.

6.6 Chapter Summary

This chapter has presented methods for including considerations with regards to the effect of grounding hazards on vessel behavior in the evaluation of safety and COLREGs compliance. If a give-way vessel is given a penalty for an insufficient course change or a stand-on vessel for not maintaining its course and speed, selected areas are checked for grounding hazards that may restrict the vessel's options. If

such restrictions are found, compensations are calculated. The redeeming effect of these considerations on the evaluation scores is presented through the evaluation of selected encounters between vessels in normal operation. The results show that compensation is only given when grounding hazards are indeed restricting the vessels' ability to perform in compliance with the COLREGs. It is also shown that a more limited maneuvering space leads to a higher compensation.

Chapter 7

Identifying Parameters for Collision Avoidance Behaviors

This chapter is based on:

[33] Inger Berge Hagen, Karen Solem Knutsen, Tor Arne Johansen, and Edmund Førland Brekke. Identification of COLREGS Parameters from Historical AIS-data. *Journal of Navigation*, 2022. unpublished/under revision.

7.1 Introduction

MASS and ASVs sharing waters with conventional ships is an inevitable consequence of the shift towards autonomy within the maritime sector. For this to be a viable and safe prospect with respect to collision avoidance, vessel interactions must be regulated. The most direct solution then seems to be the extension of existing traffic rules to also include autonomous vessels.

The COLREGs [42], which regulates the behavior of vessels during encounters at sea, arose in a world where seafaring vessels were controlled by experienced navigators and captains. The rules were therefore left purposely vague, trusting the sailors' expertise (good seamanship) in interpreting how the rules should be applied in different situations. This intentional vagueness poses a challenge when developers attempt to implement the COLREGs within the control algorithms of autonomous vessels. The question at hand is: How to transform the tacit knowledge of experienced sailors into documented information, suitable for implementation in computer programs?

One attempt at such a transformation is the concept of the ship domain. As remarked in [21], there exists an area around ships underway that navigators tend to avoid. Originally denoted the effective domain, the term ship domain, introduced in [23], has since become the more commonplace expression, defined as the area around a ship that the officers on watch (OOW) would like to maintain empty of other vessels. While [21, 23] and other earlier works were limited to information gathered by radar, the introduction of AIS provided researchers with more detailed information concerning vessels and their movements. This was exploited in [29], where AIS data recorded over a one year period in the Gulf of Pomerania was

employed in the creation of probabilistic models for the ship domains of different vessel categories (tankers, passenger and cargo ships) and different encounter types (head-on, crossing, and overtaking). Similar studies into ship domain properties that also make use of AIS data are [70, 73],which focus on areas with high traffic density, and [37], where the limits for comfortable traffic flow in narrow channels are explored. In the latter, the domain is measured in ship lengths.

While the above mentioned works aim to determine the ship domain, this chapter investigates the characteristics of actions taken to avoid the violation of this area. Whether a small course change at a large distance is preferable to a large course change at a smaller distance, or whether the size of the course change is dependent on the size or the speed of the vessels, are examples of questions that must be answered before any MASS can be termed COLREGs compliant. The answers to such questions are central, both to collision avoidance algorithms aiming towards COLREGs compliance, such as [32, 52, 102], and for the evaluation/verification of such methods, exemplified by [68, 89, 99]. As a step towards the safe coexistence of MASSs and conventional ships, this work attempts to: a) identify parameters that can be used in determining COLREGs compliance, b) ascertain acceptable values or intervals for COLREGs parameters, and c) identify correlations between parameters and external factors.

As in the previous works on ship domain, our source of information is historical AIS data. These originate from vessels in normal operation, thereby giving a realistic impression of vessel behavior. Data gathered over several years from three different areas off the coast of Norway were studied in order to obtain a sufficient number of COLREGs-related encounters for the observations regarding customary COLREGs interpretation to be reliable. A database was constructed, containing encounters where at least one of the involved vessels performed an evasive maneuver. In addition to trajectory data and vessel information, supplementary parameters characterizing the encounter and the vessels' behavior was extracted from each situation and added to the data set. These data were then examined in order to identify acceptable values for important parameters, such as the distance at CPA and TCPA at the time when an evasive maneuver is initiated. Attempts to identify determining factors for the vessel's behavior were also made, with special focus on the amount of land in the area and the encounter type.

We will start by explaining the choice of parameters for the study with regards to the COLREGs. Then follows a brief overview of AIS along with a presentation of the raw data sets and pre-processing methods employed. Techniques used for extracting relevant parameters are then explained, followed by a presentation of selected results. The article concludes with a brief discussion around the results, along with some concluding remarks in the chapter summary.

7.2 COLREGS parameters

Previous work on collision avoidance methods aiming for COLREGs compliance have focused on a subset of the steering and sailing rules concerning the conduct of vessels in sight of one another, [91]. The most commonly considered rules are rules 13-15, which describe the desired behavior in overtaking, head-on and crossing

situations. The actions required in these situations are further specified by rules 16, 17 and 8. However, several points within these rules can be regarded as open to interpretation. Below is listed three, considered by the authors as being the most pertinent.

Rule 8(a) *'Any action to avoid collision shall be ... made in **ample time** ... '*

Rule 8(b) *'Any alteration of course and/or speed to avoid collision shall ... be **large enough** to be readily apparent to another vessel observing visually or by radar'*

Rule 8(d) *'Action taken to avoid collision with another vessel shall be such as to result in passing at a **safe distance**'*

Interpreting these phrases is equal to identifying acceptable values for: (a) when an avoidance maneuver should be initiated ($TCPA_{man}$), (b) the necessary size of a course change ($\Delta\chi$) or speed change (ΔU), and (c) the appropriate distance at CPA. However, these values may differ depending on the type of situation and the vessels involved. Moreover, external factors may also affect these values. The factors focused on in this work are the amount of land in the area where the situation occurs, the speed and size of the involved vessels and the number of vessels in the vicinity.

7.3 AIS Data

The AIS is an automatic tracking system and navigational aid that allow vessels to broadcast both static and dynamic information about themselves via digital very high frequency (VHF) radio transmission, and simultaneously receive the same data from vessels nearby. The data studied in this work was gathered by the national AIS network, AIS Norway, which consists of shore-based facilities covering the area from the baseline to 40-60 nautical miles from the coast, along with satellites covering offshore areas, and is operated by the Norwegian Coastal Administration (NAC) [88].

Of the information contained in the AIS-messages, the fields most relevant to this work are the identification (MMSI) and position of the vessel, the position time stamp in coordinated universal time (UTC), SOG, COG and navigational status. The MMSI is static and entered into the device upon installation on the vessel.The remaining fields mentioned are dynamic and automatically updated from ship sensors, except for the navigational status, which must be changed manually by the OOW. Static data are transmitted every 6 minutes, or upon request, while the update rate for dynamic information depends on the vessel's speed and course alterations.

The information available is, however, limited to vessels equipped with AIS transponders, which is only required of vessels subject to the SOLAS convention, in general this will mean larger ships or passenger ships. The AIS referred to by the SOLAS is commonly known as AIS Class A, but less expensive units, termed AIS Class B, intended for non-SOLAS vessels such as domestic commercial vessels and pleasure crafts, are also available. Class B units communicate and operate in conjunction with Class A units, but has less functionality. When studying encoun-

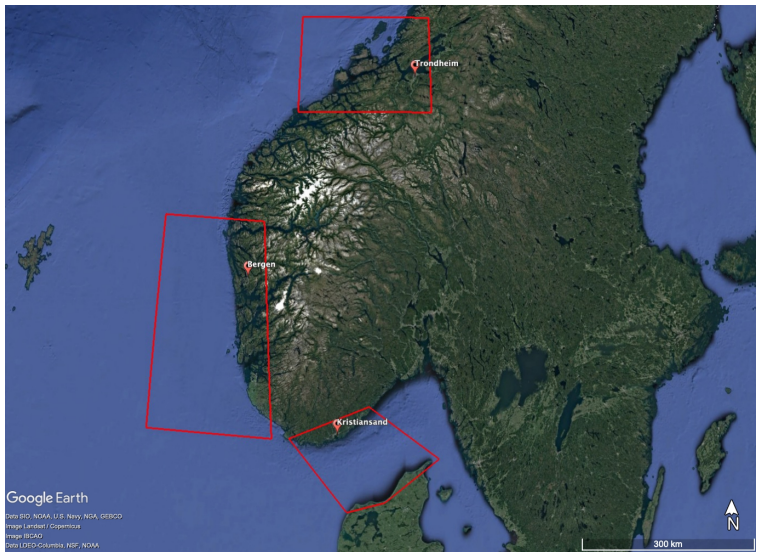

Figure 7.1: Areas where AIS data was collected, outlined in red.

ters collected from AIS data, one must therefore be aware of the possibility of the situation being influenced by vessels not visible in the data.

7.3.1 Datasets

The AIS data that form the basis for this research were gathered from the areas shown in Figure 7.1. These areas were chosen in order to capture encounters occurring in both open waters and in coastal areas where grounding hazards may restrict the vessels' movements. Data were collected for a period of three years and five months for the Northern area, and two years for the Western and Southern areas..

7.3.2 Pre-processing

The pre-processing procedure is based on the work presented in [7]. The following paragraphs describe the steps taken to extract slices from the original data set containing at least one encounter, these slices are henceforth called cases.

Masking docking sites

Locations where multiple vessels gather, such as ports, fish farms and ship-yards form clusters in the data sets. Data transmitted from such locations originate from vessels that are either docked or, if in transit, their conduct is likely to be governed by local rules or conventions and should therefore be excluded from the data sets. The density-based spatial clustering of applications with noise (DBSCAN) algorithm from [17], was employed to identify possible docking locations from the positional information of vessels with their navigational status set to "at anchor".

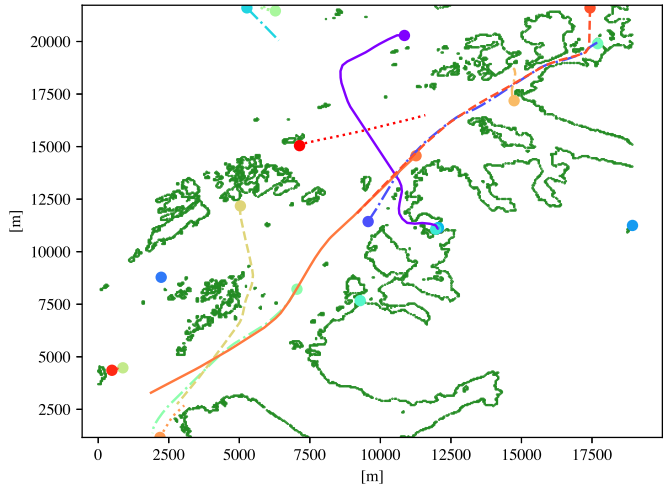

Figure 7.2: Example plot of vessel trajectories contained in one case.

These were then confirmed by manually checking for actual docking facilities at the site. A mask was placed over the site, covering an area with a radius of five kilometers (approximately 2.7 NM) around the identified dock, excluding data transmitted within that area.

Down Sampling and Case Identification

When possible, marine vessels tend to travel in rhumb line segments, making linear approximation a suitable method for down sampling. Disregarding data points where positional data can be linearly interpolated with an accuracy of ten meters[1] significantly reduces the amount of data to be processed in the case identification.

The first step in the case construction is to locate two vessels with an approximate distance at CPA of less than five kilometers (approximately 2.7 nautical mile (NM)). Around this approximate CPA, a time-frame for the case is constructed, defined as the period where the vessels are within 15 kilometers of each other. The geographical extent of the case is then found by taking the rectangular area enclosing these trajectory segments plus a margin of 10 kilometers. Data transmitted within these spatial and temporal limits are then extracted from the data set and combined into a case. A plot including all positional data from one example case is shown in Figure 7.2.

7.3.3 Interpolation

The relevant data has now been separated into smaller cases containing one or more encounters. For each case, the sample times of the AIS messages containing dynamic

[1]The approximate accuracy of AIS positional data as specified by the IMO [43].

Table 7.1: Selection of parameters included in the final data set.

Information Type	Parameter
Situation	Originating data set ID
	Originating case ID
	Date
	Situation type
	Number of vessels included in case
	Distance at CPA
Vessels	ID
	Length
	Average speed during encounter
Maneuver	Total course angle change
	Total speed change
	TCPA at maneuver start
	TCPA at maneuver end

information are synchronized using linear interpolation with a sample interval (Δt) of one minute. Relevant fields from messages containing static information, such as navigational status, ship type and length, are also added for each vessel.

7.4 Parameter Extraction

While the static parameters can be directly extracted from the case data, other information, such as situation type, must be calculated based on the trajectory data from each vessel. This is done separately for each two-vessel encounter. As in the case construction, an encounter is defined as two vessels with an approximated distance at CPA less than five kilometers. A vessel may therefore be involved in several encounters within the same case, each encounter resulting in a separate set of parameters. As a consequence, multi-vessel encounters will be divided into the appropriate number of two-vessel encounters.

An overview of the most relevant parameters can be found in Table 7.1. The remainder of this section explains how parameters are extracted from case data, and specifies the conditions that must be met for an encounter to be included in the final data set.

7.4.1 Situation Type

To investigate how the extracted parameters are affected by the type of COLREGs situation, each encounter was classified as either overtaking, crossing or head-on. For overtaking and crossing situations, the vessels involved were also assigned a role as either the stand-on or give-way vessel, cf. Rules 16 and 17. The classification method is based on an algorithm [99, Alg. 3] categorizing encounters according to the vessels' relative poses, see Figure 7.3. In addition, situations with vessels

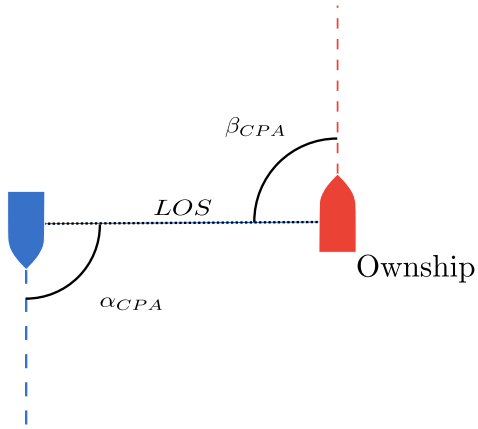

Figure 7.3: Relative pose between vessels: contact angle, $\alpha \in [-180°, 180°)$, and relative bearing $\beta \in [-180°, 180°)$.

engaged in fishing activities, i.e., navigational status set to 7, are removed from the data set, since Rule 18 could change their role or responsibility.

7.4.2 Complete / Non-complete Situations

Due to the spatial and temporal limits of the case data, some of the encounters included in the case may be incomplete and should therefore not be included in the final data set. Encounters are marked as incomplete if:

- The vessels are in a COLREGs situation at the first and/or last time step included in the case, indicating an ongoing or unresolved situation.
- Distance at CPA is less than 50 meters, indicating a collision or deliberate interaction.
- The duration of the situation is less than five minutes.
- Either vessel moves less than 100 meters.

In addition, situation specific requirements on the vessels' relative poses, given by α and β (see Figure 7.3), must be fulfilled for an encounter to be labeled as complete:
Head on: The vessels must have passed each other; $|\alpha|_{max} \geq 90° \wedge |\beta|_{max} \geq 90°$.
Overtake: The vessels must be close to parallel at CPA; $30° \leq |\alpha_{cpa}| \leq 90° \wedge 30° \leq |\beta_{cpa}| \leq 90°$.
Stay-on vessel: Must have passed give-way vessel; $|\alpha|_{min} \leq 90° \wedge |\beta|_{max} \geq 90°$.
Give-way vessel: Must have been passed by stand on vessel; $|\beta|_{min} \leq 90° \wedge |\alpha|_{max} \geq 90°$.
Crossing: One of the vessels must cross the other's line of sight; There exists a time step k within the encounter such that: $\operatorname{sign} \alpha_k \neq \operatorname{sign} \alpha_{k+1} \vee \operatorname{sign} \beta_k \neq \operatorname{sign} \beta_{k+1}$.

7.4.3 Maneuver Detection

Maneuvers are caused by a change in course angle (χ) and/or speed over ground (U). Due to differences in the nature of the signals, the detection process studies each component separately making use of the variables' derivatives, found by finite central differences.

Table 7.2: Parameter values employed in the maneuver detection procedure.

Parameter	Value	Unit
$\epsilon_{\dot{\chi}}$	0.01	rad/s
$\epsilon_{\ddot{\chi}}$	0.01	rad/s^2
$\epsilon_{\dddot{\chi}}$	0.005	rad/s^3
$\epsilon_{\dot{U}}$	0.8	m/s

Course Change

A signal change detection method ([3]) is employed to identify course changes in the data. It is based on derivatives that are smoothed by Gaussian convolution, and is similar to edge detection in image processing ([11]). A maneuver is detected at the k^{th} sample if the following conditions are fulfilled:

$$\begin{aligned} |\dot{\chi}_k| &\geq \epsilon_{\dot{\chi}}, \\ |\ddot{\chi}_k| &\leq \epsilon_{\ddot{\chi}}, \qquad \operatorname{sign} \ddot{\chi}_k \neq \operatorname{sign} \ddot{\chi}_{k-1}, \\ |\dddot{\chi}_k| &\geq \epsilon_{\dddot{\chi}}, \qquad \operatorname{sign} \dddot{\chi}_k \neq \operatorname{sign} \dot{\chi}_{k-1}, \end{aligned} \tag{7.1}$$

where $\epsilon_{\dot{\chi}}$, $\epsilon_{\ddot{\chi}}$ and $\epsilon_{\dddot{\chi}}$ are adjustable parameters, their values can be found in Table 7.2. The start and end indices (k_{man} and k_{stop}) of the maneuver are defined as the time of the nearest third derivative zero, giving the following expression for the total course change of the maneuver:

$$\Delta\chi = \chi(k_{stop}) - \chi(k_{man}) = \sum_{k_{man}}^{k_{stop}} \dot{\chi}\Delta t. \tag{7.2}$$

Speed Change

The speed changes of marine vessels tend to be short and well defined, permitting the use of a simpler detection method where only the first derivative is used. A maneuver is in progress at the k^{th} sample if the following condition is fulfilled:

$$|\dot{U}_k| \geq \epsilon_{\dot{U}}, \tag{7.3}$$

where $\epsilon_{\dot{U}}$ is an adjustable parameter, see Table 7.2. The total speed change of the maneuver is given by:

$$\Delta U = U(k_{stop}) - U(k_{man}) = \sum_{k_{man}}^{k_{stop}} \dot{U}\Delta t. \tag{7.4}$$

Evasive and Non-evasive Maneuvers

In order to exclude encounters where vessel behavior is directed by factors other than the COLREGs, only encounters where the give-way vessel performs an evasive maneuver are retained. This will exclude multi-vessel encounters where the maneuvers made are restricted by, or intended to avoid vessels not considered in the two-vessel encounter. A maneuver is tentatively marked as evasive if the following is true:

- The distance at CPA is predicted at the start and end points of the maneuver using a constant velocity (CV) model for both vessels and the maneuver causes an increase in the predicted distance at CPA.
- For head-on situations and for give-way vessels in crossing situations, any course change must be towards starboard side.

For encounters containing multiple evasive maneuvers, only the maneuver causing the largest increase in distance at CPA is included in the set of parameters.

However, these measures do not guarantee that the primary purpose of the maneuver is collision avoidance. Other possible reasons include grounding hazards and vessels not included in the situation (with or without AIS transponders). To increase the likelihood that the intention behind the maneuver is truly collision avoidance, the trajectories from each encounter is manually inspected before its parameters are added to the final data set.

7.4.4 Missing and erroneous messages

For some vessels the AIS messages do not contain information on the vessel size and the information had to be retrieved manually from an online resource, [60], using the vessels' MMSI.

7.5 Results

The procedure detailed in the previous sections produces a data set containing parameters extracted from encounters where the distance at CPA is less than 5 kilometers, and an evasive maneuver has been performed in accordance with the qualitative behavior prescribed by the COLREGs. From the 2974 cases extracted from the raw AIS data, 28421 encounters were identified. Of these, 782 encounters were considered complete, COLREGs compliant and containing both an evasive maneuver and the necessary information. The used data set thus consists of 782 entries, whereof 110 crossing, 230 overtaking and 442 head-on situations. This section presents statistics inferred from this data set and shows the relations between selected parameters.

7.5.1 External parameters

One of the questions that this work set out to answer is whether external parameters affect vessel behavior. Considered as particularly interesting is vessel size, the type of area in which the encounter occurs, and traffic density in the area.

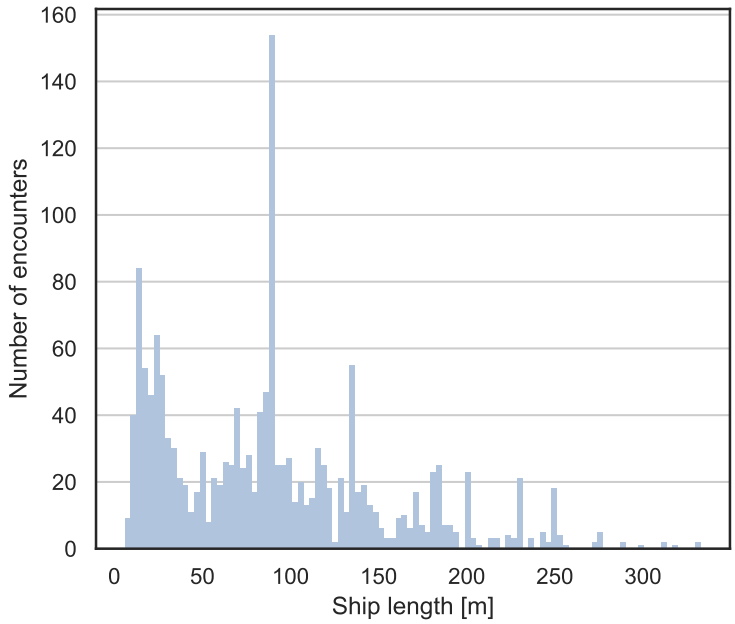

Figure 7.4: Distribution of vessel lengths in the data set, the lengths of both own ship and obstacle ship are included.

The length of a vessel is used as a representation of its size. This was chosen because of its significant effect on both ship dynamics and ship domain. While the recorded lengths in the parameter set range from 6 to 333 meters, see Figure 7.4, most (around 73%) of the vessels are between 15 and 150 meters long.

Instead of attempting to classify encounter locations into area types, such as open water, archipelago or fjord, it was chosen to calculate the percentage of land in a 14 by 14 kilometer area around the encounter, for simplicity this number will from now on be referred to as land coverage. While this classification method may seem simplistic, it is used to indicate the likelihood of a vessels' behavior being affected by grounding hazards and is sufficient for our purposes. The distribution of encounters according to percentage of land is shown in Figure 7.5. Of the 782 encounters, almost half of them occur in areas with less than 10 % land coverage.

The number of vessels included in the originating case was used as a measure for traffic density, the distribution is shown in Figure 7.6. Again, this is a simple and straight forward approach but may reveal whether traffic density is an important factor in vessel behavior.

7.5.2 Distance at CPA

The average distance at CPA with regards to situation type and land coverage is shown in Figure 7.7. When disregarding the land coverage, overtaking situations have the highest average distance at CPA at 1007 meters, followed by crossing

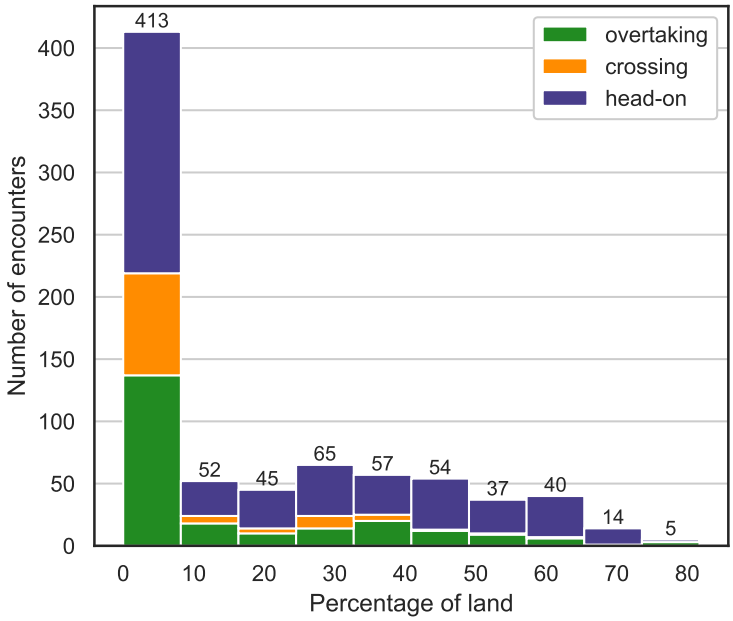

Figure 7.5: Distribution of encounters vs. the percentage of land in a 14 by 14 kilometer area surrounding the encounter, according to situation type.

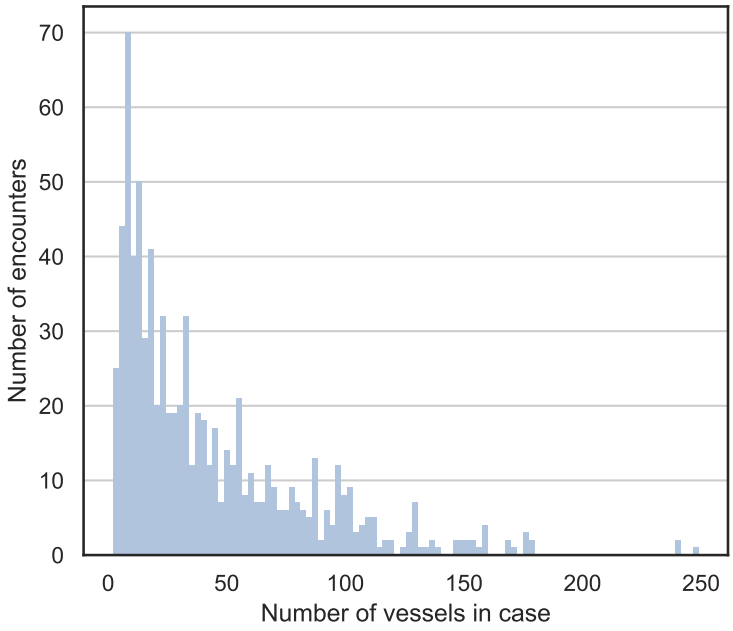

Figure 7.6: Distribution of the number of vessels in the originating case for each situation.

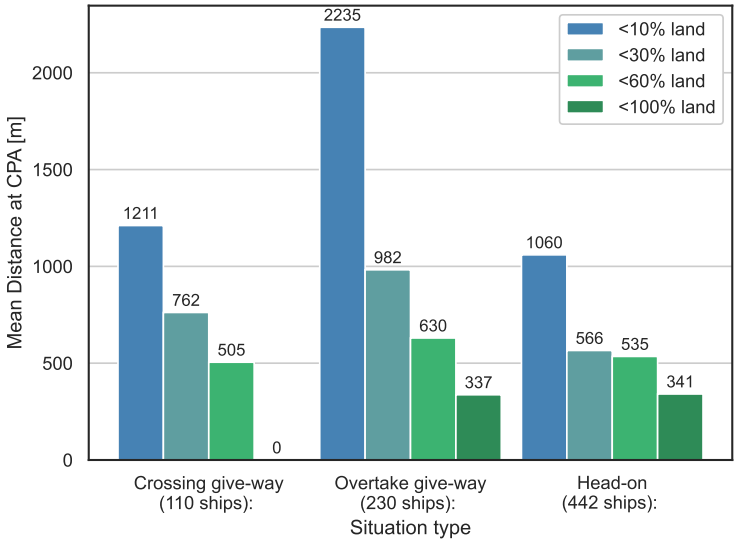

Figure 7.7: Mean distance at CPA for each situation types, according to situation type and the area's land coverage.

situations at 886 meters, and head-on situations at 597 meters. The difference between the highest and lowest is 410 meters, which is more than four ship lengths for 64% of the recorded vessels. For all situation types, the average distance at CPA decreases when the amount of land in the area increases.[2]

The relation between distance at CPA and land coverage, according to situation type, is also illustrated in Figure 7.8. Notable in this plot is the 121 overtaking situations that occurred in areas with zero land coverage, where the distance at CPA ranges from 60 to 4700 meters. The large spread in the recorded values makes it difficult to recommend a general value for distance at CPA suitable for this type of situation. For crossing situations in areas with more than 60% land coverage, only one situation fall within the category, and no recommendations can be given. For the remaining categories, the mean values appears to be a reasonable estimate for the preferred distance at CPA as practiced at sea.

The relationship between distance at CPA and the average speed of the own ship, again according to situation type, is shown in Fig 7.9. The plot shows that vessels overtaking others, not surprisingly, tend to have higher average speeds than vessels in other situations. It also appears like the lowest distance at CPA seems to increase slightly with the speed, but no strong correlations are evident in the data. With regards to vessel length, there does again seem to be a slight correlation between the length of the own ship and the distance at CPA, which can be seen in Figure 7.10.

[2]The exception is crossing situations where the average distance at CPA for the highest percentages of land is above the situation mean. However, the data set only contains one entry in this category which has been excluded from the plots to avoid misrepresenting the results since a single observation is obviously not statistically significant.

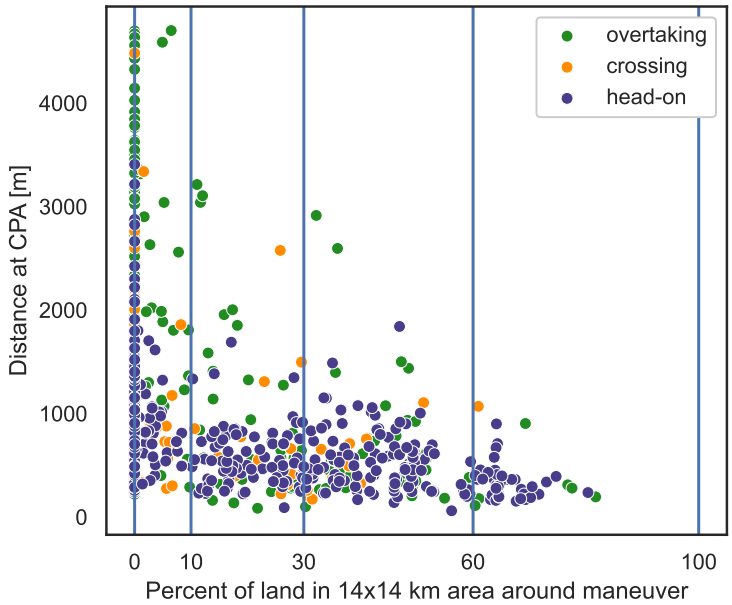

Figure 7.8: Distance at CPA vs. land coverage, according to situation type.

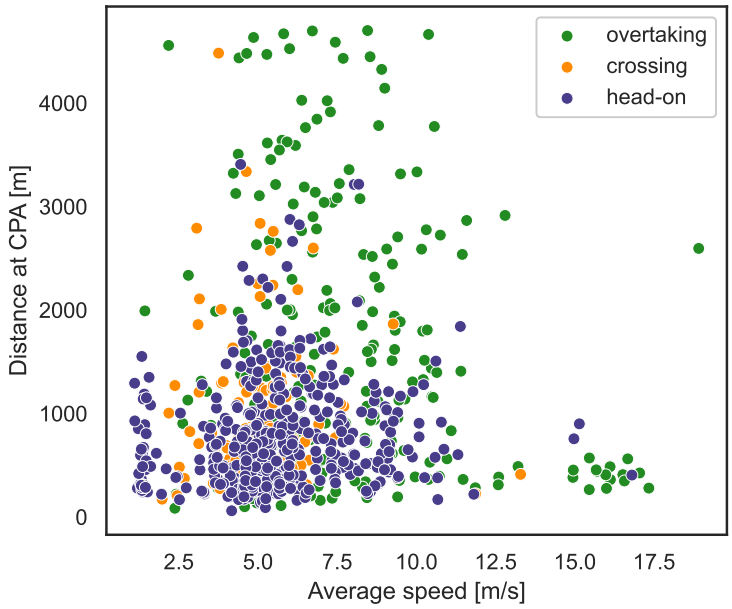

Figure 7.9: Distance at CPA vs. own ship's average speed during the encounter, according to situation type.

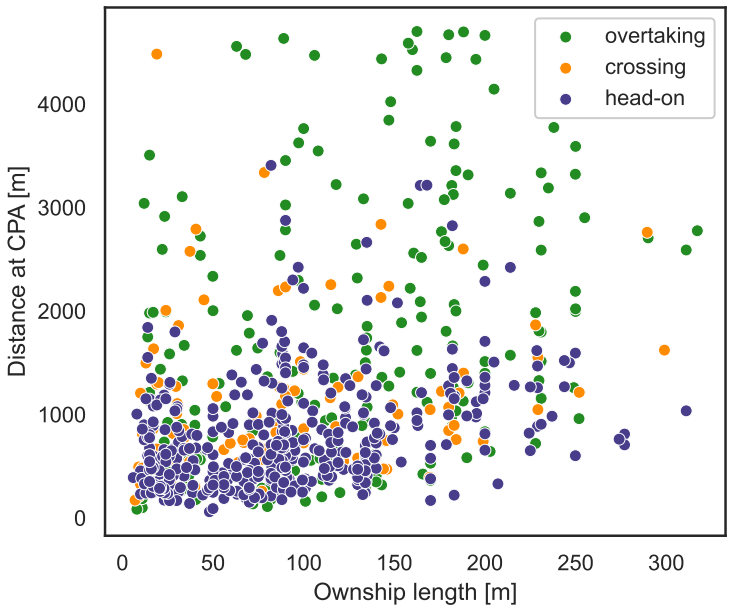

Figure 7.10: Distance at CPA vs. own ship's length during the encounter, according to situation type.

7.5.3 TCPA

The TCPA is the predicted time to CPA, assuming both vessels keep constant course and speed, and is often made available to the OOW through navigational aids. The TCPA when an evasive maneuver is initiated ($TCPA_{man}$) is therefore a parameter of interest. The means of the $TCPA_{man}$ according to land coverage, Figure 7.11, show that land coverage is a determining factor. Independent of land coverage, the mean value is 2454 seconds (40.9 minutes) for crossing situations, 2338 seconds (40.0 minutes) for overtaking situations and 1658 seconds (27.6 minutes) for head-on situations. As for the distance at CPA, encounters occurring in open waters display significantly larger values for $TCPA_{man}$. When disregarding areas with less than 10% land coverage, the mean $TCPA_{man}$ values are 1101 seconds (18.3 minutes) for crossing situations, 825 seconds (13.8 minutes) for overtaking situations and 861 seconds (14.4 minutes) for head-on situations. Again, due to a lack of data, the mean is not shown for crossing situations in areas with more than 60% land coverage.

To put this into perspective; the difference in mean $TCPA_{man}$ between crossing and overtaking situations (1101 and 825 seconds respectively) equals a distance of about 1380 meters for a vessel traveling at a speed of 10 knots, or about 5 meters per second. This represents more than four ship lengths for all the recorded vessels, and more than 8 ship lengths for 88% of them.

While it would be natural to assume that vessel speed could influence the choice of when to make a maneuver, no such connection was found in the data. This is

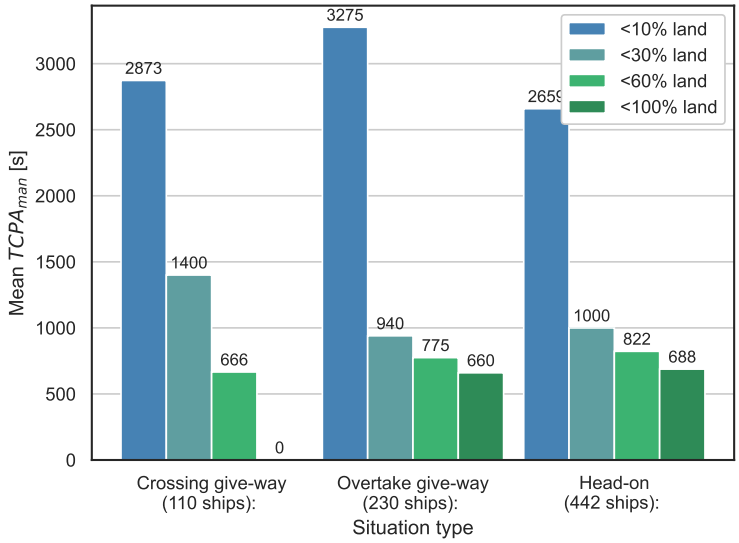

Figure 7.11: Mean predicted TCPA at maneuver start, according to situation type and the area's land coverage.

supported by Figure 7.12, which shows the $TCPA_{man}$ plotted against the own ship's average speed, similar results were found with regards to the obstacle vessel's speed.

7.5.4 Course change

A change in course angle is more readily apparent to other vessels than a change in speed, and is the preferred action to avoid collision by the COLREGs. It is thus a very relevant parameter for both collision avoidance and evaluation algorithms. In both head-on and crossing situations the COLREGs prescribe that any change in course angle should be towards starboard, while in overtaking situations both port and starboard maneuvers are allowed. In this section's plots, a negative change in course angle signifies a starboard turn, while positive values indicate port turns.

The distribution of course angle changes in overtaking situations is shown in Figure 7.13. In 102 (45%) of the 230 situations, the give-way vessel make a starboard turn, and in 125 (55%) a port turn. In absolute values, the change in course angle ranges from 0 to 42 degrees, with 76 % of the maneuvers in the 5 to 25 degrees range.

In head-on situations, the COLREGs require that changes in course angle should be to starboard, i.e. negative. The distribution of course angle changes for this situation type is shown in Figure 7.14 and ranges from 0 to -70 degrees. For this situation type 99% of the maneuvers are below 30 degrees and 66 % are in the range 5 to 15 degrees.

The course angle changes in give-way maneuvers in crossing situations, which should also be negative, fall within the range -1 to -74 degrees. Their distribution is

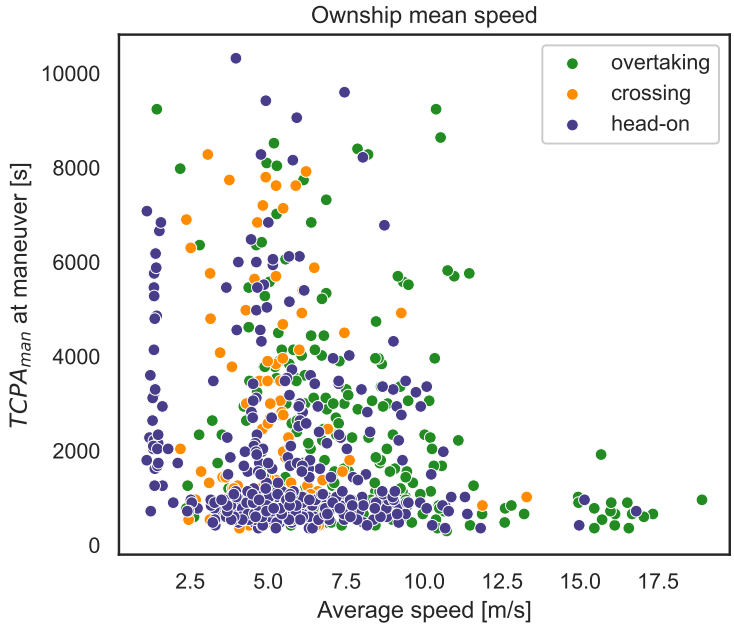

Figure 7.12: Predicted TCPA at maneuver start vs. own ship's average speed, according to situation type.

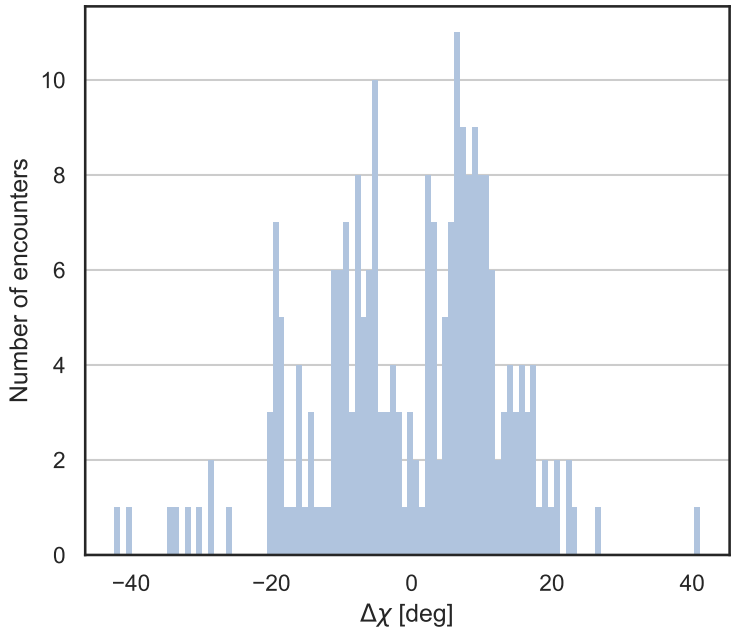

Figure 7.13: Distribution of change in course angle for the 230 overtaking maneuvers.

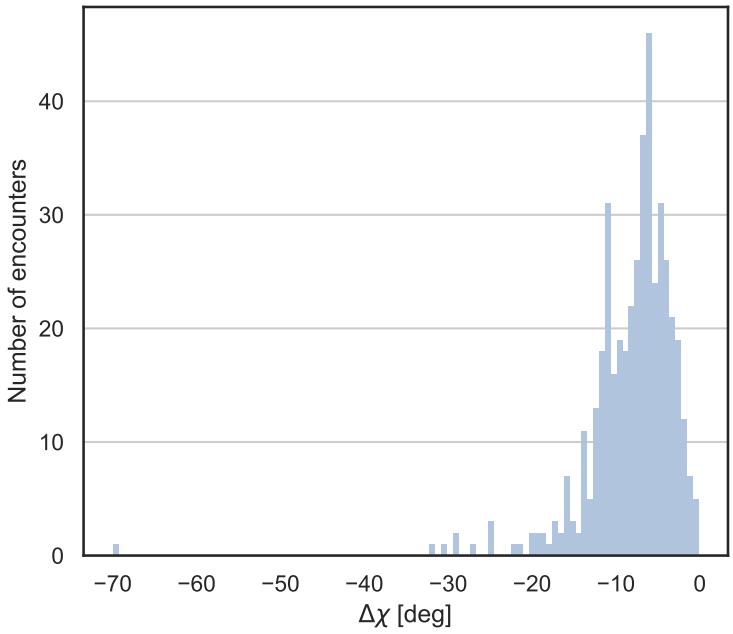

Figure 7.14: Distribution of change in course angle in 442 head-on situations.

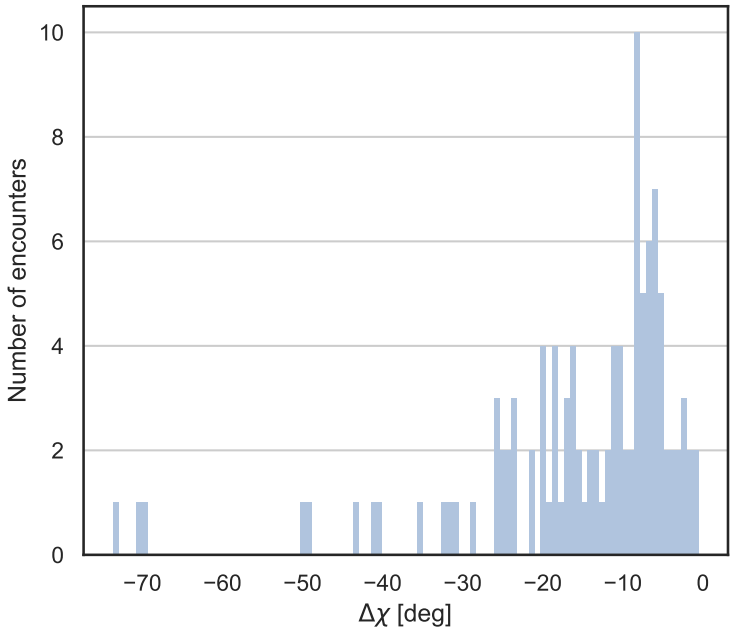

Figure 7.15: Distribution of change in course angle by give-way vessels in 110 crossing situations.

Table 7.3: Mean course angle change according to situation and land coverage. For overtaking situations, the mean is shown for all maneuvers (^{abs}), starboard turns only^{+} and port turns only^{-}.

Situation type	Land coverage			
	0 – 9%	10 – 29%	30 – 59%	60 – 100%
Head-on	−9.6°	−8.0°	−7.5°	−6.1°
Crossing	−16.2°	−11.4°	−10.6°	–
Overtaking^{+}	9.8°	8.9°	10.3°	10.3°
Overtaking^{-}	−14.8°	−8.3°	−12.4°	−12.4°
Overtaking^{abs}	11.3°	8.6°	11.6°	11.6°

shown in Figure 7.15, where 76% of the maneuvers are within the -5 to -30 degrees range.

The means of the course angle changes in the different situations according to land coverage (see Table 7.3) show that in head-on and crossing situations, there seems to be a tendency towards smaller course angle changes with increased land coverage. However, for overtaking situations there is no obvious correlation between course angle change and land coverage.

7.5.5 Speed changes

If changing the course angle to avoid collision is not practicable, the speed can be changed. For obvious reasons this type of action is most suitable for crossing situations. However, as shown in Figure 7.16, the speed changes recorded in the data set are in general too small to have a significant influence on the situation. In total, only 27 of the 782 situations have speed changes larger than 1 meter per second (about 2 knots), and it is evident that changing course is the preferred action in collision avoidance situations.

7.5.6 Traffic density

The effect of traffic density in the area with regards to the different parameters was also investigated. As an example, the distance at CPA is plotted against the number of vessels in the encounter's originating case in Figure 7.17. As expected, a low number of vessels in the area allows for a large distance at CPA, while more traffic tend to restrict the distance at CPA to lower values. There is also a tendency towards higher traffic in areas with more land coverage. This may be somewhat misleading with regards to the distance at CPA, as some of this traffic may be constrained by land, thereby not having any influence on the vessels' behavior.

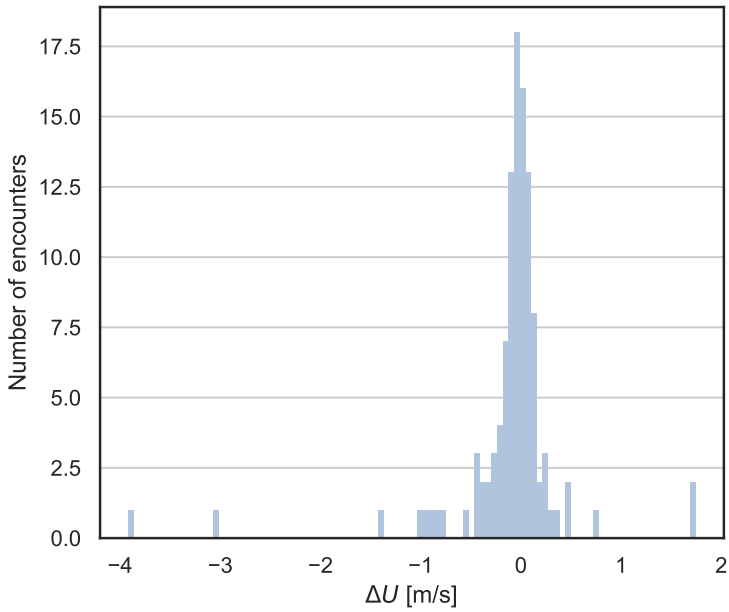

Figure 7.16: Distribution of speed changes for crossing situations, excluding situations with no changes in speed.

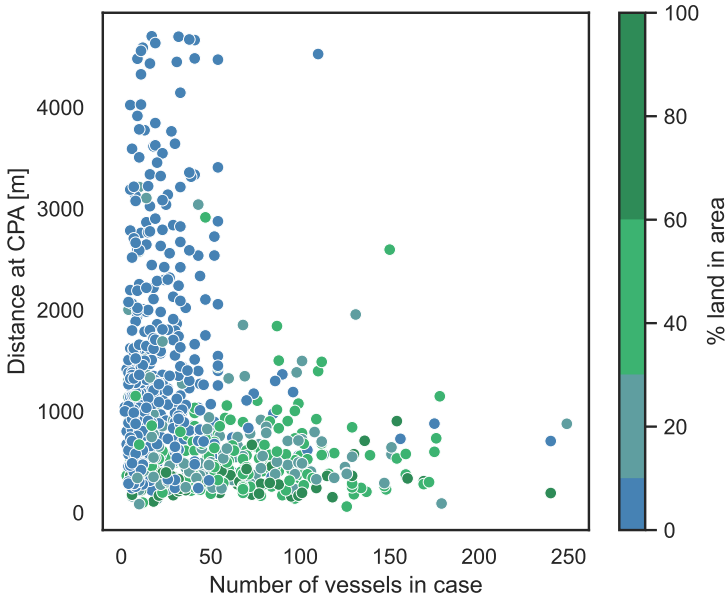

Figure 7.17: Distance at CPA vs number of vessels in originating case.

7.6 Discussion

Encounters between vessels are relatively rare and their behavior may be directed by other factors than the COLREGs. Filtering out irrelevant data and identifying encounters where the vessels behave according to the COLREGs is therefore an important task in this work. While the drastic reduction in the number of situations after filtering may seem excessive, it is necessary in order to obtain reliable information about COLREGs compliant behavior. Nevertheless, obtaining a larger selection of encounters that can produce more statistically significant results is an important task that remains for future work.

The plots presented in Section 7.5 show that vessel behavior is correlated with the percentage of land coverage in the area, but a more accurate method for classifying the area type may improve our understanding on this point. For instance, it is likely that vessels traveling in a fjord or narrow strait, where vessels often move in established lanes, will display behaviors different to those of vessels traveling in an archipelago where the vessels are restricted by multiple shallows and islands.

The presented results give an indication of customary behavior in collision avoidance situations, which may be improved if even larger data sets are studied, as further division of the data according to vessel type and size may reveal hereto undiscovered correlations. Further work is also required to identify correlations between other parameters that may have an impact on vessel behavior. This also applies to environmental influences such as wind, visibility and sea-state, which has not been considered in this work.

7.7 Chapter Summary

A procedure for identifying vessel encounters containing collision avoidance situations from recorded AIS data has been presented, along with a method for extracting parameters characterizing the evasive maneuvers performed. The technique was tested on AIS data gathered from vessels in three areas off the Norwegian coast over a period of several years, resulting in a data set containing information on how the COLREGs are currently practiced. The data are presented graphically, showing the distributions of, and relationships between relevant parameters. The data do not recommend specific values for use in methods for collision avoidance or the evaluation of these. However, for several parameters the range of recorded values along with their average do point to what should be considered as acceptable values, depending on the type of situation and the amount of land in the area. This contributes to a better understanding of what factors should be considered by collision avoidance algorithms and how these can be verified for use in autonomous vessels. The natural continuation of this work is to obtain a larger dataset providing more statistically significant results, and further the investigation into determining factors for vessel behavior.

Chapter 8

Concluding Remarks and Future Work

The purpose of this chapter is twofold. It primarily serves as a resume of the outcomes of the works presented in Chapters 2 to 6. Additionally, it aims to place these contributions within the wider context of not just previous works on the topics, but also a suggested outline of the road ahead.

8.1 Conclusions

Part I - Tracking: This part investigated the feasibility of tracking a kayak using a lidar sensor. The tracking approach forming the main contribution of this chapter, employs a single-target EOT method, where the target is modeled by a stick approximation. The method's performance was investigated through a simulation study and the results were verified through testing on recorded lidar data.

While the results show promise, there are still many possibilities for future improvements and extensions. A natural continuation of the work would include testing the method on data collected by a lidar sensor with a higher vertical resolution than the one used in the presented work. This would determine what measures should be taken to remedy the lack of measurements between beams. To be of real use in urban environments the system should also be extended with target models for other vessel types that are likely to be encountered in an urban environment. This can also be combined with an image detection algorithm to identify the type of target from camera images, and thereby aid in the selection of an appropriate target model.

Part II - Collision Avoidance: The second part of this thesis proposed a method for COLREGs compliant collision avoidance, suitable for integration within existing guidance and control architectures for marine vessels. The presented method implements an MPC-based approach with a restricted number of alternative control behaviors, thereby avoiding many of the disadvantages of numerical optimization. This formulation also facilitates integration of additional constraints, with their importance and influence weighted according to human priorities.

Increasing the number of decision points, i.e., time steps where the control behaviors can be modified, did not produce significant changes to the resulting behavior. However, the calculation of a possible return point proved a significant improvement to prediction accuracy for the vessels' future movements. When transmitted to an operator, this information provides a better foundation for decision making. This can be useful to operators aboard the vessel itself, those aboard other vessels in the vicinity or to a supervisor located at a remote SCC with remote-control capabilities.

Due to the ease of including additional constraints into the proposed method it is natural to consider the inclusion of grounding hazards and land as a logical next step. Efforts are currently underway to achieve this, but there are still unresolved challenges to be met. Thought must also be given to the likelihood of differences in the collision avoidance behavior of vessels in open waters and vessels operating in waters where their movements are restricted. This would indicate that efforts should also be put into adapting the method to produce slightly different behaviors according to situation and location. This can be achieved by modifications to the cost-function, situation specific tuning or a combination of the two. The current tuning of the presented algorithm was obtained through experimentation, which is a laborious and time-consuming task. The prospect of multiple tunings therefore encourages investigation into automatic tuning, using for instance machine learning.

Another avenue for future exploration is improving the predictions for the movements of obstacle vessels, which is especially important when the maneuvering space is restricted. One approach to achieving this is the inclusion of vessel dynamics in the prediction model, this can for instance be based on the obstacle's size. A second, more challenging approach, is to include expected obstacle behavior in the predictions. This would include considerations regarding COLREGs compliance, grounding hazards and possibly location specific expectations.

Part III - Evaluation: This final part explores the topic of COLREGs compliance in terms of evaluation and identification. This includes a method for evaluating the behavior of vessels in collision avoidance encounters along with a study into the properties of behaviors displayed by vessels in normal operation. Automatic evaluation of COLREGs behavior is a vital component in simulation-based verification schemes, but can also be a useful aid in the development of collision avoidance algorithms as a tool for identifying problematic behaviors. For the latter application, a finite set of predefined scenarios may be sufficient to produce useful results. The former will, however, depend on methods for generating and selecting scenarios that explore the limits of the systems being tested. They must also provide estimates of the results' reliability. This development of such frameworks is therefore an important topic for future research.

The presented study of COLREGs compliant behavior, according to current practices at sea, provides necessary information for the tuning of the evaluation algorithm. It also identifies factors that influence that behavior and therefore should be accounted for both in the evaluation process, but also in the collision avoidance algorithms themselves. The results show that the type of situation and the amount

of land in the vicinity are, as expected, the most influential of the factors studied. However, the size of the available data sets limited the number of encounters included in the study which put restrictions on which factors could be investigated. Future investigations should therefore aim to include a higher number of encounters in order to investigate additional factors and provide results with a greater statistical significance.

8.2 Other Remarks

This thesis touch upon several distinct, yet related topics, and while the methods presented in each chapter can be viewed as separate contributions to their own distinct fields, they are better viewed as connected parts of the puzzle leading to the realization of autonomous ships.

The EOT method presented in Chapter 2 is a contribution specifically aimed towards the implementation of autonomous vessels as urban ferries. This application allows for the use of existing infrastructures, which facilitates the task of communication between the vessel and the SCC responsible for supervising the ferries. The experience gained through the operation of such centers will provide valuable information for the development and deployment of autonomous ships in more isolated areas where communication related issues pose an additional challenge.

Even assuming perfect communication, it will be desirable for the vessels to be able to operate autonomously, thereby reducing the need for intervention to a minimum. The collision avoidance algorithm presented in Part II is a contribution towards this goal. Until SCCs for seagoing vessels become a reality, the method's easy integration into existing systems along with its short term planning abilities also make it suitable as a decision support system. Such an approach will enable the collection of valuable data regarding any discrepancies between the algorithms' recommendations and the navigator's decisions which can be used to further improve the method. Coherence between the two will on the other hand help building confidence in the system, easing the transition into conditional autonomy.

This transition will require that the autonomy system, as any other system aboard a marine vessel, is verified by the proper authorities. The work of Part III is a step towards this in that it contains contributions both the with respect to the evaluation process itself, but also to the definition of the evaluation criteria. Whether simulation-based approaches will be used in the verification of ASVs also depends on the development of methods assuring sufficient test-space coverage and acceptable levels of uncertainty in the results.

As a last remark, it must be said that the diversity of topics covered does limit the time dedicated to each. However, this somewhat holistic approach also gives useful insights into the connections and dependencies between the respective systems, and brings to light the complexity of many of the challenges that must be met, before autonomous ships will rule the waves.

References

[1] Melih Akdag, Tor Inge Fossen, and Tor Arne Johansen. Collaborative Collision Avoidance for Autonomous Ships Using Informed Scenario-Based Model Predictive Control. In *14th IFAC Conference on Control Applications in Marine Systems, Robotics, and Vehicles*, Copenhagen, 2022.

[2] Yaakov Bar-Shalom and Xiao-Rong Li. *Multitarget-Multisensor Tracking: Principles and Techniques*. YBS Publishing, Storrs, CT, 1995.

[3] Michele Basseville and Igor V. Nikiforov. *Detection of abrupt changes: theory and application*, volume 104. prentice Hall Englewood Cliffs, 1993.

[4] Fuat Beser and Tulay Yildirim. Colregs based path planning and bearing only obstacle avoidance for autonomous unmanned surface vehicles. *Procedia Computer Science*, 131:633–640, jan 2018. ISSN 1877-0509. doi: 10.1016/J.PROCS.2018.04.306.

[5] Simon Blindheim and Tor Arne Johansen. Electronic Navigational Charts for Visualization, Simulation, and Autonomous Ship Control. *IEEE Access*, 10:3716–3737, 2021. ISSN 2169-3536. doi: 10.1109/ACCESS.2021.3139767.

[6] Edmund Brekke and Mandar Chitre. A multi-hypothesis solution to data association for the two-frame SLAM problem. *The International Journal of Robotics Research*, 34(1):43–63, 2015. ISSN 0278-3649. doi: 10.1177/0278364914545674.

[7] Olav Buset Vassbotn. Analysis of ship collision risk encounters and colreg behaviours using machine learning and ais data. Msc, Norwegian University of Science and Technology (NTNU), 2022.

[8] Raphael Cagienard, Pascal Grieder, Eric C. Kerrigan, and Manfred Morari. Move blocking strategies in receding horizon control. *Journal of Process Control*, 17(6):563–570, 2007.

[9] Charmane V. Caldwell, Damion D. Dunlap, and Emmanuel G. Collins. Motion planning for an autonomous underwater vehicle via sampling based model predictive control. In *OCEANS 2010 MTS/IEEE SEATTLE*, pages 1–6. IEEE, 2010.

[10] Sable Campbell, Wasif Naeem, and George W. Irwin. A review on improving the autonomy of unmanned surface vehicles through intelligent collision avoidance manoeuvres. *Annual Reviews in Control*, 36(2):267–283, 2012. ISSN 1367-5788. doi: 10.1016/J.ARCONTROL.2012.09.008.

[11] John Canny. A computational approach to edge detection. *IEEE Transactions on Pattern Analysis and Machine Intelligence*, PAMI-8(6):679–698, nov 1986. ISSN 0162-8828. doi: 10.1109/TPAMI.1986.4767851.

[12] Ki-Yin Chang, Gene Eu Jan, and Ian Parberry. A Method for Searching Optimal Routes with Collision Avoidance on Raster Charts. *Journal of Navigation*, 56(3):371–384, sep 2003. ISSN 0373-4633. doi: 10.1017/S0373463303002418.

[13] Alfred Norman Cockcroft and Jan Nanne Frits Lameijer. Part B - Steering and sailing rules. In *Guide to the Collision Avoidance Rules*, pages 11–104. Butterworth-Heinemann, Oxford, 7 edition, 2012.

[14] Lester Eli Dubins. On Curves of Minimal Length with a Constraint on Average Curvature, and with Prescribed Initial and Terminal Positions and Tangents. *American Journal of Mathematics*, 79(3):497, jul 1957. ISSN 00029327. doi: 10.2307/2372560.

[15] Bjørn-Olav H. Eriksen and Morten Breivik. MPC-Based mid-level collision avoidance for ASVs using nonlinear programming. In *Conference on Control Technology and Applications (CCTA)*, pages 766–772, Kohala Coast,Hawaii, 2017. ISBN 978-1-5090-2182-6. doi: 10.1109/CCTA.2017.8062554.

[16] Bjørn-Olav H. Eriksen, Morten Breivik, Kristin Y. Pettersen, and Martin S. Wiig. A modified dynamic window algorithm for horizontal collision avoidance for AUVs. In *IEEE Conference on Control Applications (CCA)*, pages 499–506, 2016. ISBN 978-1-5090-0755-4. doi: 10.1109/CCA.2016.7587879.

[17] Martin Ester, Hans-Peter Kriegel, Jörg Sander, Xiaowei Xu, et al. A density-based algorithm for discovering clusters in large spatial databases with noise. In *kdd*, volume 96, pages 226–231, 1996.

[18] European Maritime Safety Agency. Annual Overview of Marine Casualties and Incidents 2020, 2020. ISSN 1098-6596.

[19] Thor I. Fossen. *Handbook of Marine Craft Hydrodynamics and Motion Control*. John Wiley & Sons, Ltd, 2011.

[20] Dieter Fox, Wolfram Burgard, and Sebastian Thrun. The dynamic window approach to collision avoidance. *IEEE Robotics & Automation Magazine*, 4 (1):23–33, mar 1997. ISSN 10709932. doi: 10.1109/100.580977.

[21] Yahei Fujii and Kenichi Tanaka. Traffic capacity. *Journal of Navigation*, 24 (4):543–552, oct 1971. ISSN 0373-4633. doi: 10.1017/S0373463300022384.

[22] Ravi Gondhalekar and Jun ichi Imura. Least-restrictive move-blocking model predictive control. *Automatica*, 46(7):1234–1240, 2010. ISSN 0005-1098.

[23] Elisabeth M. Goodwin. A statistical study of ship domains. *Journal of Navigation*, 28(3):328–344, jul 1975. ISSN 0373-4633. doi: 10.1017/S0373463300041230.

[24] Karl Granström, Christian Lundquist, and Umut Orguner. Tracking Rectangular and Elliptical Extended Targets Using Laser Measurements. In *14th International Conference on Information Fusion*, pages 592–599, Chicago, Illinois, 2011. IEEE.

[25] Karl Granström, Stephan Reuter, Daniel Meissner, and Alexander Scheel. A multiple model PHD approach to tracking of cars under an assumed rectangular shape. In *17th International Conference on Information Fusion (FUSION)*, pages 1–8, Salamanca, 2014. IEEE. ISBN 9788490123553.

[26] Karl Granström, Marcus Baum, and Stephan Reuter. Extended Object Tracking: Introduction, Overview and Applications. *Journal of Advances in Information Fusion*, 12(2):139–174, 2017. ISSN 1557-6418.

[27] Karl Granström, Stephan Reuter, Maryam Fatemi, and Lennart Svensson. Pedestrian tracking using Velodyne data - Stochastic optimization for extended object tracking. In *Intelligent Vehicles Symposium (IV)*, pages 39–46, Redondo Beach, CA, 2017. IEEE. ISBN 9781509048038. doi: 10.1109/IVS.2017.7995696.

[28] Karl Granström, Lennart Svensson, Stephan Reuter, Yuxuan Xia, and Maryam Fatemi. Likelihood-based data association for extended object tracking using sampling methods. *IEEE Transactions on Intelligent Vehicles*, 3 (1):30 – 45, 2018. ISSN 2379-8904. doi: 10.1109/TIV.2017.2788184.

[29] Lucjan Gucma and Krzysztof Marcjan. Examination of ships passing distances distribution in the coastal waters in order to build a ship probabilistic domain. *Scientific Zeszyty Naukowe Akademii Morskiej w Szczecinie*, 32 (104):34–40, 2012.

[30] Inger Berge Hagen. Collision Avoidance for ASVs using Model Predictive Control. Msc, Norwegian University of Science and Technology (NTNU), 2017.

[31] Inger Berge Hagen and Edmund Brekke. Kayak tracking using a direct lidar model. In *Global Oceans 2020: Singapore–US Gulf Coast*, pages 1–7. IEEE, 2020.

[32] Inger Berge Hagen, D. Kwame Minde Kufoalor, Edmund Førland Brekke, and Tor Arne Johansen. MPC-based Collision Avoidance Strategy for Existing Marine Vessel Guidance Systems. In *IEEE International Conference on Robotics and Automation*, Brisbane, QLD, 2018.

[33] Inger Berge Hagen, Karen Solem Knutsen, Tor Arne Johansen, and Edmund Førland Brekke. Identification of COLREGS Parameters from Historical AIS-data. *Journal of Navigation*, 2022. unpublished/under revision.

[34] Inger Berge Hagen, D. Kwame Minde Kufoalor, Edmund Førland Brekke, and Tor Arne Johansen. Scenario-based model predictive control with several steps for colregs compliant ship collision avoidance. In *14th IFAC Conference on Control Applications in Marine Systems, Robotics and Vehicles (CAMS)*, 2022. in press.

[35] Inger Berge Hagen, Martin Navarsete Murvold, Tor Arne Johansen, and Edmund Førland Brekke. Grounding Hazard Considerations in Evaluation of COLREGS Collision Avoidance Algorithms. *IEEE Transactions on Intelligent Transportation Systems*, 2022. unpublished/under revision.

[36] Inger Berge Hagen, Olav Vassbotn, Morten Skogvold, Tor Arne Johansen, and Edmund Førland Brekke. Safety and COLREGS Evaluation for Marine Collision Avoidance Algorithms. *Ocean Engineering*, 2022. unpublished/under revision.

[37] Martin Gamborg Hansen, Toke Koldborg Jensen, Tue Lehn-Schiøler, Kristina Melchild, Finn Mølsted Rasmussen, and Finn Ennemark. Empirical ship domain based on ais data. *Journal of Navigation*, 66(6):931–940, nov 2013. ISSN 0373-4633. doi: 10.1017/S0373463313000489.

[38] Eivind Sørum Henriksen. Automatic testing of maritime collision avoidance methods with sensor fusion. Msc, Norwegian University of Science and Technology, 2018.

[39] Honda Motor Co., Ltd. Honda to Begin Sales of Legend with New Honda SENSING Elite, 2021. URL `https://global.honda/newsroom/news/2021/4210304eng-legend.html`. Accessed: 2022-08-15.

[40] Xia Hong, C.J. Harris, and P.A. Wilson. Autonomous ship collision free trajectory navigation and control algorithms. In *1999 7th IEEE International Conference on Emerging Technologies and Factory Automation. Proceedings ETFA '99 (Cat. No.99TH8467)*, volume 2, pages 923–929. IEEE, 1999. ISBN 0-7803-5670-5. doi: 10.1109/ETFA.1999.813090.

[41] Yamin Huang, Linying Chen, Pengfei Chen, Rudy R. Negenborn, and P. H. A. J. M. Van Gelder. Ship collision avoidance methods: State-of-the-art. *Safety Science*, 121:451–473, 2020. doi: 10.1016/j.ssci.2019.09.018.

[42] International Maritime Organization (IMO). Colregs - international regulations for preventing collisions at sea, 1972.

[43] International Maritime Organization (IMO). Resolution a.1106(29), revised guidelines for the onboard operational use of shipborne automatic identification systems (ais), 2015. URL `https://edocs.imo.org/Final`.

[44] SAE International. SAE J3016: Taxonomy and Definitions for Terms Related to On-Road Motor Vehicle Automated Driving Systems, Revision September 2016.

[45] International Maritime Organization (IMO). SOLAS-International Convention for the Safety of Life at Sea, 1974.

[46] International Maritime Organization (IMO). Autonomous ships: regulatory scoping exercise completed, 2021. URL `https://www.imo.org/en/MediaCentre/PressBriefings/pages/MASSRSE2021.aspx`.

[47] International Network for Autonomous Ships. Autonomous ships test areas, 2022. URL `http://www.autonomous-ship.org/testarea.html`. Accessed: 2022-08-12.

[48] Ornulf Jan Rodseth, Havard Nordahl, and Asa Hoem. Characterization of Autonomy in Merchant Ships. In *2018 OCEANS - MTS/IEEE Kobe Techno-Oceans (OTO)*, pages 1–7. IEEE, may 2018. ISBN 978-1-5386-1654-3. doi: 10.1109/OCEANSKOBE.2018.8559061.

[49] Tor Arne Johansen, Tristan Perez, and Andrea Cristofaro. Ship Collision Avoidance and COLREGS Compliance Using Simulation-Based Control Behavior Selection With Predictive Hazard Assessment. *IEEE Transactions on Intelligent Transportation Systems*, 17(12):3407–3422, dec 2016. ISSN 1524-9050.

[50] Martin Keller, Carsten Hass, Alois Seewald, and Torsten Bertram. A Model Predictive Approach to Emergency Maneuvers in Critical Traffic Situations. In *IEEE 18th International Conference on Intelligent Transportation Systems*, pages 369–374, Las Palmas, 2015. ISBN 978-1-4673-6596-3. doi: 10.1109/ITSC.2015.69.

[51] O. Khatib. Real-time obstacle avoidance for manipulators and mobile robots. In *Proceedings. 1985 IEEE International Conference on Robotics and Automation*, volume 2, pages 500–505, 1985. doi: 10.1109/ROBOT.1985.1087247.

[52] Hyo-Gon Kim, Sung-Jo Yun, Young-Ho Choi, Jae-Kwan Ryu, and Jin-Ho Suh. Collision avoidance algorithm based on colregs for unmanned surface vehicle. *Journal of Marine Science and Engineering*, 9(8):863, 2021. ISSN 2077–1312. doi: 10.3390/jmse9080863.

[53] Kristian Kjerstad. Collision Avoidance System for Ships Utilizing Other Vessels' Intentions. Msc, Norwegian University of Technology and Science, 2020.

[54] D. Kwame Minde Kufoalor, Erik Wilthil, Inger Berge Hagen, Edmund Førland Brekke, and Tor Arne Johansen. Autonomous COLREGs-Compliant Decision Making using Maritime Radar Tracking and Model Predictive Control. In *2019 18th European Control Conference (ECC)*, pages 2536–2542. IEEE, jun 2019. ISBN 978-3-907144-00-8.

[55] D. Kwame Minde Kufoalor, Tor Arne Johansen, Edmund Førland Brekke, Arild Hepsø, and Keith Trnka. Autonomous maritime collision avoidance: Field verification of autonomous surface vehicle behavior in challenging scenarios. *Journal of Field Robotics*, 37(3):387–403, apr 2020. ISSN 1556-4959.

[56] Yoshiaki Kuwata and Jonathan P. How. Cooperative distributed robust trajectory optimization using receding horizon milp. *IEEE Transactions on Control Systems Technology*, 19(2):423–431, 2010.

[57] Yoshiaki Kuwata, Michael T. Wolf, Dimitri Zarzhitsky, and Terrance L. Huntsberger. Safe maritime autonomous navigation with COLREGS, using velocity obstacles. *IEEE Journal of Oceanic Engineering*, 39(1), 2014. ISSN 03649059. doi: 10.1109/JOE.2013.2254214.

[58] Jiechao Liu, Paramsothy Jayakumar, Jeffrey L. Stein, and Tulga Ersal. An mpc algorithm with combined speed and steering control for obstacle avoidance in autonomous ground vehicles. In *Dynamic Systems and Control Conference*, volume 57267, page V003T44A003. American Society of Mechanical Engineers, 2015.

[59] Zhixiang Liu, Youmin Zhang, Xiang Yu, and Chi Yuan. Unmanned surface vehicles: An overview of developments and challenges. *Annual Reviews in Control*, 41:71–93, 2016. ISSN 1367-5788. doi: 10.1016/J.ARCONTROL.2016.04.018.

[60] Marine Traffic. MarineTraffic: Global Ship Tracking Intelligence | AIS Marine Traffic, 2022. URL `https://www.marinetraffic.com`.

[61] Maritime Safety Committee (MSC). Outcome of the Regulatory Scoping Exercise for the use of Maritime Autonomous Surface Ships (MASS), 2021.

[62] Luis Martinez-Gomez and Thierry Fraichard. Collision avoidance in dynamic environments: An ICS-based solution and its comparative evaluation. In *IEEE International Conference on Robotics and Automation*, pages 100–105, 2009. ISBN 978-1-4244-2788-8. doi: 10.1109/ROBOT.2009.5152536.

[63] Mercedes-Benz Group AG. The front runner in automated driving and safety technologies, 2022. URL `https://group.mercedes-benz.com/innovation/case/autonomous/drive-pilot-2.html`. Accessed: 2022-08-15.

[64] Paal Kristian Eknes Minne. Automatic testing of maritime collision avoidance algorithms. Msc, Norwegian University of Science and Technology, 2017.

[65] Signe Moe and Kristin Y. Pettersen. Set-based Line-of-Sight (LOS) path following with collision avoidance for underactuated unmanned surface vessel. In *24th Mediterranean Conference on Control and Automation (MED)*, pages 402–409, 2016. ISBN 978-1-4673-8345-5. doi: 10.1109/MED.2016.7535964.

[66] Maritime Safety Comittee (MSC). RESOLUTION MSC.137(76) (adopted on 4 December 2002) Standards for Ship Manoeuvrability, 2002.

[67] Peter Niedfeldt and Randal Beard. Convergence and Complexity Analysis of Recursive-RANSAC: A New Multiple Target Tracking Algorithm. *IEEE Transactions on Automatic Control*, 61(2):456 – 461, 2015. doi: 10.1109/TAC.2015.2437518.

[68] Tom Arne Pedersen, Jon Arne Glomsrud, and Odd Ivar Haugen. Towards simulation-based verification of autonomous navigation systems. In *Proceedings of the International Seminar on Safety and Security of Autonomous Vessels (ISSAV) and European STAMP Workshop and Conference (ESWC) 2019*, 2019. doi: 10.2478/9788395669606-00.

[69] Tom Arne Pedersen, Jon Arne Glomsrud, Else-Line Ruud, Aleksander Simonsen, Jarle Sandrib, and Bjørn-Olav Holtung Eriksen. Towards simulation-based verification of autonomous navigation systems. *Safety Science*, 129, sep 2020. ISSN 0925-7535. doi: 10.1016/J.SSCI.2020.104799.

[70] Z. Pietrzykowski and J. Magaj. Ship domain as a safety criterion in a precautionary area of traffic separation scheme. *TransNav : International Journal on Marine Navigation and Safety of Sea Transportation*, 11(1), 2017. doi: 10.12716/1001.11.01.10.

[71] Riccardo Polvara, Sanjay Sharma, Jian Wan, Andrew Manning, and Robert Sutton. Obstacle Avoidance Approaches for Autonomous Navigation of Unmanned Surface Vehicles. *Journal of Navigation*, 71(1):241–256, 2018. ISSN 0373-4633. doi: 10.1017/S0373463317000753.

[72] Ivan Porres, Sepinoud Azimi, and Johan Lilius. Scenario-based Testing of a Ship Collision Avoidance System. In *2020 46th Euromicro Conference on Software Engineering and Advanced Applications (SEAA)*, pages 545–552. IEEE, 2020. ISBN 978-1-7281-9532-2. doi: 10.1109/SEAA51224.2020.00090.

[73] Stephan Procee, Clark Borst, René van Paassen, Max Mulder, and V Bertram. Using augmented reality to improve collision avoidance and resolution. In *Proceedings of the 17th International Conference on Computer and IT Applications in the Maritime Industries, Pavone, Italy*, pages 14–16, 2018.

[74] S. Joe Qin and Thomas A. Badgwell. A survey of industrial model predictive control technology. *Control Engineering Practice*, 11(7):733–764, 2003. ISSN 0967-0661.

[75] Ørnulf Jan Rødseth. Assessing business cases for autonomous and unmanned ships. In *Technology and Science for the Ships of the Future*, pages 1033–1041. IOS Press, 2018.

[76] Hans Rosling. The magic washing machine, 2010. URL `https://www.ted.com/talks/hans_rosling_the_magic_washing_machine?utm_campaign=tedspread&utm_medium=referral&utm_source=tedcomshare`. Accessed: 2022-08-15.

[77] Kristian Amundsen Ruud, Edmund Førland Brekke, and Jo Eidsvik. Lidar extended object tracking of a maritime vessel using an ellipsoidal contour model. In *2018 Sensor Data Fusion: Trends, Solutions, Applications (SDF)*, pages 1–6. IEEE, 2018.

[78] Michael Schuster and Johannes Reuter. Target tracking in marine environment using automotive radar and laser range sensor. In *20th International Conference on Methods and Models in Automation and Robotics (MMAR)*, pages 965–970, Miedzyzdroje, 2015. IEEE. ISBN 978-1-4799-8701-6. doi: 10.1109/MMAR.2015.7284009.

[79] SFI AutoShip. Annual Report 2021 SFI AutoShip, 2021.

[80] Shutterstock. Shutterstock, 2022. URL `https://www.shutterstock.com`. Acessed: 2022-08-10.

[81] Sjøfartsdirektoratet | Norwegian Maritime Authorithy. World's first test area for autonomous ships opened, 2016. URL `https://www.sdir.no/en/news/news-from-the-nma/worlds-first-test-area-for-autonomous-ships-opened/`. Accessed: 2022-08-12.

[82] Paul G. Stankiewicz and Galen E. Mullins. Improving Evaluation Methodology for Autonomous Surface Vessel COLREGS Compliance. In *OCEANS 2019 - Marseille*, pages 1–7. IEEE, 2019. ISBN 978-1-7281-1450-7. doi: 10.1109/OCEANSE.2019.8867549.

[83] Thomas Statheros, Gareth Howells, and Klaus Mcdonald-Maier. Autonomous Ship Collision Avoidance Navigation Concepts, Technologies and Techniques. *Journal of Navigation*, 61(1):129–142, 2008. doi: 10.1017/S037346330700447X.

[84] Rafal Szlapczynski. A New Method of Ship Routing on Raster Grids, with Turn Penalties and Collision Avoidance. *Journal of Navigation*, 59(1):27–42, jan 2005. ISSN 0373-4633. doi: 10.1017/S0373463305003528.

[85] Cheekuang Tam, Richard Bucknall, and Alistair Greig. Review of Collision Avoidance and Path Planning Methods for Ships in Close Range Encounters. *Journal of Navigation*, 62(3):455–476, 2009. doi: 10.1017/S0373463308005134.

[86] Trym Tengesdal, Tor Arne Johansen, and Edmund Brekke. Risk-based autonomous maritime collision avoidance considering obstacle intentions. In *FUSION conference*, 2020.

[87] Trym Tengesdal, Tor A. Johansen, and Edmund F. Brekke. Ship collision avoidance utilizing the cross-entropy method for collision risk assessment. *IEEE Trans. Intelligent Transportation Systems*, 2022.

[88] The Norwegian Coastal Administration. AIS Norway, 2019. URL `https://www.kystverket.no/en/navigation-and-monitoring/ais/ais-norge/`. Accessed: 2021-04-15.

[89] Tobias Rye Torben, Jon Arne Glomsrud, Tom Arne Pedersen, Ingrid B. Utne, and Asgeir J. Sørensen. Automatic simulation-based testing of autonomous ships using Gaussian processes and temporal logic. *Proceedings of the Institution of Mechanical Engineers, Part O: Journal of Risk and Reliability*, page 1748006X2110692, jan 2022. ISSN 1748-006X. doi: 10.1177/1748006X211069277.

[90] Anete Vagale, Robin T. Bye, and Ottar L. Osen. Evaluation of Path Planning Algorithms of Autonomous Surface Vehicles Based on Safety and Collision Risk Assessment. In *Global Oceans 2020: Singapore – U.S. Gulf Coast*, pages 1–8, 2020. doi: 10.1109/IEEECONF38699.2020.9389481.

[91] Anete Vagale, Robin T. Bye, Rachid Oucheikh, Ottar L. Osen, and Thor I. Fossen. Path planning and collision avoidance for autonomous surface vehicles II: a comparative study of algorithms. *Journal of Marine Science and Technology*, pages 1–17, 2021. ISSN 0948-4280. doi: 10.1007/s00773-020-00790-x.

[92] Anete Vagale, Rachid Oucheikh, Robin T. Bye, Ottar L. Osen, and Thor I. Fossen. Path planning and collision avoidance for autonomous surface vehicles I: a review. *Journal of Marine Science and Technology*, pages 1–15, 2021. ISSN 0948-4280. doi: 10.1007/s00773-020-00787-6.

[93] Andrea Vedaldi, Hailin Tin, Paolo Favaro, and Stefano Soatto. KALMANSAC: Robust filtering by consensus. In *Tenth IEEE International Conference on Computer Vision (ICCV'05)*, volume 1, pages 633–640, Beijing, 2005. IEEE. ISBN 076952334X. doi: 10.1109/ICCV.2005.130.

[94] Ning Wang, Yuncheng Gao, Zhongjiu Zheng, Hong Zhao, and Jianchuan Yin. A Hybrid Path-Planning Scheme for an Unmanned Surface Vehicle. In *2018 Eighth International Conference on Information Science and Technology (ICIST)*, pages 231–236. IEEE, jun 2018. ISBN 978-1-5386-3782-1. doi: 10.1109/ICIST.2018.8426161.

[95] Erik F. Wilthil, Andreas L. Flåten, and Edmund F. Brekke. A target tracking system for ASV collision avoidance based on the PDAF. In *Sensing and Control for Autonomous Vehicles: Applications to Land, Water and Air Vehicles*, volume 474, pages 269–288. Springer International Publishing, 2017. ISBN 978-3-319-55372-6. doi: 10.1007/978-3-319-55372-6_13.

[96] Kyle L. Woerner. *Multi-contact protocol-constrained collision avoidance for autonomous marine vehicles*. PhD thesis, Massachusetts Institute of Technology, 2016.

[97] Kyle L. Woerner and Michael R. Benjamin. Real-Time Automated Evaluation of COLREGS-Constrained Interactions Between Autonomous Surface Vessels and Human Operated Vessels in Collaborative Human-Machine Partnering Missions. In *2018 OCEANS - MTS/IEEE Kobe Techno-Oceans (OTO)*, pages 1–9, 2018. ISBN 9781538616543. doi: 10.1109/OCEANSKOBE.2018.8559422.

[98] Kyle L. Woerner, Michael R. Benjamin, Michael Novitzky, and John J. Leonard. Collision Avoidance Road Test for COLREGS-Constrained Autonomous Vehicles. In *OCEANS 2016 MTS/IEEE Monterey*, pages 1–6, 2016. ISBN 9781509015375.

[99] Kyle L. Woerner, Michael R. Benjamin, Michael Novitzky, and John J. Leonard. Quantifying protocol evaluation for autonomous collision avoidance: Toward establishing COLREGS compliance metrics. *Autonomous Robots*, 43 (4):967–991, 2019. ISSN 15737527. doi: 10.1007/s10514-018-9765-y.

[100] Yara International ASA. Yara Birkeland | Yara International, 2022. URL `https://www.yara.com/news-and-media/press-kits/yara-birkeland-press-kit/`. Accessed: 2022-08-11.

[101] Boliang Yi, Stefan Gottschling, Jens Ferdinand, Norbert Simm, Frank Bonarens, and Christoph Stiller. Real time integrated vehicle dynamics control and trajectory planning with MPC for critical maneuvers. In *2016 IEEE Intelligent Vehicles Symposium (IV)*, pages 584–589, Gothenburg, 2016. ISBN 978-1-5090-1821-5. doi: 10.1109/IVS.2016.7535446.

[102] Luman Zhao and Myung-Il Roh. Colregs–compliant multiship collision avoidance based on deep reinforcement learning. *Ocean Engineering*, 191:106436, 2019. doi: 10.1016/J.OCEANENG.2019.106436.

ISBN 978-82-326-6737-6 (printed ver.)
ISBN 978-82-326-5298-3 (electronic ver.)
ISSN 1503-8181 (printed ver.)
ISSN 2703-8084 (online ver.)

NTNU
Norwegian University of
Science and Technology